Mesh Free Methods for Differential Models in Financial Mathematics

Abdelmgid Osman Mohammed Sidahmed

A Thesis submitted in partial fulfillment of the requirements for the degree of Doctor of Philosophy in the Department of Mathematics and Applied Mathematics at the Faculty of Natural Sciences, University of the Western Cape

Supervisor: Prof. Kailash C. Patidar

May 2011

KEYWORDS

Computational Finance

Option Pricing

Mesh Free Methods

Radial Basis Functions

European and American put Options

Exotic Options

Heston's Model

Free Boundary Problems

Numerical Methods

Analysis of Numerical Methods

ABSTRACT

Mesh Free Methods for Differential Models in Financial Mathematics

by

A.O.M. Sidahmed

PhD thesis, Department of Mathematics and Applied Mathematics, Faculty of Natural Sciences, University of the Western Cape.

Many problems in financial world are being modeled by means of differential equation. These problems are time dependent, highly nonlinear, stochastic and heavily depend on the previous history of time. A variety of financial products exists in the market, such as forwards, futures, swaps and options. Our main focus in this thesis is to use the numerical analysis tools to solve some option pricing problems. Depending upon the inter-relationship of the financial derivatives, the dimension of the associated problem increases drastically and hence conventional methods (for example, the finite difference methods or finite element methods) for solving them do not provide satisfactory results. To resolve this issue, we use a special class of numerical methods, namely, the mesh free methods. These methods are often better suited to cope with changes in the geometry of the domain of interest than classical discretization techniques. In this thesis, we apply these methods to solve problems that price standard and non-standard options. We then extend the proposed approach to solve Heston's volatility model. The methods in each of these cases are analyzed for stability and thorough comparative numerical results are provided.

May 2011.

DECLARATION

I declare that *Mesh Free Methods for Differential Models in Financial Mathematics* is my own work, that it has not been submitted before for any degree or examination at any other university, and that all sources I have used or quoted have been indicated and acknowledged by complete references.

Abdelmgid Osman Mohammed Sidahmed May 2011

Signed ....

ACKNOWLEDGEMENT

First and foremost, I would like to thank the Almighty Allah (Glory to Him) who gave me the strength to do this research and made all difficult tasks very easy.

I would like to express my deepest and sincere gratitude to my supervisor, Prof. Kailash C. Patidar. Without his great ideas and big efforts, this work would not have been done. Special thanks to his family.

I would also like to thanks AL-Neelain University for funding my PhD programme. Particularly, Prof. Ismail Hamid El-Sanusi (the Secretary of the Scientific Affairs, at the AL-Neelain University) and Prof. Mohammed Abdul Jalil Mohammed (the Dean of Faculty of Mathematical Sciences at the AL-Neelain University) who have been of great assistance throughout the programme.

I acknowledge the senior students and staff of the Department of Mathematics and Applied Mathematics, University of the Western Cape.

I do not have words to express my thanks for the help and moral support that I received from my friends Eihab, Zakariya, Hasim, Khabir, Mushal, Gasim and Sara. They were always part of my difficult times.

Lastly, I appreciate the support of my extended family for all their love and encouragement, in particular, to my parents (Osman & Manar) who raised me with the love of science and supported me in all my pursuits, and my brothers and sisters for their all time support. I am very grateful to them.

DEDICATION

I dedicate this work to my parents who have devoted their lives for us and who have been giving their continuous blessings to me for success; to my dear brothers and sister with whom I shared big portion of my life; and to my supervisor who has been very kind and friendly.

Contents

List of Tables

List of Figures

List of Publications

Part of this thesis has been submitted in the form of the research papers listed below. We also have some technical reports whose revised form is being submitted to prestigious international journals for publications.

1. K.C. Patidar and A.O.M. Sidahmed, An Efficient Meshfree Method for Option Pricing Problems. In T.E. Simos, G. Psihoyios and Ch. Tsitouras (eds.), *Numerical Analysis and Applied Mathematics, Proceedings of the International Conference on Numerical Analysis and Applied Mathematics (ICNAAM 2010)*, published by American Institute of Physics (AIP) Conference Proceedings, Vol. 1281, New York, 2010, pp. 1824-1827.

2. K.C. Patidar and A.O.M. Sidahmed, Efficient meshfree method for pricing European and American put options on a non-dividend paying asset, submitted for publication.

3. K.C. Patidar and A.O.M. Sidahmed, A mesh free method for pricing exotic options, submitted for publication.

4. K.C. Patidar and A.O.M. Sidahmed, A radial point interpolation method to price options, submitted for publication.

5. K.C. Patidar and A.O.M. Sidahmed, Efficient meshfree method for pricing European and American put options on a dividend paying asset, submitted for publication.

6. K.C. Patidar and A.O.M. Sidahmed, A mesh free method for solving the Heston's volatility model, Report Nr. UWC-MRR 2011/19, University of the Western Cape, 2011.

7. K.C. Patidar and A.O.M. Sidahmed, An efficient meshfree method for option pricing problems, Report Nr. UWC-MRR 2010/05, University of the Western Cape, 2010.

8. D. Bahuguna, K.C. Patidar and A.O.M. Sidahmed, Existence, uniqueness and meshfree approximation of a solution of Merton's model for pricing jump diffusion process, Report Nr. UWC-MRR 2010/14, University of the Western Cape, 2010.

9. M.H.M. Khabir, K.C. Patidar and A.O.M. Sidahmed, Investigation of Some Numerical Methods for Option Pricing Problems, Report Nr. UWC-MRR 2009/11, University of the Western Cape, 2009.

10. K.C. Patidar and A.O.M. Sidahmed, On numerical methods for pricing exotic options, Report Nr. UWC-MRR 2008/08, University of the Western Cape, 2008.

Chapter 1

General introduction

There is a growing interest in pricing financial derivatives that can be used to minimize losses caused by price fluctuations of the underlying assets. These assets are financial objects whose value is known at present but is liable to change in future. A variety of financial products exists in the financial market, such as futures, forwards, swaps and options. In this thesis we will concentrate on options particularly on American options (which are the standard options) and the exotic options, e.g., barrier options (which are non-standard options). Such options have become so popular that in many cases more money is invested in them than in the underlying asset due to the fact that they are extremely attractive to the investors, both for speculation and hedging.

Even though the American options can be exercised before the maturity date, in practice, they are rarely exercised early. This is because any option has a non-negative time value and is usually worth more unexercised. Where American and European options are otherwise identical (having the same strike price, etc.), the American option will be worth at least as much as the European one (which it entails). If it is worth more, then the difference is a guide to the likelihood of early exercise which results into a free boundary problem. However, relatively much less attention has been paid for solving such free-boundary problem (related in pricing the American options) directly. Unlike the evaluation of the expected pay-off, solving the free-boundary problem has two important advantages. Firstly, it provides the optimal exercise policy. Secondly, it provides the complete pricing function.

Though the American option pricing problem has been the focus of several numerical methods in the past three decades, it still retains a prominent position amongst fundamental problems of interest in finance. Most numerical methods in literature calculate the price of the option for a given time to expiration and stock price. These methods exploit the representation of the price as the expected pay-off under the risk-neutral measure. Relatively a smaller number of methods attempt to solve the related free-boundary problem directly. Solving the free-boundary problem explicitly provides the entire price function as well as the optimal exercise boundary.

On the other hand, an exotic option is a derivative which has features making it more complex than commonly traded products (e.g., vanilla options like European and American options). These products are usually traded over-the-counter (OTC), or are embedded in structured notes. An exotic option can have the features that the payoff at maturity depends not just on the value of the underlying index at maturity, but at its value at several times during the contracts life (it could be an Asian option depending on some average, a lookback option depending on the maximum or minimum, a barrier option which ceases to exist if a certain level is reached or not by the underlying, a digital option, range options, etc.). Even products traded actively in the market can have the characteristics of exotic options, such as convertible bonds, whose valuation can depend on the price and volatility of the underlying equity, the credit rating, the level and volatility of interest rates, and the correlations between these factors.

Under the exotic options, we will be dealing with the barrier and Asian options. In finance, a barrier option is a type of financial option where the option to exercise depends on the underlying crossing or reaching a given barrier level. These options were created to provide the insurance value of an option without charging much premium. These options are similar in some ways to ordinary options. There are put and calls, as well as of European and American style. But they become activated or, on the contrary, null and void only if the underlier reaches a predetermined level (barrier).

The four main types of barrier options are: Up-and-out, Down-and-out, Up-and-in, and Down-and-in barrier options. In a nutshell, the barrier options have a payoff that switches on or off depending on whether the asset crosses a pre-defined level (barrier). Moreover, unlike other standard options, the barrier options are path-dependent, and hence their valuation is not straightforward. The value of the option at any time depends not just on the underlying at that point, but also on the path taken by the underlying. The classical Black-Scholes approach does not directly provide us the value of these options and hence we need to use some more complex methods.

For further understanding on option pricing, below we present some more information which is fairly standard. However, to keep the thesis readable and self-contained, we give a very brief discussion on some of the issues from [43, 96].

1.1 Option pricing: a brief overview

An option is the right (but not an obligation) to buy or sell a risky asset at a pre-specified fixed price within a specified period. The underlying asset typically is a stock, or a parcel of shares of a company. Other examples of underlying include stock indices, currencies, or commodities.

There are two types of options: call and put. The call option gives the holder the right to buy the underlying for an agreed price E (called the strike price) by the date T (maturity time). The put option gives the holder the right to sell the underlying for the price E by the date T.

At time t the holder of the option can choose to

- sell the option at its current market price (at $t < T$),
- retain the option and do nothing,
- exercise the option ($t \leq T$), or
- let the option expire worthless ($t \geq T$).

It should be noted that every option can be exercised at any time $t \leq T$. For European options exercise is only permitted at expiration T. American options can be exercised at any time up to and including the expiration date.

The value of the option, denoted by V, usually depends on the price of the underlying, which is denoted by S.

The payoff $V(S, T)$ of a European call option at expiration date T is given by

$$V(S_T, T) = \begin{cases} 0 & \text{in case } S_T \leq E \ \text{ (option expires worthless)} \\ S_T - E & \text{in case } S_T > E \ \text{ (option is exercised).} \end{cases} \tag{1.1.1}$$

Hence

$$V(S_T, T) = \max(S_T - E, 0), \tag{1.1.2}$$

or

$$V(S_T, T) = (S_T - E, 0)^+, \tag{1.1.3}$$

where the notation $(x, 0)^+$ means x if it is non-negative, otherwise 0.

For a European put option, exercising only makes sense in case $S < E$. The payoff $V(S, T)$ of a put at expiration time T is

$$V(S_T, T) = \begin{cases} E - S_T & \text{in case } S_T < E \ \text{ (option is exercised)} \\ 0 & \text{in case } S_T \geq E \ \text{ (option is worthless).} \end{cases} \tag{1.1.4}$$

Hence

$$V(S_T, T) = \max(E - S_T, 0), \tag{1.1.5}$$

or

$$V(S_T, T) = (E - S_T, 0)^+. \tag{1.1.6}$$

Figures 1.1.1 and 1.1.2 shows the payoff function for European call and put options, respectively [96].

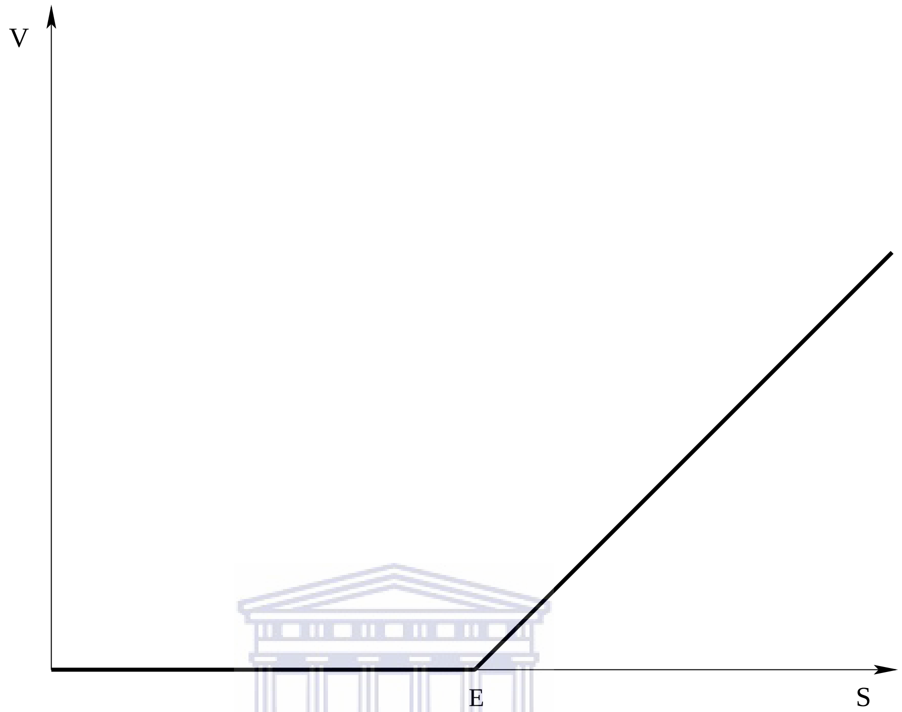

Figure 1.1.1: Payoff of European call option

1.1.1 Itô's lemma

The price of any derivative is a function of the stochastic variables underlying the derivative and time [43]. The variable x has a drift rate of a and a variance rate of b^2. Suppose that the value of a variable x follows the Itô process

$$dx = a(x,t)dt + b(x,t)dz, \tag{1.1.7}$$

where dz is a Wiener process and a and b are functions of x and t.

Itô's lemma shows that a function G of x and t follows the process

$$dG = \left(\frac{\partial G}{\partial x}a + \frac{\partial G}{\partial t} + \frac{1}{2}\frac{\partial^2 G}{\partial x^2}b^2\right)dt + \frac{\partial G}{\partial x}bdz, \tag{1.1.8}$$

where dz is the same Wiener process as in equation (1.1.7). Thus, G also follows an

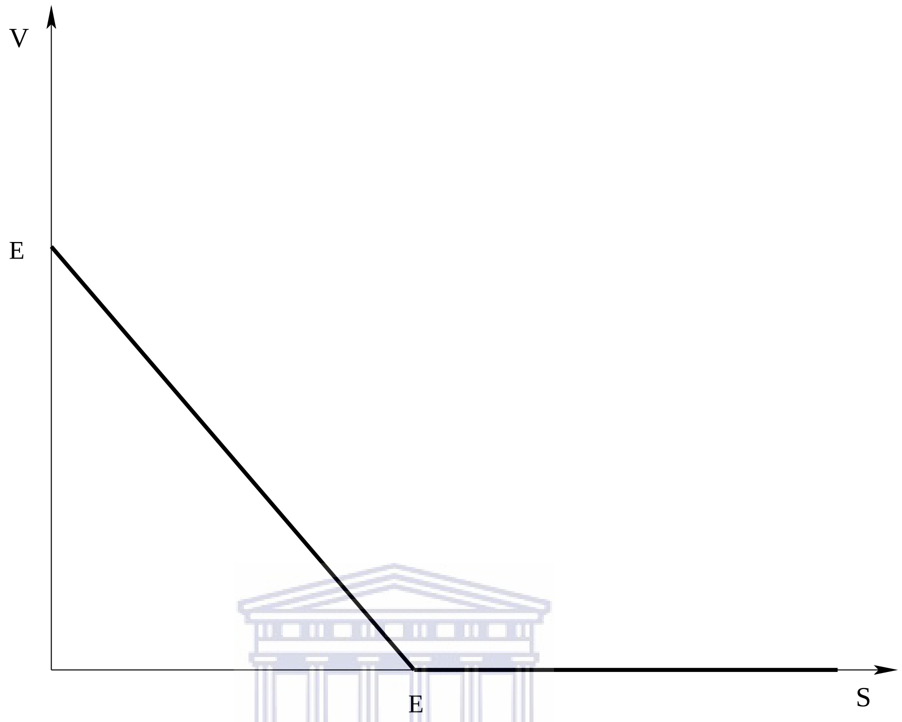

Figure 1.1.2: Payoff of European put option

Itô process. It has a drift rate of

$$\frac{\partial G}{\partial x}a + \frac{\partial G}{\partial t} + \frac{1}{2}\frac{\partial^2 G}{\partial x^2}b^2,$$

and a variance rate of

$$\frac{\partial G}{\partial x}b.$$

The standard deviation of the change in a short period of time Δt should be proportional to the stock price and leads to the model

$$dS = \mu S dt + \sigma S dz, \tag{1.1.9}$$

where σ is the volatility of the stock price S and μ is the expected rate of return.

Substituting equation (1.1.8) into (1.1.9) we get

$$dG = \left(\frac{\partial G}{\partial S}\mu S + \frac{\partial G}{\partial t} + \frac{1}{2}\frac{\partial^2 G}{\partial S^2}\sigma^2 S^2\right) dt + \frac{\partial G}{\partial S}\sigma S dz. \tag{1.1.10}$$

Note that both S and G are affected by the same underlying source of uncertainty, dz.

1.1.2 The classical Black-Scholes-Merton differential equation and Black-Scholes formula

The assumptions that are used to derive the Black-Scholes-Merton differential equation are as follows:

- The stock price follows the stochastic process with μ and σ constant.
- The short selling of securities with full use of proceeds is permitted.
- There are no transactions costs or taxes. All securities are perfectly divisible.
- There are no dividends during the life of the derivative.
- There are no riskless arbitrage opportunities.
- Security trading is continuous.
- The risk-free rate of interest, r, is constant and the same for all maturities.

Suppose that f is the price of a call option or other derivative contingent on S. The variable f must be some function of s and t. Hence, from equation (1.1.10) we obtain

$$df = \left(\frac{\partial f}{\partial S}\mu S + \frac{\partial f}{\partial t} + \frac{1}{2}\frac{\partial^2 f}{\partial S^2}\sigma^2 S^2\right) dt + \frac{\partial f}{\partial S}\sigma S dz. \tag{1.1.11}$$

The discrete versions of equations (1.1.9) and (1.1.11) are

$$\Delta S = \mu S \Delta t + \sigma S \Delta z, \tag{1.1.12}$$

and

$$\Delta f = \left(\frac{\partial f}{\partial S} \mu S + \frac{\partial f}{\partial t} + \frac{1}{2} \frac{\partial^2 f}{\partial S^2} \sigma^2 S^2 \right) \Delta t + \frac{\partial f}{\partial S} \sigma S \Delta z, \tag{1.1.13}$$

where Δf and ΔS are the changes in f and S in a small time interval Δt.

Define Π as the value of the portfolio

$$\Pi = -f + \frac{\partial f}{\partial S} S. \tag{1.1.14}$$

The change $\Delta\Pi$ in the value of the portfolio in the time interval Δt is given by

$$\Delta\Pi = -\Delta f + \frac{\partial f}{\partial S} \Delta S. \tag{1.1.15}$$

Substituting equations (1.1.12) and (1.1.13) into equation (1.1.15) we obtain

$$\begin{aligned} \Delta\Pi &= -\left(\frac{\partial f}{\partial S} \mu S + \frac{\partial f}{\partial t} + \frac{1}{2} \frac{\partial^2 f}{\partial S^2} \sigma^2 S^2 \right) \Delta t + \frac{\partial f}{\partial S} \sigma S \Delta z \\ &\quad + \frac{\partial f}{\partial S} (\mu S \Delta t + \sigma S \Delta z) \\ &= -\frac{\partial f}{\partial S} \mu S \Delta t + \left(-\frac{\partial f}{\partial t} - \frac{1}{2} \frac{\partial^2 f}{\partial S^2} \sigma^2 S^2 \right) \Delta t - \frac{\partial f}{\partial S} \sigma S \Delta z \\ &\quad + \frac{\partial f}{\partial S} \mu S \Delta t + \frac{\partial f}{\partial S} \sigma S \Delta z. \end{aligned} \tag{1.1.16}$$

Further simplification leads to

$$\Delta\Pi = \left(-\frac{\partial f}{\partial t} - \frac{1}{2} \frac{\partial^2 f}{\partial S^2} \sigma^2 S^2 \right) \Delta t. \tag{1.1.17}$$

Because this equation does not involve Δz, the portfolio must be riskless during time Δt. The assumptions listed above imply that the portfolio must instantaneously earn the same rate of return as other short–term risk-free securities. If it earned more than this return, arbitrageurs could make a riskless profit by borrowing money to buy the portfolio; if it earned less, they could make a riskless profit by shorting the portfolio and buying risk-free securities. It follows that

$$\Delta\Pi = r\Pi\Delta t, \tag{1.1.18}$$

where r is the risk-free interest rate.

Substitutions from equations (1.1.14) and (1.1.17) into (1.1.18), gives

$$\left(\frac{\partial f}{\partial t} + \frac{1}{2}\frac{\partial^2 f}{\partial S^2}\sigma^2 S^2\right)\Delta t = r\left(f - \frac{\partial f}{\partial S}S\right)\Delta t, \tag{1.1.19}$$

which implies

$$\frac{\partial f}{\partial t} + rS\frac{\partial f}{\partial S} + \frac{1}{2}\sigma^2 S^2\frac{\partial^2 f}{\partial S^2} = rf. \tag{1.1.20}$$

Equation (1.1.20) is the Black-Scholes-Merton differential equation. It should be noted that most of the option pricing problems following a differential equation approach will have a variant of the above equation with some initial (or final) conditions and appropriate boundary conditions using which one can find the solution of the governing problem.

The Black-Scholes formulas for the prices at time zero of a European call and put options on a non-dividend-paying stock are

$$V_{\text{Call}} = S_0 N(d_1) - Ee^{-rT}N(d_2), \tag{1.1.21}$$

and

$$V_{\text{Put}} = Ee^{-rT}N(-d_2) - S_0 N(-d_1), \tag{1.1.22}$$

where

$$d_1 = \frac{\ln(S_0/E) + (r + \frac{1}{2}\sigma^2)T}{\sigma\sqrt{T}}, \tag{1.1.23}$$

and

$$d_2 = \frac{\ln(S_0/E) + (r - \frac{1}{2}\sigma^2)T}{\sigma\sqrt{T}} = d_1 - \sigma\sqrt{T}. \tag{1.1.24}$$

In the above, $N(\cdot)$ is the cumulative probability distribution function for a standard normal distribution.

1.1.3 Options on dividend-paying assets

A simple modification of the modeling process allows the payment of a continuous and constant dividend yield on the underlying asset. This dividend yield is usually denoted by D and is the continuously compounded proportion over a year. The equivalent of equation (1.1.9) is as follows

$$dS = (\mu - D)Sdt + \sigma Sdz. \tag{1.1.25}$$

The derivation approach is similar to the one described before, and therefore the modified Black-Scholes equation is

$$\frac{\partial f}{\partial t} + (r - D)S\frac{\partial f}{\partial S} + \frac{1}{2}\sigma^2 S^2 \frac{\partial^2 f}{\partial S^2} - rf = 0. \tag{1.1.26}$$

With the addition of a dividend yield D, the value of a European call option on a dividend-paying stock and a European put option on a dividend paying stock at time zero are

$$V_{\text{Call}} = e^{-DT}S_0N(\widetilde{d}_1) - Ee^{-rT}N(\widetilde{d}_2), \tag{1.1.27}$$

and

$$V_{\text{Put}} = Ee^{-rT}N(-\widetilde{d}_2) - S_0e^{-DT}N(-\widetilde{d}_1), \tag{1.1.28}$$

where

$$\widetilde{d}_1 = \frac{\ln(S_0/E) + (r - D + \frac{1}{2}\sigma^2)T}{\sigma\sqrt{T}},$$

and

$$\widetilde{d}_2 = \frac{\ln(S_0/E) + (r - D - \frac{1}{2}\sigma^2)T}{\sigma\sqrt{T}} = \widetilde{d}_1 - \sigma\sqrt{T}.$$

As before, $N(\cdot)$ is the cumulative probability distribution function for a standard normal distribution.

1.1.4 Greeks

In mathematical finance, the Greeks are quantities that are used to represent the sensitivities of the price of derivatives such as options to a change in underlying parameters on which the value of an instrument or portfolio of financial instruments is dependent. In some cases, these also called the risk sensitivities [1], risk measures [71] or hedge parameters [19]. Below we give a brief discussion on them.

Delta: The delta of an option defined as the rate of change of the option price with respect to the price of the underlying asset. The seller of the option or its portfolio should buy Δ shares of the underlying asset to hedge the risk inherited in selling the option or portfolio.

$$\Delta = \frac{\partial V}{\partial S}, \tag{1.1.29}$$

where V is a price of the option and S is the stock price.

For a European call option on a non-dividend-paying stock,

$$\Delta(\text{Call}) = N(d_1). \tag{1.1.30}$$

For a European put option on a non-dividend-paying stock,

$$\Delta(\text{Put}) = N(d_1) - 1, \tag{1.1.31}$$

where d_1 and d_2 are defined as in equations (1.1.23) and (1.1.29) respectively.

Theta: The theta (Θ) of a portfolio of options, is the rate of change of the value of the portfolio with respect to the passage of time with all else remaining the same, i.e.,

$$\Theta = \frac{\partial V}{\partial t}. \tag{1.1.32}$$

For a European call option on a non-dividend-paying stock,

$$\Theta_{\text{Call}} = -\frac{S_0 N'(d_1)\sigma}{2\sqrt{T}} - rEe^{-rT}N(d_2), \tag{1.1.33}$$

where d_1 and d_2 are defined as in equations (1.1.23) and (1.1.24), respectively, and

$$N'(x) = \frac{1}{\sqrt{2\pi}}e^{-x^2/2}. \tag{1.1.34}$$

For a European put option on the stock,

$$\Theta_{\text{Put}} = -\frac{S_0 N'(d_1)\sigma}{2\sqrt{T}} - rEe^{-rT}N(-d_2). \tag{1.1.35}$$

Gamma: The gamma (Γ) of an option on an underlying asset, is the rate of change of the option's delta with respect to the price of the underlying asset. It is the second partial derivative of the portfolio with respect to asset price, i.e.,

$$\Gamma = \frac{\partial^2 V}{\partial S^2}. \tag{1.1.36}$$

For a European call or put option on a non-dividend-paying stock, the gamma is given by

$$\Gamma = \frac{N'(d_1)}{S_0\sigma\sqrt{T}}, \tag{1.1.37}$$

where d_1 is defined as in equation (1.1.23) and $N'(x)$ is as given by equation (1.1.34).

Vega: The sensitivity of the option to changes in volatility is known as 'Vega' which is the rate of change of the value of the option with respect to the volatility of the underlying asset and is given by

$$\text{vega} = \frac{\partial V}{\partial \sigma}. \tag{1.1.38}$$

If the absolute value of vega is high, the option's value is very sensitive to small changes in volatility. For a European call or put option on a non-dividend-paying stock, vega is given by

$$\text{vega} = S_0\sqrt{T}N'(d_1), \tag{1.1.39}$$

where d_1 is defined as in equation (1.1.23) and the formula for $N'(x)$ is given by equation (1.1.34).

Rho: The sensitivity of the option to changes in interest rate is known as 'rho' which is the rate of change of the value of the option with respect to the interest rate and is given by

$$\text{rho} = \frac{\partial V}{\partial r}. \tag{1.1.40}$$

For a European call option on a non-dividend-paying stock,

$$\text{rho}_{\text{Call}} = ETe^{-rT}N(d_2), \tag{1.1.41}$$

where d_2 is defined as in equation (1.1.24). For a European put option,

$$\text{rho}_{\text{Put}} = -ETe^{-rT}N(-d_2). \tag{1.1.42}$$

1.2 A brief overview of mesh free methods

Our numerical methods will largely be based on the so-called mesh free methods. These methods, nowadays, are being used in many different areas of sciences and engineering, for example, scattered data modeling, problems involving moving discontinuities such as cracks and shocks, multi-scale resolution, non-uniform sampling, computer graphics, neural networks, etc. The salient features of mesh free methods which make them very powerful are the following:

- In mesh free methods the connectivity of the nodes is determined at run-time, hence no a-priori mesh is required.
- No mesh alignment sensitivity is required. This is a serious problem in mesh-based algorithms.
- Continuity of shape functions: The shape functions of mesh free methods can be constructed to have any desired order of continuity.
- Convergence: For the same order of consistency numerical experiments suggest that the convergence results of the mesh free methods are often considerably better than the results obtained by mesh-based shape functions.

In the traditional finite difference, finite element and finite volume methods, the spatial domain is discretized into meshes [67]. A mesh is defined as any of the open spaces or interstices between the strands of a net that is formed by connecting nodes in a predefined manner.

The mesh free method is used to establish a system of algebraic equations for the whole problem domain without the use of a predefined mesh. Mesh free methods essentially use a set of nodes scattered within the problem domain as well as on the boundaries to represent the problem domain and its boundaries.

Applications of mesh free methods [28] can be found in

- many different areas of science and engineering via scattered data modeling (e.g., fitting of potential energy surfaces in chemistry),

- many different areas of science and engineering via solution of partial differential equations,
- non-uniform sampling (e.g., medical imaging),
- computer graphics (e.g., image warping),
- learning theory, neural networks and data mining (e.g., support vector machines),
- optimization, etc.

The key idea of the mesh free methods is to provide accurate and stable numerical solutions for integral equations or PDEs with all kinds of possible boundary conditions with a set of arbitrarily distributed nodes (or particles) without using any mesh that provides the connectivity of these nodes or particles.

1.2.1 Different approaches of constructing the mesh free shape functions

Smooth Particle Hydrodynamics Approach [6]: Probably the oldest of the mesh free methods is the smooth particle hydrodynamics (SPH) method [68]. A rationale for this method was provided by invoking the notion of a kernel approximation for solution $u(x)$ on a domain Ω generated by

$$u^h(x) = \int_\Omega W(x-\xi,h)u(\xi)d\xi, \tag{1.2.1}$$

where $u^h(x)$ is the approximation, $W(x-\xi,h)$ is a kernel or weight function, and h is a measure of the size of the support.

The weight function W is a monotonically decreasing function and satisfies the following properties

$$
\begin{aligned}
W(x-\xi,h) &> 0 \quad \text{over } \Omega && (1.2.2)\\
W(x-\xi,h) &= 0 \quad \text{out side } \Omega && (1.2.3)\\
\int_\Omega W(x-\xi,h)d\xi &= 1 && (1.2.4)\\
W(s,h) &\to \delta(s) \ \text{ as } \ h \to 0. && (1.2.5)
\end{aligned}
$$

Three commonly used weight functions are the exponential, cubic spline and quartic spline functions. These are:

The exponential weight function

$$
W(\overline{d}) = \begin{cases} e^{-(\frac{\overline{d}}{\alpha})^2} & \text{for } \overline{d} \leq 1 \\ 0 & \text{for } \overline{d} > 1, \end{cases} \tag{1.2.6}
$$

the cubic spline weight function

$$
W(\overline{d}) = \begin{cases} \frac{2}{3} - 4\overline{d}^2 + 4\overline{d}^3 & \text{for } \overline{d} \leq \frac{1}{2} \\ \frac{4}{3} - 4\overline{d} + 4\overline{d}^2 - \frac{4}{3}\overline{d}^3 & \text{for } \frac{1}{2} < \overline{d} \leq 1 \\ 0 & \text{for } \overline{d} > 1, \end{cases} \tag{1.2.7}
$$

and the quartic spline weight function

$$
W(\overline{d}) = \begin{cases} 1 - 6\overline{d}^2 + 8\overline{d}^3 - 3\overline{d}^4 & \text{for } \frac{1}{2} < \overline{d} \leq 1 \\ 0 & \text{for } \overline{d} > 1. \end{cases} \tag{1.2.8}
$$

In SPH methods, the following weight function is often used (for 1-D problems):

$$
W(\overline{d}) = \frac{2}{3h} \begin{cases} 1 - \frac{2}{3}\overline{d}^2 + \frac{3}{4}\overline{d}^3 & \text{for } \overline{d} \leq 1 \\ \frac{1}{4}(2-\overline{d})^3 & \text{for } 1 < \overline{d} < 2 \\ 0 & \text{for } \overline{d} \geq 2, \end{cases} \tag{1.2.9}
$$

where α is constant, $\overline{d} = d/h$ and h is the smoothing length.

The idea in SPH is to obtain a simple formula for $u^h(x)$ in terms of nodal values $u_I \equiv u(x_I),\ I = 1$ to n_N. The most straightforward quadrature approaches are usually used. For example, in one dimension, the quadrature can be performed by the trapezoidal rule, which gives

$$u^h(x) = \sum_I W(x - x_I) u_I \Delta x_I, \tag{1.2.10}$$

for a sequentially numbered set of nodes x_I. For interior nodes, Δx_I is

$$\Delta x_I = (x_{I+1} - x_{I-1})/2. \tag{1.2.11}$$

On the left end,

$$\Delta x_{n_N - 1} = (x_{I+1} - x_b)/2, \tag{1.2.12}$$

where x_b is coordinate of the left boundary, with a similar expression on the right. The sum needs to be taken only over the point x_I where $w(x - x_I) > 0$.

In multi-dimensions, the quadrature is more difficult to come to the grips with. Generally, formulas of the type

$$u^h(x) = \sum_I W(x - x_I) u_I \Delta V_I, \tag{1.2.13}$$

are used, where ΔV_I represents the volume of node I.

Equation (1.2.13) can be written in the following form

$$u^h = \sum_I \phi_I(x) u_I, \tag{1.2.14}$$

where $\phi_I(x)$ are the SPH shape functions given by

$$\phi_I(x) = W(x - x_I)\Delta V_I. \tag{1.2.15}$$

Moving Least-Squares Approach [6]: In this approach, we let $u(x)$ be the function of a field variable defined in the domain Ω. The approximation of $u(x)$ at point x is denoted as $u^h(x)$. The Moving Least-Squares (MLS) approximates the field function in the form of series representation

$$u^h(x) = \sum_{j=1}^{m} p_j(x)a_j(x) \equiv \mathbf{P^T}(\mathbf{x})\mathbf{a}(\mathbf{x}), \tag{1.2.16}$$

where m is the number of terms of monomials (polynomial basis), $p_i(x)$ are monomial basis functions, and $\mathbf{a}(x)$ is a vector of coefficients given by

$$\mathbf{a}(\mathbf{x}) = [a_0(x)\ ,\ a_1(x)\ ,\ \cdots\ ,\ a_m(x)]^T, \tag{1.2.17}$$

which are functions of x.

In 1D space, a complete polynomial basis of order m is given by

$$\mathbf{P}(\mathbf{x}) = [P_0(x), P_1(x), \cdots, P_m(x)]^T = [1, x, x^2, \cdots, x^m], \tag{1.2.18}$$

whereas in 2D space, it is given by

$$\mathbf{P}(\mathbf{x}) = \mathbf{P}(x, y) = [1, x, y, xy, x^2, y^2, \cdots, x^m, y^m]^T, \tag{1.2.19}$$

Assuming the support domain of x contains a set of n local nodes $x_1, x_2, \cdots, x_n$, equation (1.2.16) is then used to calculate the approximated values of the field function at the nodes

$$u^h(x, x_I) = P^T(x_I)a(x), \quad I = 1, 2, \cdots, n. \tag{1.2.20}$$

A functional of weighted residual is then constructed using the approximated values of the field function and the nodal parameters $u_I = u(x_I)$ as

$$
\begin{aligned}
J &= \sum_{I}^{n} W(x-x_I)[u^h(x,x_I) - u(x_I)]^2 && (1.2.21)\\
&= \sum_{I}^{n} W(x-x_I)[P^T(x_I)a(x) - u(x_I)]^2, && (1.2.22)
\end{aligned}
$$

where $W(x-x_I)$ is a weight function, and u_I is the nodal parameter of the field variable at node I with compact support the same weight functions as in SPH are used.

Equation (1.2.22) can be rewritten in the form

$$J = (Pa-u)^T W(x)(Pa-u), \tag{1.2.23}$$

where

$$u = [u_1, u_2, \cdots u_n]^T, \tag{1.2.24}$$

$$P = \begin{bmatrix} p_1(x_1) & p_2(x_1) & \dots & p_m(x_1) \\ p_1(x_2) & p_2(x_2) & \dots & p_m(x_2) \\ \vdots & \vdots & \ddots & \vdots \\ p_1(x_n) & p_2(x_n) & \dots & p_m(x_n) \end{bmatrix} \tag{1.2.25}$$

and

$$W(x) = \begin{bmatrix} W(x-x_1) & 0 & \dots & 0 \\ 0 & W(x-x_1) & \dots & 0 \\ \vdots & \vdots & \ddots & \vdots \\ 0 & 0 & \dots & W(x-x_1) \end{bmatrix}. \tag{1.2.26}$$

To find the coefficients $\mathbf{a}(x)$, we obtain the extremum of J by

$$\frac{\partial J}{\partial a} = A(x)\mathbf{a}(x) - B(x)u = 0, \tag{1.2.27}$$

where A is called the moment matrix and is given by

$$A(x) = P^T W(x) P. \tag{1.2.28}$$

Also

$$B(x) = P^T W(x). \tag{1.2.29}$$

Therefore, we have

$$\mathbf{a}(x) = A^{-1}(x) B(x) u. \tag{1.2.30}$$

The approximation $u^h(x)$ can then be expressed as

$$u^h(x) = \sum_{I=1}^{n} \phi_I^k(x) u_I, \tag{1.2.31}$$

where the shape functions are given by

$$\Phi^k = [\phi_1^k(x) \cdots \phi_n^k(x)] = P^T(x) A^{-1}(x) B(x), \tag{1.2.32}$$

where k is the order of the polynomial basis.

Point Interpolation Method [67]: In this approach, a function $u(x)$ is defined in the problem domain Ω with a number of scattered field nodes. For a point of interest x_Q, the field function $u(x)$ is approximated using the following series representation:

$$u^h(x, x_Q) = \sum_{i=1}^{n} B_i(x) a_i(x_Q), \tag{1.2.33}$$

where $B_i(x)$ are the basis functions, n is the number of nodes in support domain of a given point x_Q, and $a_i(x_Q)$ is a coefficient for the basis function $B_i(x)$ corresponding to the given point x_Q.

The Point Interpolation Method (PIM) obtains its approximation by letting the interpolation function passing through the function values at each scattered node.

The formulation of polynomial PIM starts with the following representation:

$$u^h(x, x_Q) = \sum_{i=1}^{n} p_i(x) a_i(x_Q) = P(x) a(x_Q), \tag{1.2.34}$$

where $p_i(x)$ is the basis function of monomials, n is the number of nodes in support domain of a given point x_Q, and $a_i(x_Q)$ is a coefficient for the monomial $p_i(x)$ corresponding to the given point x_Q. The vector $\mathbf{a}$ is defined as

$$\mathbf{a}(x_Q) = [a_1, a_2, a_3, \cdots, a_n]^T. \tag{1.2.35}$$

The coefficients a_i in equation (1.2.34) can be determined by enforcing that equation (1.2.34) be satisfied at the n nodes in support domain of point x_Q. At node i we can have equation

$$u_i = P^T(x_i) a_i, \quad i = 1 \text{ to } n, \tag{1.2.36}$$

where u_i is the nodal value of u at $x = x_i$.

Equation (1.2.36) can be written in the matrix form

$$U_s = P_Q a, \tag{1.2.37}$$

where U_s is the vector that collects the values of field variables at all the n nodes in the support domain:

$$U_s = [u_1, u_2, \cdots, u_n]^T, \tag{1.2.38}$$

and P_Q is called the moment matrix given by

$$P_Q = [P^T(x_1), P^T(x_2), \cdots, P^T(x_n)]^T. \tag{1.2.39}$$

Using equation (1.2.37) and assuming that the inverse of the moment matrix P_Q exists, we can have

$$a = P_Q^{-1} U_s. \tag{1.2.40}$$

Substituting equation (1.2.40) into equation (1.2.34), we obtain

$$u^h(x) = \sum_{i=1}^{n} \phi_i(x) u_i, \tag{1.2.41}$$

or in matrix form

$$u^h(x) = \mathbf{\Phi}(x)\mathbf{U}_s, \tag{1.2.42}$$

where $\mathbf{\Phi}(x)$ is a matrix of PIM shape functions ϕ_i defined by

$$\mathbf{\Phi}(x) = P^T(x) P_Q^{-1} = [\phi_1, \phi_2, \phi_3, \cdots, \phi_n]. \tag{1.2.43}$$

1.2.2 Radial basis functions

A radial basis function [67] interpolant takes the form

$$u^h(x) = \sum_{i=1}^{n} R_i(x) a_i = \mathbf{R}^T \mathbf{a}, \tag{1.2.44}$$

where $\mathbf{a}$ is a vector of unknown constants, and $\mathbf{R}_i$ is i-th radial basis functions.

There are two kinds of radial basis functions: the piecewise smooth and the infinitely smooth radial functions. For the infinitely smooth radial basis functions, we have a shape parameter, c. The closer this parameter is to 0, the flatter the radial function becomes. Table 1.2.1 contains a list of most widely used radial basis functions whereas Figure 1.2.1 shows the surface of some of these functions. The specific radial basis functions that will be used in the thesis are indicated in individual chapters.

The vectors of coefficients $\mathbf{a}$ in equation (1.2.44) are determined by enforcing interpolation passing through all the n local support nodes selected by means of support domain. The interpolation has the form

$$\mathbf{d}_s = \mathbf{R}\mathbf{a}, \tag{1.2.45}$$

where $\mathbf{d}_s$ is the vector that collects all the field nodal variables at the n local nodes and $\mathbf{R}$ is the moment matrix of RBF expressed as

$$\mathbf{R} = \begin{bmatrix} R_1(r_1) & R_2(r_1) & \dots & R_n(r_1) \\ R_1(r_2) & R_2(r_2) & \dots & R_n(r_2) \\ \vdots & \vdots & \ddots & \vdots \\ R_1(r_n) & R_2(r_n) & \dots & R_n(r_n) \end{bmatrix}, \tag{1.2.46}$$

where

$$r_k = [(x_k - x_i)^2 + (y_k - y_i)^2]^{1/2}. \tag{1.2.47}$$

Because the distance is directionless, we have

$$R_i(r_j) = R_j(r_i). \tag{1.2.48}$$

Therefore, the moment matrix $\mathbf{R}$ is symmetric. This symmetry property of $\mathbf{R}$ hints that $\mathbf{R}$ will likely be symmetric positive definite (SPD), and hence invertible. It is indeed proven true [109]. A unique solution for vectors of coefficients $\mathbf{a}$ can then be obtained if the inverse of $\mathbf{R}$ exists

$$\mathbf{a} = \mathbf{R}^{-1}\mathbf{d}_s. \tag{1.2.49}$$

Substituting equation (1.2.53) into equation (1.2.44) leads to

$$u^h(x) = \mathbf{R}^T\mathbf{R}^{-1}\mathbf{d}_s = \phi(x)\mathbf{d}_s, \tag{1.2.50}$$

where the matrix of shape functions has the form

$$\boldsymbol{\Phi}(x) = [R_1(x), R_2(x), \cdots, R_n(x)]\mathbf{R}^{-1} \tag{1.2.51}$$

$$= [\phi_1(x), \phi_2(x), \cdots, \phi_n(x)], \tag{1.2.52}$$

in which $\phi_k(x)$ is the shape function for the k^{th} node and is given by

$$\phi_k(x) = \sum_{i=1}^{n} R_i(x) S_{ik}^a, \tag{1.2.53}$$

where S_{ik}^a is the $(i,k)^{\text{th}}$ element of matrix $\mathbf{R}^{-1}$, which is a constant matrix for given locations of the n nodes in the support domain.

Table 1.2.1: Some well-known radial basis functions used in the literature

Name of RBF	$\phi(r), r \geq 0$	Type	References
Multiquadric	$\sqrt{r^2+c^2}$	Smooth, global	Islam *et al.* [46]
Inverse multiquadric	$\frac{1}{\sqrt{r^2+c^2}}$	Smooth, global	Islam *et al.* [46]
Inverse quadratic	$\frac{1}{r^2+c^2}$	Smooth, global	Islam *et al.* [46]
Gaussian	$e^{-(cr)^2}$	Smooth, global	Fornberg and Piret [31]
Cubic	$\|r\|^3$	Piecewise smooth, global	Fornberg and Piret [31]
Thin plate spline	$r^2 \ln\|r\|$	Piecewise smooth, global	Fornberg and Piret [31]

The direct method expressed in equations (1.2.44) and (1.2.45) entails inverting the collocation matrix R in order to find the expansion coefficients, thus the RBF interpolant. We now consider the invertibility of the collocation matrices associated with the most common radial functions from the sources [28, 89] and [110]:

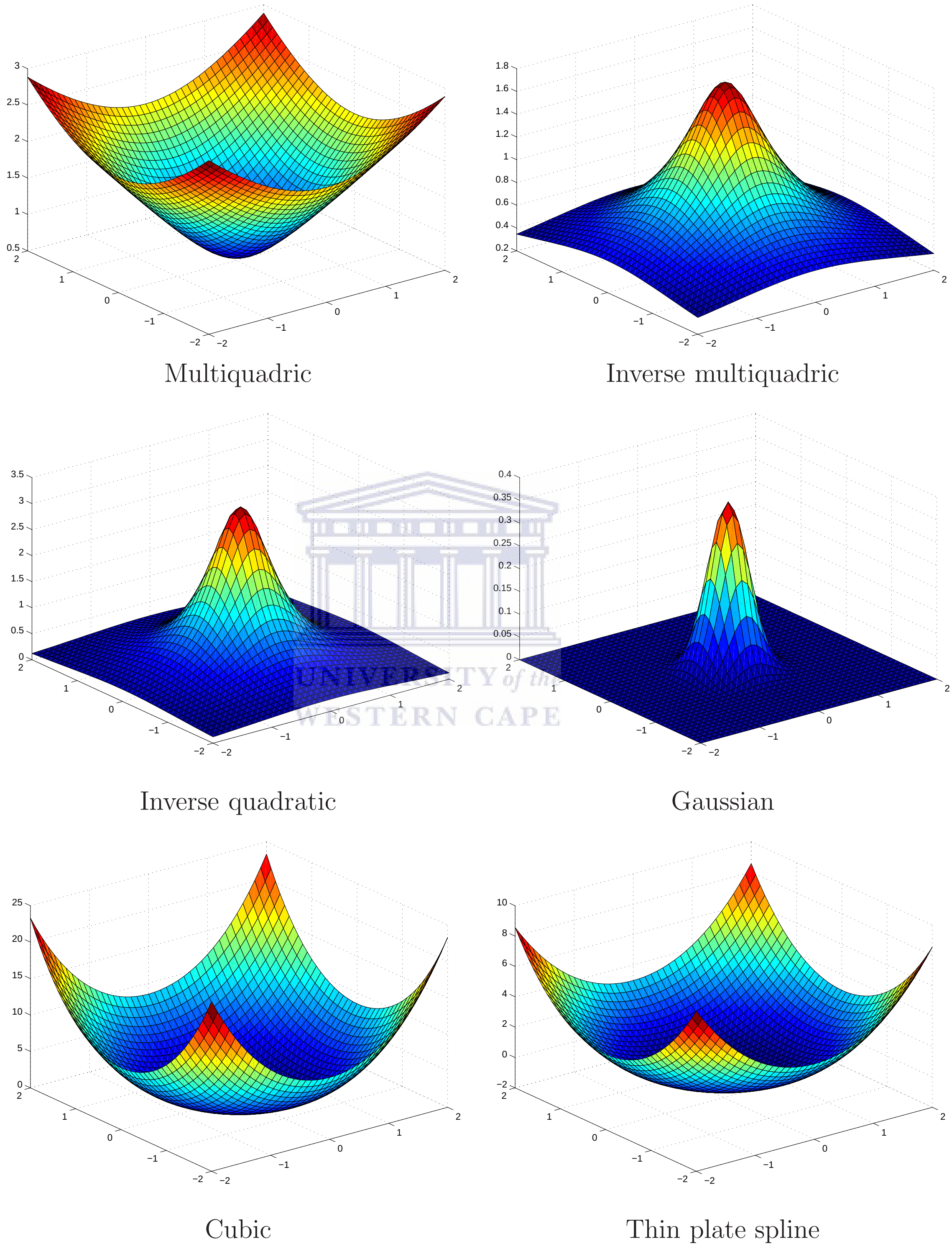

Figure 1.2.1: The most commonly used radial functions

Definition 1.2.1 Positive Definite Matrices. *A real symmetric matrix A is called strictly positive definite if its associated quadratic form is positive*

$$\sum_{j=1}^{n}\sum_{k=1}^{n} c_j c_k A_{jk} > 0, \tag{1.2.54}$$

for all non-vanishing coefficients $c \in \mathbb{R}^n$. Consequently, the eigenvalues of a positive definite matrix are all strictly positive.

Theorem 1.2.1 *Assume that d is any positive integer and that the points $x_i \in \mathbb{R}^d$, $i = 1, 2, \cdots, n$, are all distinct. If ϕ can be written in the form*

$$\phi(r) = \int_0^{\infty} e^{-\alpha r^2} w(\alpha) d\alpha, \tag{1.2.55}$$

where $w(\alpha) \geq 0$ for $\alpha \geq 0$ and $\int_\delta^\infty w(\alpha)d\alpha > 0$ for some $\delta > 0$, then the collocation matrix A with entries $A_{i,j} = \phi(x_i - x_j)$ is positive definite.

Definition 1.2.2 Completely monotonic functions. *A function $\phi(r) = \int_0^\infty e^{-\alpha r^2} w(\alpha)d\alpha$, $r \geq 0$, where $w \geq 0$ is said to be completely monotonic on $[0, \infty)$ if, when considering*

$$\psi(r) = \phi(r^{1/2}) = \int_0^{\infty} e^{-\alpha r} w(\alpha) d\alpha, \tag{1.2.56}$$

- *$\psi(r) \geq 0$, and*
- *$(-1)^k \psi^{(k)}(r) \geq 0$, $r \geq 0$ for all positive integers k.*

Theorem 1.2.2 *$\phi(r)$ can be expressed as $\phi(r) = \int_0^\infty e^{-\alpha r^2} w(\alpha)d\alpha$ if and only if $\psi(r) \geq 0$, $r \geq 0$ is completely monotonic.*

Examples of completely monotonic functions:

- Gaussian: $\phi(r) = e^{-c^2 r^2}$,
- Generalized inverse multiquadric: $\phi(r) = (1 + (cr)^2)^{\beta}$, $\beta < 0$.

By virtue of the fact that these radial functions are completely monotonic, they give rise to strictly positive definite collocation matrices.

Theorem 1.2.3 *Let* $\psi(r) = \phi(r^{1/2}) \in C^0[0,\infty)$, $\psi(r) > 0$ *for* $r > 0$, *and* $\psi\prime(r)$ *completely monotone but not constant on* $(0,\infty)$. *Then, for any set of* n *distinct points* $\{x_j\}_{j=1}^n$, *the* $n\times n$ *matrix* A *with entries* $A_{i,j} = \phi(\|x_i x_j\|)$ *is non-singular. Furthermore, for* $n \geq 2$, *the matrix has* $n-1$ *negative eigenvalues and one positive eigenvalue.*

Examples of radial functions to which Theorem 1.2.3 applies:

- $\phi(r) = r$,
- $\phi(r) = (1 + (cr)^2)^{1/2}$.

So, although these radial functions do not give rise to strictly positive definite matrices, they nonetheless give rise to invertible matrices, permitting the interpolant to be uniquely solvable unconditionally via (1.2.45).

1.3 Literature review on use of mesh free methods for other problems

The work presented in this thesis is largely based on the applications of mesh free methods and therefore below we provide a little survey on the approaches that used these methods in the past.

The earliest work in mesh free methods originated about thirty years ago. However, the research efforts devoted to them until recently are miniscule. The starting point which seems to have the longest continuous history is the smooth particle hydrodynamics (SPH) method. Lucy [70] used it for modeling astrophysical phenomena without boundaries such as exploding stars and dust clouds. Compared to other methods in these times of prolific academicians, the rate of publications was very modest for many years and is mainly reflected in the work of Monaghan [76].

Probably the most widely cited pioneering work that used the RBF approach was that of Kansa [53]. He first used it for solving some problems in computational fluid dynamics. He presented a powerful, enhanced multiquadrics (MQ) scheme developed for spatial approximations for these problems. The MQ is a grid free scheme suited for scattered data and represents surfaces and bodies in an arbitrary number of dimensions. The associated multiquadratic function is continuously differentiable and integrable and is capable of representing functions with steep gradients and very high accuracy. In fact, in [54], Kansa used Multiquadric RBFs for parabolic, hyperbolic and elliptic PDEs. He showed that MQ is not only exceptionally accurate, but is more efficient than finite difference schemes which require many more operations to achieve the same degree of accuracy.

Swegle *et al.* [98] showed the origin of the so-called tensile instability through a dispersion analysis of the linearized equations and proposed a viscosity term to stabilize it.

Belytschko *et al.* [6] examined meshless approximations based on moving least squares, kernels, and partitions of unity. They showed that the three methods are in most cases identical except for the important fact that partitions of unity enable p-adaptivity to be achieved.

Johnson and Beissel [49] proposed a normalized smoothing function algorithm that can improve the accuracy of smooth particle hydrodynamics impact computations. Their approach consists of adjusting the standard smoothing functions for every node (and every cycle) such that the normal strain rates are computed exactly for conditions of constant strain rates (linear velocity distributions). This, in turn, generally improves accuracy for non-uniform strain rates and therefore significantly improves the accuracy for free boundaries, for non-uniform arrangements of SPH nodes, and for small smoothing distances.

Sharan [97] used the multiquadric (MQ) approximation scheme for the solution of elliptic partial differential equations with Dirichlet and Neumann boundary conditions. They took two-dimensional Laplace, Poisson, and biharmonic equations describing the various physical processes as the test examples.

Giinther and Liu [35] described a computational algorithm based on d'Alembert's principle that can be used for general constraints both in meshless methods and finite elements. They developed a method of partitioning meshless shape functions suitable for imposing linear boundary conditions and then extended the approach for nonlinear constraints.

Fedoseyev *et al.* [29] formulated an improved Kansa-MQ method with PDE collocation on the boundary (MQ-PDECB). They added an additional set of nodes adjacent to the boundary and, correspondingly, added an additional set of collocation equations obtained via collocation of the PDE on the boundary. They applied the MQ-PDECB method to several model 1D and 2D linear and nonlinear elliptic PDEs and have presented results of their numerical experiments.

Li *et al.* [64] developed a meshless method for modeling groundwater contaminant transport using collocation method with radial basis functions. Their numerical results are presented for several cases: pure diffusion; advection and dispersion for continuous source; advection and dispersion for instantaneous source; advection and dispersion for patch-source. They showed that from the results their method is accurate.

Gao-lian and Xiao-wei [34] proposed a new mesh free method in which the derivatives at each node were constructed using whole derivative formulas through the nodes selected around the node using local Cartesian frame in an autonomous manner. They tested the method with a numerical example, and obtained a reliable solution with high accuracy and efficiency.

Wen *et al.* [108] reproduced a mesh free method based on kernel approximation and point collocation for analysis of metal ring compression. They introduced corrected kernel functions to the stabilization of free-surface boundary conditions. The solution of symmetric ring compression problem is compared with a conventional finite element solution.

Islam *et al.* [46] presented a mesh free technique for the numerical solution of the regularized long wave (RLW) equation. They used a global collocation method using the radial basis functions (RBFs). They tested the accuracy of their method in terms of L_2 and L_∞ error norms.

Islam *et al.* [47] discussed a classical radial basis functions (RBFs) collocation (Kansa's) method for the numerical solution of the coupled Korteweg-de Vries (KdV) equations, coupled Burgers' equations, and quasi-nonlinear hyperbolic equations. They assessed the accuracy of their method in terms of the error in L_1 and L_2 norms, number of nodes in the domain of influence, time step length; and parameter free and parameter dependent RBFs. They performed numerical experiments to demonstrate the accuracy and robustness of the method for the three classes of partial differential equations (PDEs).

Kindelan *et al.* [59] introduced a radial basis function collocation method for computing solutions to the time-dependent radiative transfer equation. They used finite differences to discretize the time coordinate, a discrete ordinate method to discretize the directional variable, and an expansion in radial basis functions to approximate the spatial dependence of the solution.

Tatari *et al.* [101] proposed a technique for solving partial differential equations using radial basis functions. The radial basis functions are very suitable instruments for solving partial differential equations of various types. However, the matrices which result from the discretization of the equations are usually ill-conditioned especially in higher dimensional problems. They proposed a method for solving the partial differential equations and generalized to solve higher-dimensional problems.

Some mesh free methods or element free methods have been developed and achieved significant progress in recent years, such as the smooth particle hydrodynamics (SPH) [92], the element-free Galerkin (EFG) [6], the reproducing kernel particle method (RKPM) [66].

Wang and Liu [106] proposed a point interpolation meshless method based on combining radial and polynomial basis functions. The interpolation function obtained passes through all scattered points in an influence domain and thus shape functions are of delta function property. This makes the implementation of essential boundary conditions much easier than the meshless methods based on the moving least-squares approximation. In addition, the partial derivatives of shape functions are easily obtained.

In [107], Wang *et al.* proposed an algorithm to solve Biots consolidation problem using meshless method called a radial point interpolation method (radial PIM). In time domain they proposed fully implicit integration scheme to avoid spurious ripple effect. They studied some examples with structured and unstructured nodes and compared with closed-form solution or finite element method solutions.

Dai *et al.* [24] presented a mesh free model for the static and dynamic analysis of functionally graded material (FGM) plates based on the radial point interpolation method (RPIM). They studied the convergence rate and accuracy and compared with the finite element method (FEM).

The RPIM has the following advantages ([69]):

- The shape function has the Kronecker delta property, which facilitates easy treatment of the essential boundary conditions.
- The moment matrix used in constructing shape functions is always invertible for irregular nodes.
- The polynomials can be exactly reproduced up to desired order by polynomial augmentation.

Some of these properties make the RPIM as a very powerful tool when solving complex problems like those considered in this chapter as well as their possible extensions to price multi-asset options.

1.4 Literature review on methods for option pricing problems

There are two main approaches to study the problems in finance: a statistical approach and a differential equation approach. Our research is focused on the Differential Equation approach and therefore most of the literature that we present in this thesis will be based on this approach.

Two classical references for the Black-Scholes theory are the paper [7] in which Black and Scholes derive the key equation and the paper [73] by Merton which adds a rigorous mathematical analysis.

Most of the numerical methods for American options exploit the representation of the option price as expected pay-off under the risk-natural measure and calculate the price for a given time to expiration and stock price, they do not solve the related free boundary problem explicitly.

Landau [61] Wu and Kwok [113] Nielsen *et al.* [80] apply a non-linear transformation to fix the boundary and solve the resulting non-linear problem using Front-fixing methods. On the other hand, Nielsen *et al.* [80] applied penalty methods by eliminating the free-boundary and adding a non-linear penalty term to the PDE.

Friedman [32] discussed relations of the free-boundary formulation to the variational inequality formulation. The method developed in Brennan and Schwartz [9] is justified rigorously through the use of variational inequalities in Jaillet *et al.* [48].

Chiarella *et al.* [17] present a path-integral approach to price American puts by using Hermite polynomials to represent the price function for any given time, rather than by storing price values at discrete grid points (as in binomial methods and the method by Brennan and Schwartz [9]).

Zhao *et al.* [115] gave three ways of combining compact finite difference methods for American option price on a single asset with methods for dealing with this optimal exercise boundary. The first one is the compact finite difference method which uses the implicit condition that solutions of the transformed partial differential equation be nonnegative to detect the optimal exercise value. The second one is the compact finite difference method that solves an algebraic nonlinear equation obtained by Pantazopoulos [84] at every time step. The third one is the compact finite difference method that refines the free boundary value by a method developed by Adesi [3].

In [18], Chiarella *et al.* considered the problem of numerically evaluating American options under the combined stochastic volatility and jump-diffusion model of Bates [4]. They extended the method of lines solution proposed by Meyer [74] for pricing American options under jump-diffusion dynamics to allow for stochastic volatility. One of the strengths of their method is that the option price, delta, gamma, and the free boundary are all computed as part of the solution process. As a benchmark for the method of lines, they considered two finite difference schemes. The first is a standard two-dimensional Crank-Nicholson implicit scheme solved using projected successive over-relaxation (PSOR) techniques, with appropriate adjustments to deal with the integral over the jumps term. They used this algorithm with a large order of discretization as the 'true' solution for the option price. The second method they considered is a generalization of the component-wise splitting algorithm of Ikonen and Toivanen [44] to include jump-diffusion.

Muthuraman [78] presented a computational method (based on Finite Elements and Finite Difference) that efficiently solves the free-boundary problem to obtain the price function as well as the optimal exercise boundary. He showed that this method provides a monotone sequence of boundaries that converges to the optimal exercise boundary. At the end, he presented runtime and error comparisons, and compared his approach against the 10000-step binomial tree method, the method of Brennan and Schwartz [9] the front-fixing method, penalty method and the integral method. He also computed the hedge ratios using the integral method and compared it to those computed using the moving boundary method because the integral method has the advantage of being able to compute the hedge ratios (Greeks) of American option without numerical differentiation.

As far as the barrier options are concerned, we mention below some of the works:

Platen and West [90] proposed a consistent approach to the pricing of weather derivatives. They showed that the classical actuarial pricing methodology is a particular case of the fair pricing concept. They constructed a discrete time model to approximate historical weather characteristics. They derived fair prices of some particular weather derivatives by using historical and Gaussian residuals.

Khaliq *et al.* [56] developed a strongly stable (L-stable) and highly accurate method for pricing exotic options. Their method is based on Padé schemes and also utilizes partial fraction decomposition to address issues regarding accuracy and computational efficiency.

In [99], Sun *et al.* developed an algorithm to price the barrier options in the presence of proportional transaction costs. Using the optimal portfolio framework, they computed numerically barrier options prices by using a Markov chain approximation to the continuous-time singular stochastic optimal control problem when the utility function is of exponential type. As a result, they obtain two option prices which correspond the upper boundary and lower boundary of no-transaction region.

Rambeerich *et al.* [91] considered exponential time integration schemes for fast numerical pricing of European, American, barrier and butterfly options when the stock price follows a dynamics described by a jump-diffusion process. The resulting pricing equation which is in the form of a partial integro-differential equation is approximated in space using finite elements. Their methods required the computation of a single matrix exponential. They demonstrated the method using a wide range of numerical tests that the combination of exponential integrator and finite element discretizations with quadratic basis functions. They made Comparisons with other time-stepping methods to illustrate the effectiveness of their methods.

Some other works related to the European and /or American options [2, 5, 12, 13, 15, 16, 21, 27, 30, 39, 52, 55, 57, 65, 72, 75, 79, 81, 88, 87, 104, 111, 114, 115, 116], exotic options[11, 14, 22, 33, 36, 41, 43, 50, 82, 86, 93, 94, 95, 102, 105, 118] and multi-asset options [20, 40, 45, 62, 83, 88, 103, 117].

Some of the books that are dealing with various issues (including options) in financial mathematics are [8, 25, 60, 96].

It should be noted that there are many other relevant works that we are not listing here, simply because we will be focusing on them more in the individual chapters where they are reviewed further.

1.5 Outline of the thesis

We have organized the rest of this thesis as follows.

In Chapter 2, we develop efficient mesh free methods based on the radial basis functions (RBFs) to solve European and American option pricing problems in computational finance. The application of RBFs leads to system of differential equations which are then solved by a time integration scheme. This is done by using a θ-method. The main difficulty in pricing the American options lies in the fact that these options are allowed to be exercised at any time before their expiry. Such an early exercise right purchased by the holder of the option results into a free boundary problem. We use a small penalty term to remove the free boundary. The method is analyzed for stability. Numerical results describing the payoff functions and option values are also presented.

In Chapter 3, we extend the method presented in Chapter 2 to solve problems for pricing American and European put options on a dividend paying asset. The resulting method is analyzed for stability. Comparative numerical results along with evaluation of some Greeks are presented at the end.

In Chapter 4, the mesh free method is presented for pricing two type of exotic options, namely, European barrier and European Asian options. Using the RBF approximation, we obtain a system of ordinary differential equations which is then solved by a time integration technique. As compared to the work done in Goto *et al.* [36], in this chapter we provide a simplified presentation of the approach. We also analyzed the method for stability which was not done in the above mentioned work. Furthermore, the proposed approach in this chapter is extended to solve problems of pricing European style double barrier options and digital options. Finally, we present some numerical experiments using a number of radial basis functions.

In Chapter 5, we introduce a radial point interpolation method (RPIM) to price European and American put options. To resolve the difficulties associated in solving this free boundary problem in the case of American options, we add a penalty term to the governing partial differential equation. The proposed method is analyzed for stability. Some comparative numerical results are also presented.

In Chapter 6, we extend the mesh free method to price some put options of European and American type for the Heston's model [38]. In the case of American style options, we use an update procedure to solve the free boundary problem. The resulting method is analyzed for stability and comparative numerical results are presented.

Finally, in Chapter 7, we provide some concluding remarks and discuss the scope for the future research.

Before we start the next chapter, we list some of the very important notations in Table 1.5.1 that are used throughout the thesis.

Table 1.5.1: Some notations used in the thesis

Parameter	Descriptions
E	Strike price
r	Risk-free interest rate
σ	Volatility of the stock price
$V(S,t)$	Value of European option at time t
$P(S,t)$	Value of American option at time t
S	Asset (Stock) price
T	Maturity time
c	Shape function parameter
D	Dividend paying asset
K	Barrier value
ϑ	Market price of risk
ρ	Correlation between the two underlying assets
α	Mean-reversion rate
β	Long-term mean

Chapter 2

A mesh free method for pricing options on a non-dividend paying asset

In this chapter, we develop efficient mesh free methods based on the radial basis functions (RBFs) to solve European and American option pricing problems in computational finance. The application of RBFs leads to systems of differential equations which are then solved by a time integration scheme. This is done by using a θ-method. The main difficulty in pricing the American options lies in the fact that these options are allowed to be exercised at any time before their expiry. Such an early exercise right purchased by the holder of the option results into a free boundary problem. We use a small penalty term to remove the free boundary. The method is analyzed for stability. Numerical results describing the payoff functions and option values are also presented along with valuation of option's delta and gamma.

2.1 Introduction

Options are frequently priced by means of partial differential equations (PDEs). The work in this chapter deals with the standard options (European and American options).

A large amount of work has already been done to solve the PDEs representing European options. However, the same for American options is not fully explored.

Researchers have attempted to solve these problems using a variety of techniques. Fasshauer *et al.* [27] studied multi-asset American options. They considered a penalty method which allows the removal of the free and moving boundary by adding a small and continuous penalty term to the Black-Scholes equation. Zhao *et al.* [115], developed three compact finite difference methods for American options on a single asset.

Chawla *et al.* [16] described generalized trapezoidal formulas (GTF(α) schemes, α a positive parameter) for the valuation of American options and compared their performance with that of the Crank-Nicolson's scheme. They found that the Crank-Nicolson's scheme suffers oscillations near the exercise price where the payoff is either non-differentiable or discontinuous. In comparison the GTF(1/3) scheme could provide consistently superior approximations for valuation of American options.

Khaliq *et al.* [55] considered the numerical solution of American option problems using a penalty approach followed by semi-discretization of the resulting partial differential equation on a fixed domain. They used a second-order linearly implicit time stepping method to estimate option values. Their numerical results indicate that a constraint on the time step-size due to the explicit treatment of the penalty term is not more restrictive than that of the linearly implicit first-order methods.

In [57], Khaliq *et al.* developed adaptive θ-methods for solving the Black-Scholes PDE for American options.

Nielsen *et al.* [81] presented a penalty method for solving multi-asset American put option problems. They added a small nonlinear penalty term to the Black-Scholes equation to remove the free and moving boundary imposed by the early exercise feature of the contract. They derived explicit, semi-implicit and fully implicit finite difference schemes.

Liao and Khaliq [65] proposed an unconditionally stable high-order compact finite difference scheme to compute both the option price and the hedging parameter delta.

On the other hand, the methods based on mesh free approximations have been used a lot for problems in other domains of science and engineering, see e.g., [53, 54, 101]. One of these popular mesh free methods are those based on the radial basis functions (RBFs). Wua and Hon [114] used such an approximation for solving diffusion type problems under free boundary condition. In their work, the numerical solution of the Black-Scholes equation for pricing American options, which is a classical heat diffusion equation under free boundary value condition, is obtained and compared with the traditional binomial method for numerical verification.

In this work, we construct a mesh free method based on RBFs to solve European and American option pricing problems. For American put option we remove the free boundary by adding a small penalty term. The basic idea behind the use of RBFs is to use interpolation with a linear combination of basis functions of the same type. A variety of RBFs are found in the literature. The two RBFs that we will use in this chapter are Gaussian and Multi-quadratic.

The rest of the chapter is organized as follows. Two option pricing problems are described in Section 2.2. Section 2.3 deals with the application of radial basis functions to solve these problems. The stability analysis of the numerical methods is presented in Section 2.4. Finally some numerical results along with a discussion on them are given in Section 2.5.

2.2 Problem description

The options give the owner the right, but not the obligation, to buy (in the case of a call option) or sell (in the case of a put option) an asset at a specified price and time. If the owner of the contract exercises this right, the counter-party is obliged to carry out the transaction. A thorough discussion on them can be found in any standard text on financial derivatives, see, e.g., Hull [43]. In this chapter, we are considering the European and American options. A European option can only be exercised on the expiration date whereas the American option can be exercised at any time before the expiration date.

The European option satisfies the following Black-Scholes equation

$$\frac{\partial V}{\partial t} + \frac{1}{2}\sigma^2 S^2 \frac{\partial^2 V}{\partial S^2} + rS\frac{\partial V}{\partial S} - rV = 0, \tag{2.2.1}$$

where r is the risk-free interest rate, σ is the volatility of the stock price, and $V(S,t)$ is the option value at time t for the stock's price S.

The initial condition is given by the terminal payoff

$$V(S,T) = \begin{cases} \max(E - S, 0) & \text{for put} \\ \max(S - E, 0) & \text{for call} \end{cases} \tag{2.2.2}$$

and the boundary conditions are given by

$$V(S,T) = \begin{cases} V(0,t) = Ee^{-r(T-t)}, & V(S,t) \to 0 \ \text{ as } \ S \to \infty \qquad \text{for put} \\ V(0,t) = 0, & V(S,t) \to S \ \text{ as } \ S \to \infty \qquad \text{for call} \end{cases} \tag{2.2.3}$$

where T is the maturity time and E is the strike price of the option.

The exact solution of equation (2.2.1) with the initial condition (2.2.2) and the boundary conditions (2.2.3) is given by [112]

$$V(S,T) = \begin{cases} Ee^{-r(T-t)}N(-d_2) - SN(-d_1) & \text{for put} \\ SN(d_1) - Ee^{-r(T-t)}N(d_2) & \text{for call} \end{cases} \tag{2.2.4}$$

where $N(\cdot)$ is the cumulative distribution function of the standard normal distribution with

$$d_1 = \frac{\log(S/E) + (r + \frac{1}{2}\sigma^2)(T-t)}{\sigma\sqrt{T-t}} \tag{2.2.5}$$

and

$$d_2 = \frac{\log(S/E) + (r - \frac{1}{2}\sigma^2)(T-t)}{\sigma\sqrt{T-t}}. \tag{2.2.6}$$

On the other hand, the American option problem takes the form of a free-boundary problem. The early exercise constraint leads to the following model for the value $P(S,t)$ of an American put to sell the underlying asset [55]:

$$\begin{aligned}
&\frac{\partial P}{\partial t} + \frac{1}{2}\sigma^2 S^2 \frac{\partial^2 P}{\partial S^2} + rS\frac{\partial P}{\partial S} - rP = 0, \quad S > S_f(t),\ 0 \le t < T\\
&P(S,T) = \max(E - S, 0), \quad S \ge 0,\\
&\frac{\partial P}{\partial S}(S_f, t) = -1,\\
&P(S_f(t), t) = E - S_f(t),\\
&\lim_{S\to\infty} P(S,t) = 0,\\
&S_f(T) = E,\\
&P(S,t) = E - S, \quad 0 \le S < S_f(t),
\end{aligned} \tag{2.2.7}$$

where $S_f(t)$ represents the free boundary, σ is the volatility of the underlying asset, r is the risk-free interest rate, and E is the exercise price of the option. Since early exercise is permitted, the value P of the option must satisfy

$$P(S,t) \ge \max(E - S, 0), \quad S \ge 0,\ 0 \le t \le T. \tag{2.2.8}$$

In next section, we explain how the RBFs (explained in detail in Chapter 1) are used to solve the above option pricing problems.

2.3 Application of radial basis functions in pricing options

To proceed with, let us assume that $x_1, x_2, \cdots, x_N$ be a given set of distinct points in $\mathbb{R}^d,\ d \ge 1$. The basic idea behind the use of RBFs is that we interpolate the function by a linear combination of RBFs of the same type as follows

$$F(x) = \sum_{i=1}^{N} a_i \phi(\|x - x_i\|), \tag{2.3.1}$$

where $\|.\|$ denotes the Euclidean norm, a_i are unknown scalars and ϕ denotes the radial basis function.

Assume that we want to interpolate the given values $f_i = f(x_i)$, $i = 1, \cdots, N$. The unknown scalars a_i are chosen in such a way that $F(x_j) = f_j$ for $j = 1, \cdots, N$. This results in the following linear system of equations

$$A\mathbf{z} = \mathbf{f}, \tag{2.3.2}$$

where $A_{i,j} = \phi(\|x_i - x_j\|)$, $\mathbf{z} = [a_1, \cdots, a_N]$ and $\mathbf{f} = [f_1, \cdots, f_N]$.

We apply this procedure to the two option pricing problems mentioned in the previous section.

2.3.1 Pricing European options on a non-dividend paying asset

We approximate the unknown function V (the value of the European option) using the radial basis functions as

$$V(S,t) \approx \sum_{j=1}^{N} a_j(t)\phi(\|S - x_j\|), \tag{2.3.3}$$

where a_j are unknown coefficients and $\phi(\|S - x_j\|)$ are the RBFs. We will use the following Gaussian radial basis functions for this problem

$$\phi(S) = e^{-\|S - x_j\|^2/c^2}, \tag{2.3.4}$$

where c is a positive parameter.

Collocating at the N points x_j $(j = 1, 2, \cdots, N)$, equation (2.2.1) becomes

$$\frac{\partial V(x_i,t)}{\partial t} + \frac{1}{2}\sigma^2 S_i^2 \frac{\partial^2 V(x_i,t)}{\partial S^2} + rS_i \frac{\partial V(x_i,t)}{\partial S} - rV(x_i,t) = 0. \tag{2.3.5}$$

Differentiating (2.3.3) we get

$$\frac{\partial V(x_i,t)}{\partial t} = \sum_{j=1}^{N} \frac{da_j(t)}{dt}\phi(\|S-x_j\|), \tag{2.3.6}$$

$$\frac{\partial V(x_i,t)}{\partial S} = \sum_{j=1}^{N} a_j \frac{\partial \phi(\|S-x_j\|)}{\partial S}, \tag{2.3.7}$$

$$\frac{\partial^2 V(x_i,t)}{\partial S^2} = \sum_{j=1}^{N} a_j \frac{\partial^2 \phi(\|S-x_j\|)}{\partial S^2}. \tag{2.3.8}$$

Now from (2.3.4) we have

$$\frac{\partial \phi(\|S-x_j\|)}{\partial S} = -\frac{2(S-x_j)}{c^2} e^{-\|S-x_j\|^2/c^2} \tag{2.3.9}$$

and

$$\frac{\partial^2 \phi(\|S-x_j\|)}{\partial S^2} = \frac{4(S-x_j)^2-2c^2}{c^4} e^{-\|S-x_j\|^2/c^2}. \tag{2.3.10}$$

Substituting equations (2.3.6)-(2.3.10) into (2.3.5), we obtain

$$\sum_{j=1}^{N} \frac{d}{dt}(a_j(t))\phi(\|x_i-x_j\|) + \frac{1}{2}\sigma^2 x_i^2 \sum_{j=1}^{N} a_j(t)\left[\frac{4(x_i-x_j)^2-2c^2}{c^4}\phi(\|x_i-x_j\|)\right]$$
$$+rx_i \sum_{j=1}^{N} a_j(t)\left[\frac{-2(x_i-x_j)}{c^2}\phi(\|x_i-x_j\|)\right] - r\sum_{j=1}^{N} a_j(t)\phi(\|x_i-x_j\|) = 0. \tag{2.3.11}$$

We write equation (2.3.11) in form of a system of differential equations as

$$\Phi \frac{d\mathbf{a}}{dt} + \mathbf{R}\mathbf{a} = 0, \tag{2.3.12}$$

where

$$\Phi_{ij} = e^{-\|x_i-x_j\|^2/c^2} \tag{2.3.13}$$

and

$$\mathbf{R}_{ij} = \frac{1}{2}\sigma^2 x_i^2 \left(\frac{4(x_i - x_j)^2 - 2c^2}{c^4}\right)\Phi_{ij} + r x_i \left(\frac{-2(x_i - x_j)}{c^2}\right)\Phi_{ij} - r\Phi_{ij}. \qquad (2.3.14)$$

To solve the system described by equation (2.3.12), we use a θ-method

$$\Phi\frac{\mathbf{a}^{n+1} - \mathbf{a}^n}{\Delta t} + \theta R\mathbf{a}^{n+1} + (1-\theta)R\mathbf{a}^n = 0, \qquad (2.3.15)$$

with the initial condition given by the first part of equation (2.2.2) and boundary conditions given by the first part of equation (2.2.3).

We can rewrite equation (2.3.15) as

$$[\Phi - (1-\theta)\Delta t\mathbf{R}]a^n = [\Phi + \theta\Delta t\mathbf{R}]a^{n+1}, \qquad (2.3.16)$$

$$a^n = [\Phi - (1-\theta)\Delta t\mathbf{R}]^{-1}[\Phi + \theta\Delta t\mathbf{R}]a^{n+1}. \qquad (2.3.17)$$

Equation (2.3.3) applied at all collocation points can be written in the matrix form as

$$\mathbf{V} = \Phi\mathbf{a}. \qquad (2.3.18)$$

Using equation (2.3.18), equation (2.3.17) can be written as

$$V^n = \Phi[\Phi - (1-\theta)\Delta t\mathbf{R}]^{-1}[\Phi + \theta\Delta t\mathbf{R}]\Phi^{-1}V^{n+1}. \qquad (2.3.19)$$

The above equation is solved along with (2.2.2) and the first part of equation (2.3.3) to obtain the numerical solution. Also the form of this equation should be read in context to the computing process because in the problems like those considered in this chapter, we usually have a final boundary value problem rather than an initial boundary value problem. To this end, note that the scheme given by (2.3.16) corresponding to $\theta = 0,\ 0.5,$ and 1 are the implicit Euler, Crank-Nicolson and explicit Euler methods, respectively.

2.3.2 Pricing American options on a non-dividend paying asset

To solve the American option problem (2.2.7), which is a free boundary problem, we approximate the model by adding a penalty term. This leads to a nonlinear partial differential equation on a fixed domain.

We consider the initial-boundary value problem

$$\frac{\partial P_\epsilon}{\partial t} + \frac{1}{2}\sigma^2 S^2 \frac{\partial^2 P_\epsilon}{\partial S^2} + rS\frac{\partial P_\epsilon}{\partial S} - rP_\epsilon + \frac{\epsilon C}{P_\epsilon + \epsilon - q(S)} = 0, \tag{2.3.20}$$

with the initial condition as the first part of equation (2.2.2), and the boundary conditions as

$$P_\epsilon(0,t) = E, \qquad \lim_{S\to\infty} P_\epsilon(S,t) = 0, \tag{2.3.21}$$

where $C \geq rE$, $q(S) = E - S$, and $0 < \epsilon \ll 1$.

Using Multiquadric radial basis functions (mentioned in Table 1.2.1) we find

$$\frac{\partial \phi(S - x_j)}{\partial S} = \frac{(S - x_j)}{\sqrt{(S - x_j)^2 + c^2}} \tag{2.3.22}$$

and

$$\frac{\partial^2 \phi(x_i - x_j)}{\partial S^2} = \frac{c^2}{\sqrt{((x_i - x_j)^2 + c^2)^3}}. \tag{2.3.23}$$

By inserting equations (2.3.3), (2.3.6)-(2.3.8), (2.3.22) and (2.3.23) into equation (2.3.20) we get

$$\begin{aligned}
&\sum_{j=1}^{N} \frac{d}{dt}(a_j(t))\phi(x_i - x_j) + \frac{1}{2}\sigma^2 x_i^2 \sum_{j=1}^{N} a_j(t)\left[\frac{c^2}{\sqrt{((x_i - x_j)^2 + c^2)^3}}\right] \\
&+ r x_i \sum_{j=1}^{N} a_j(t)\left[\frac{(x_i - x_j)}{\sqrt{(x_i - x_j)^2 + c^2}}\right] - r\sum_{j=1}^{N} a_j(t)\phi(x_i - x_j) \\
&+ \frac{\epsilon C}{\sum_{j=1}^{N} a_j(t)\phi(x_i - x_j) + \epsilon - q(S)} = 0.
\end{aligned} \tag{2.3.24}$$

We write equation (2.3.24) in the form of a system of differential equations

$$\Phi \frac{d\mathbf{a}}{dt} + \mathbf{R}\mathbf{a} + Q(\mathbf{a}) = 0, \tag{2.3.25}$$

where

$$\Phi_{ij} = \sqrt{(x_i - x_j)^2 + c^2}, \quad i, j = 1, \cdots, N, \tag{2.3.26}$$

$$Q(\mathbf{a}) = \frac{\epsilon C}{\Phi_i \mathbf{a} + \epsilon - q(x_i)}, \quad i = 1, \cdots, N$$

with Φ_i denoting the i-th row of the matrix Φ and

$$\mathbf{R}_{ij} = \frac{1}{2}\sigma^2 x_i^2 \left(\frac{c^2}{\sqrt{((x_i - x_j)^2 + c^2)^3}} \right) + r x_i \left(\frac{(x_i - x_j)}{\sqrt{(x_i - x_j)^2 + c^2}} \right) - r\Phi_{ij}. \tag{2.3.27}$$

Using θ-method, equation (2.3.25) becomes

$$\Phi \frac{\mathbf{a}^{n+1} - \mathbf{a}^n}{\Delta t} + \theta R \mathbf{a}^{n+1} + (1-\theta) R \mathbf{a}^n + \theta Q(\mathbf{a}^{n+1}) + (1-\theta) Q(\mathbf{a}^n) = 0. \tag{2.3.28}$$

Consequently, the nonlinear penalty term gives rise to a nonlinear system of equations whose solution is typically found by a modified Newton method. However, by replacing a^n in the penalty term by a^{n+1}(as in [55]), the linearly implicit scheme corresponding to equation (2.3.28) is given by

$$\Phi \frac{\mathbf{a}^{n+1} - \mathbf{a}^n}{\Delta t} + \theta R \mathbf{a}^{n+1} + (1-\theta) \mathbf{R}\mathbf{a}^n + Q(\mathbf{a}^{n+1}) = 0, \tag{2.3.29}$$

with the initial condition given by the first part of equation (2.2.2) and boundary conditions given by equation (2.2.3).

2.4 Stability analysis of the numerical method

To proceed with the stability analysis, let us define the error at the n^{th} time level by

$$e^n = V^n_{\text{exact}} - V^n_{\text{app}}, \tag{2.4.1}$$

where V^n_{exact} is the exact solution and V^n_{app} is the numerical solution obtained by either (2.3.15) or (2.3.29).

For the scheme given by (2.3.15) the error equation at $(n+1)^{th}$ level can be written as

$$e^n = Be^{n+1}, \tag{2.4.2}$$

where B is the amplification matrix given by

$$B = \Phi^{-1}[\Phi + \theta\Delta tR][\Phi - (1-\theta)\Delta tR]^{-1}\Phi.$$

The numerical scheme is stable if $\rho(B) \leq 1$, where $\rho(B)$ is the spectral radius of B. Substituting B in equation (2.4.2) and simplifying, we obtain

$$[\Phi - (1-\theta)\Delta t\mathbf{R}]\Phi^{-1}e^n = [\Phi + \theta\Delta t\mathbf{R}]\Phi^{-1}e^{n+1}. \tag{2.4.3}$$

This implies

$$[I - (1-\theta)\Delta tM]e^n = [I + \theta\Delta tM]e^{n+1} \tag{2.4.4}$$

where $M = R\Phi^{-1}$ and $I \in \mathbb{R}^{N\times N}$ is the identity matrix.

It is clear from equation (2.4.4) that the numerical scheme is stable if all the eigenvalues of the matrix $[I - (1-\theta)\Delta tM]^{-1}[I + \theta\Delta tM]$ are less than unity, which means that

$$\left| \frac{1 + \theta\Delta t\lambda_M}{1 - (1-\theta)\Delta t\lambda_M} \right| \leq 1, \tag{2.4.5}$$

where λ_M represent the eigenvalues of the matrix M.

Now we consider different cases. Firstly, when $\theta = 1$, we have explicit Euler method.

The above condition for stability becomes

$$|1 + \Delta t \lambda_M| \leq 1, \tag{2.4.6}$$

which upon simplification implies that the explicit Euler method will be stable if

$$\Delta t \geq \frac{-2}{\lambda_M} \quad \text{and} \quad \lambda_M \leq 0. \tag{2.4.7}$$

Secondly, when $\theta = 0$, we have implicit Euler method which is unconditionally stable as can be seen from (2.4.5) because $\lambda_M \leq 0$. Finally, when $\theta = 0.5$, we have the Crank-Nicholson's method. Even in this case, the inequality (2.4.5) will hold as long as $\lambda_M \leq 0$ and this does happen. Therefore the Crank-Nicholson's method is unconditionally stable. The stability analysis for (2.3.29) can be done along the similar lines.

2.5 Numerical results and discussion

Using the RBF approach, the resulting problems for European and American put options on a non-dividend paying asset are solved via Crank-Nicolson's method (i.e., $\theta = 0.5$) with $\Delta t = 0.01$. Results are presented in Table 2.5.1.

The parameters used for the simulations for European put option problem are: $r = 0.05,\ \sigma = 0.2,\ D = 0,\ E = 10,\ t_0 = 0,\ T = 0.5,\ S_0 = 0$ and $S_{max} = 30$. We have set the parameter c in the radial basis function as $2h$ where $h = (S_{max} - S_0)/(N-1)$. The first column in this table represents values of the asset price S, the second column represents the exact solution and the other three columns indicated the numerical values of the European put option that we obtain using the radial basis function approach with 21, 41 and 101 nodes, respectively.

For the American put options, we choose $r = 0.1,\ \sigma = 0.2,\ D = 0,\ E = 1,\ t_0 = 0,\ T = 1, \epsilon = 0.01,\ S_0 = 0,$ and $S_{max} = 2$. We again use the Crank-Nicolson method with $\Delta t = 0.01$. Using the multiquadratic radial basis function $\sqrt{r^2 + c^2}$, we obtain reasonably accurate results in the sense that they are very close to those obtained by

Fasshauer in [27]. This can be seen from Table 2.5.2. In Table 2.5.3 and Table 2.5.4,

Table 2.5.1: Values of European put option using radial basis functions on a non-dividend paying asset

S	Exact	RBF21	RBF41	RBF101
2	7.7531	7.7525	7.7533	7.7531
4	5.7531	5.7533	5.7533	5.7531
6	3.7532	3.7528	3.7529	3.7532
7	2.7568	2.7659	2.7594	2.7572
8	1.7987	1.8510	1.8080	1.8003
9	0.9880	1.0079	0.9908	0.9886
10	0.4420	0.5280	0.4628	0.4454
11	0.1606	0.2087	0.1754	0.1629
12	0.0483	0.0499	0.0504	0.0486
13	0.0124	0.0206	0.0147	0.0127
14	0.0028	0.0040	0.0035	0.0029
15	0.0006	0.0003	0.0006	0.0006
16	0.0001	0.0002	0.0001	0.0001

RBF21: radial basis functions with 21 nodes.

RBF41: radial basis functions with 41 nodes.

RBF101: radial basis functions with 101 nodes.

Table 2.5.2: Values of American put option using radial basis functions on a non-dividend paying asset

S	RBF21	RBF41	RBF101
0.6	4.00E-01	4.00E-01	4.00E-01
0.7	3.00E-01	3.00E-01	3.00E-01
0.8	2.02E-01	2.02E-01	2.02E-01
0.9	1.17E-01	1.17E-01	1.17E-01
1.0	5.97E-02	6.02E-02	6.03E-02
1.1	2.88E-02	2.92E-02	2.93E-02
1.2	1.37E-02	1.40E-02	1.41E-02
1.3	6.75E-03	7.02E-03	7.22E-03
1.4	3.62E-03	3.91E-03	4.25E-03

RBF21: radial basis functions with 21 nodes.

RBF41: radial basis functions with 41 nodes.

RBF101: radial basis functions with 101 nodes.

we tabulate the mean errors and root mean square errors (RMSE).

Table 2.5.3: Mean and RMS Errors for European put options for difference values of N with $\Delta t = 0.01$

N	Mean error	RMSE
21	1.76E-02	3.14E-02
41	4.30E-03	9.90E-03
61	1.60E-03	4.20E-03
81	1.10E-03	2.30E-03
101	7.05E-04	1.60E-03
121	4.08E-04	1.10E-03
141	3.69E-04	8.60E-04

Table 2.5.4: Mean and RMS Errors for European put options for difference values of Δt with $N = 101$

Δt	Mean error	RMSE
0.1	8.28E-04	1.80E-03
0.01	7.05E-04	1.60E-03
0.001	7.05E-04	1.60E-03
0.0001	7.05E-04	1.60E-03

Finally, figures 2.5.1, 2.5.2 and 2.5.3 depict some special cases for European and American options as indicated in the figure captions.

The accuracy of the mesh free methods solution depends on the choice of the shape parameter c. The choice of the optimal value of this parameter is still an open problem (see [31], [67]). Many researchers chose it as $c = 2h$, where $h = (S_{max} - S_0)/(N - 1)$. However, we have done some numerical simulations to find the appropriate value of this parameter. We plot the values of the shape parameter versus max-error in order for us to determine the optimal value of this shape parameter. From Figure 2.5.4 we found that the optimal value of shape parameters using Gaussian RBFs is in the approximately of 0.79.

Since the radial basis functions are infinitely differentiable, the computations of the derivatives of the options values are readily available from the derivatives of the basis functions. Then using equation (2.3.7) we can calculate the value of the delta of an option, which is the rate of change of the option value with respect to the asset price.

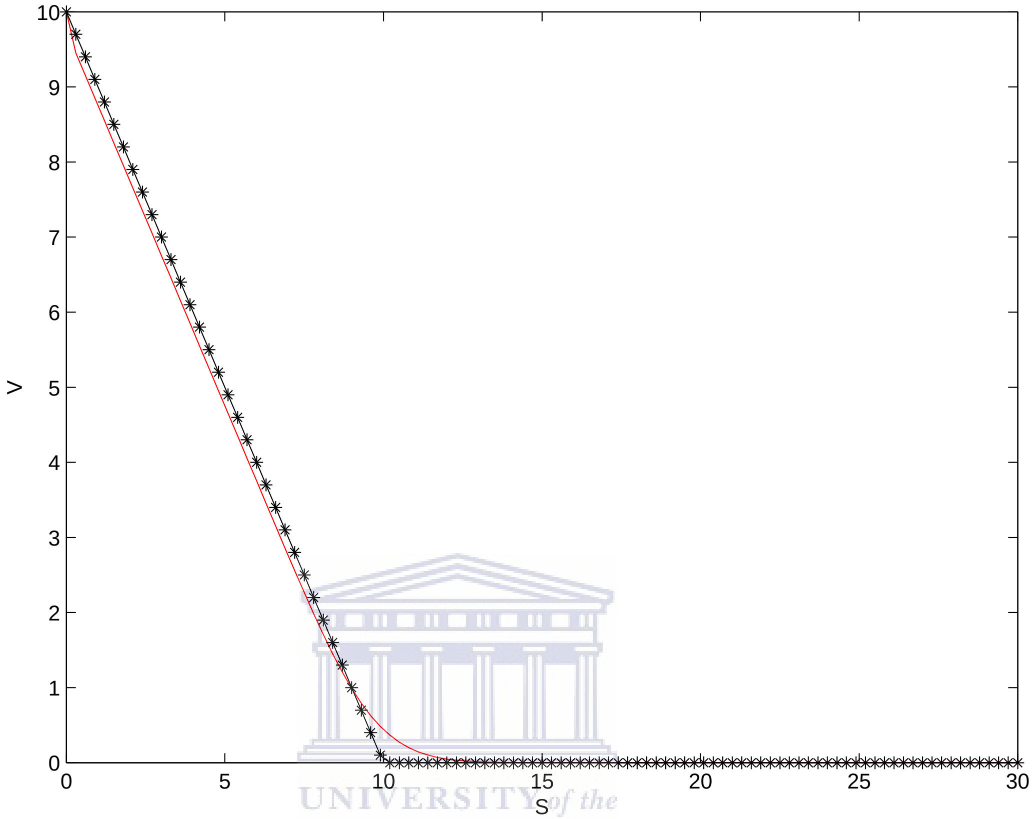

Figure 2.5.1: Values of the European put on a non-dividend paying asset at t_0 using 101 points and $r = 0.05,\ \sigma = 0.2,\ E = 10,\ t_0 = 0,\ T = 0.5,\ S_0 = 0$ and $S_{\max} = 30$. The curve with '*' shows payoff whereas the solid curve represents the value of the option

Table 2.5.5 and Table 2.5.6 give the values of delta for European and American put options using radial point interpolation method. It is clear from the results presented in these tables that the numerical values of the option's delta lie between -1 and 0 which is in agreement with what is mentioned in Hull [43]. Furthermore, in Table 2.5.7 we compare the option's delta for American put with some other works seen in the literature and found that our results are comparable with those obtained by others. Figure 2.5.5 shows the values of European delta put option using radial point interpolation method.

We also calculate the gamma (Γ) of a portfolio of options on an underlying asset which is the rate of change of the portfolio's delta with respect to the price of the

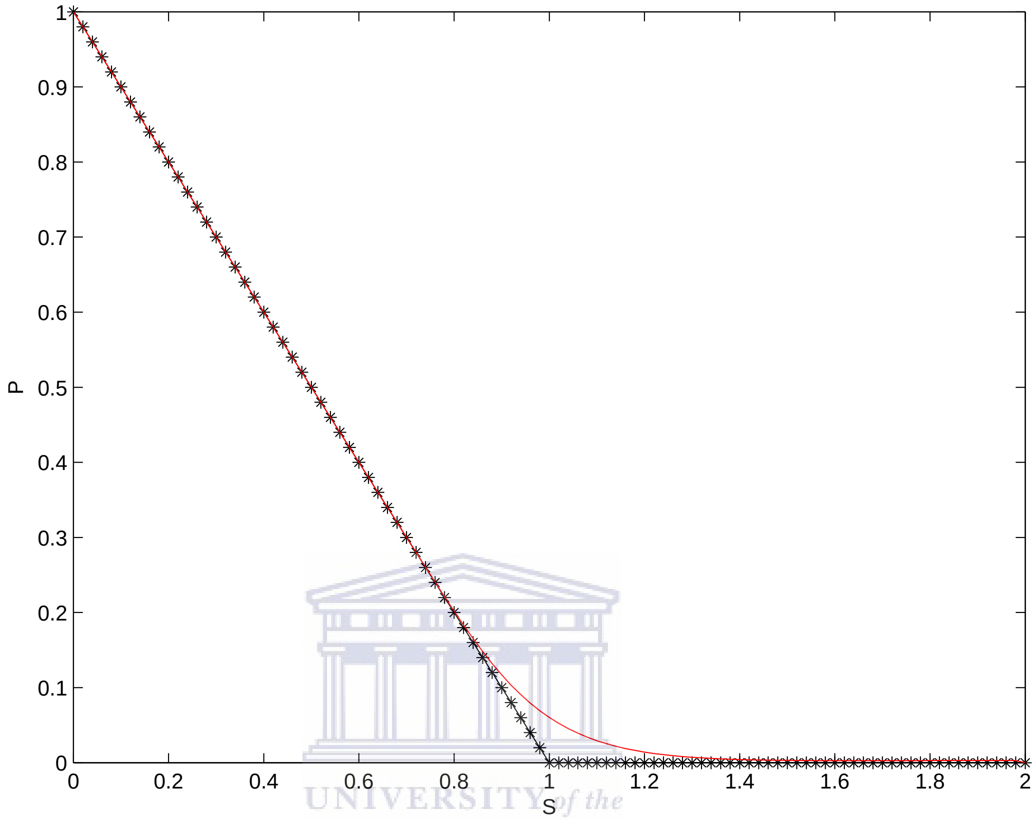

Figure 2.5.2: Values of an American put on a non-dividend paying asset at t_0 using 101 points and $r = 0.1, \sigma = 0.2, E = 1, T = 1, \epsilon = 0.01$. The curve with '*' shows payoff whereas the solid curve represents the value of the option

underlying asset. To do so, we use (2.3.8). It is the second partial derivative of the portfolio with respect to the asset price. If the absolute value of gamma is large, delta is highly sensitive to the price of the underlying asset. Table 2.5.8 gives the values of gamma for European put options. The first column in this table represents the values of the asset price S, the second column represents the analytical values of option's gamma and the third column represents the numerical values of it using the proposed approach.

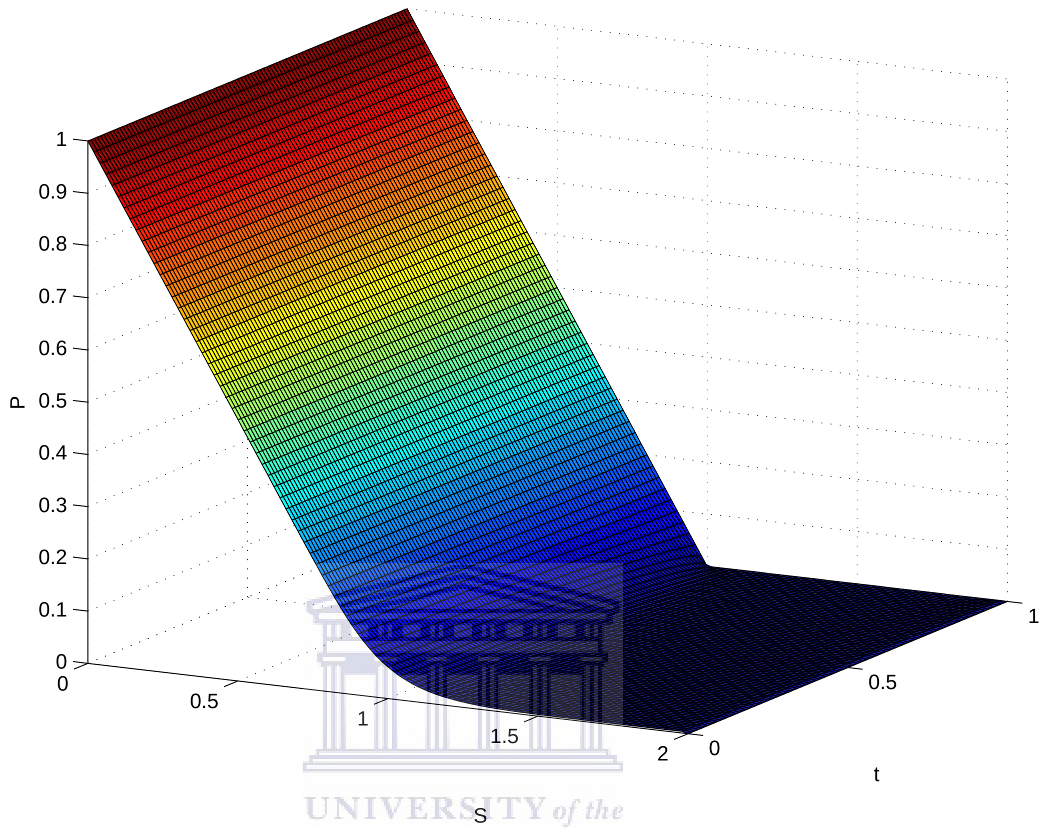

Figure 2.5.3: Values of American put option on a non-dividend paying asset using radial basis functions

Table 2.5.5: Values of option's delta (Δ) for European put on a non-dividend paying asset

S	Analytic values of option's Δ	Numerical values of option's Δ
6.0000	-0.9996	-0.9992
7.0000	-0.9885	-0.9879
8.0000	-0.9083	-0.9066
9.0000	-0.6906	-0.6902
10.0000	-0.4023	-0.4031
11.0000	-0.1784	-0.1798
12.0000	-0.0622	-0.0625
13.0000	-0.0177	-0.0181
14.0000	-0.0043	-0.0044
15.0000	-0.0009	-0.0012
16.0000	-0.0002	0.0010

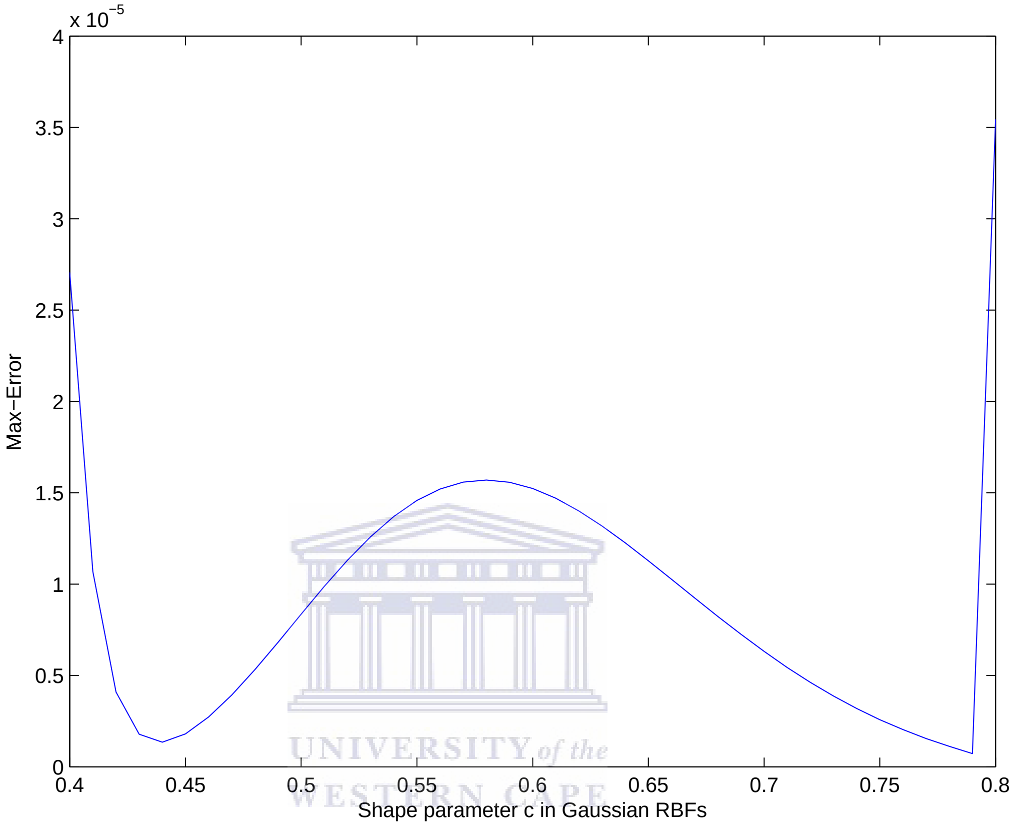

Figure 2.5.4: Effect of parameter c to computational error using radial basis functions

Table 2.5.6: Values of option's delta (Δ) for American put on a non-dividend paying asset

S	American delta (Δ)
0.6	-0.9999
0.7	-0.9964
0.8	-0.9480
0.9	-0.7201
1.0	-0.4218
1.1	-0.2152
1.2	-0.1010
1.3	-0.0445
1.4	-0.0183

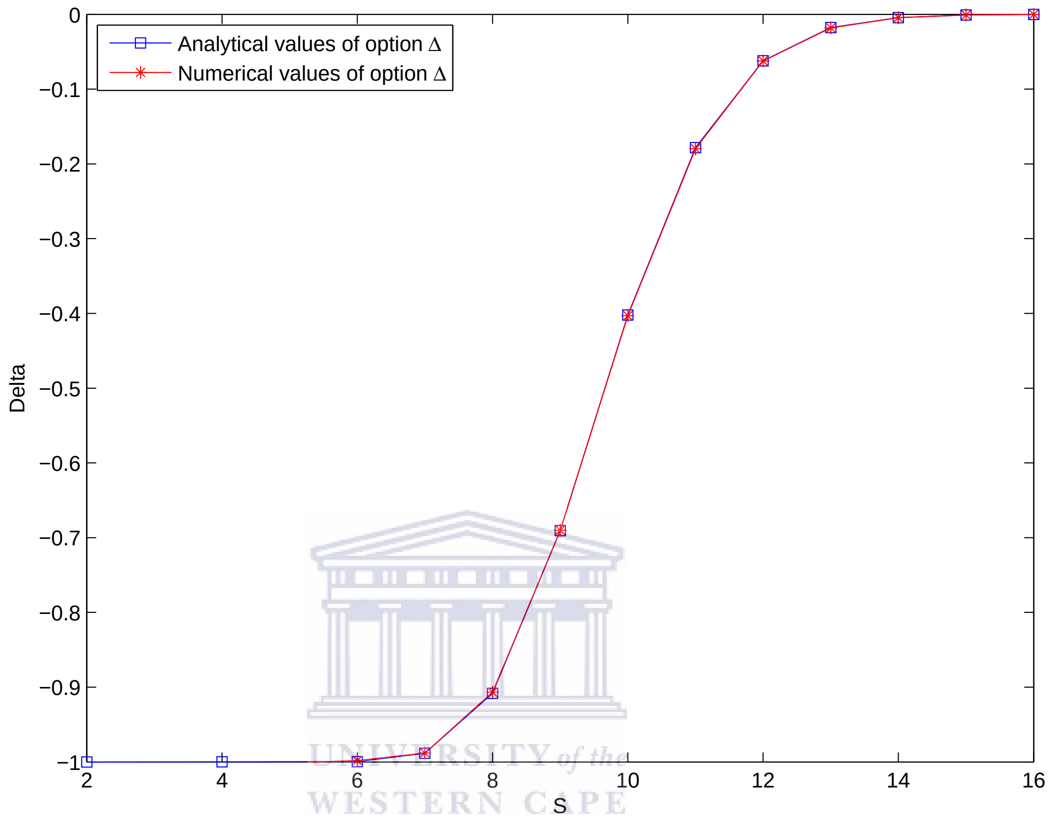

Figure 2.5.5: Analytical and numerical values for option's delta (Δ) of European put on a non-dividend paying asset

Table 2.5.7: Comparison of option's delta (Δ) for American put options on a non-dividend paying asset

S	LUBA	EXP	QFK	RBFs
80	-1.0000	-1.0000	-1.0000	-0.9997
90	-0.6173	-0.6207	-0.6212	-0.6220
100	-0.3588	-0.3582	-0.3581	-0.3602
110	-0.2108	-0.2109	-0.2108	-0.2129
120	-0.1256	-0.1257	-0.1256	-0.1280

LUBA: Lower and Upper bound Approximations [10].

EXP: The multipiece Exponention [51].

QFK: Quadrature Formula of Kim equations [52].

RBF: Radial Basis Function approach proposed in this chapter.

Table 2.5.8: Values of option's gamma (Γ) for European put on a non-dividend paying asset

S	Analytic values of option's Γ	Numerical values of option's Γ
6.0000	0.0016	0.0014
7.0000	0.0303	0.0315
8.0000	0.1455	0.1461
9.0000	0.2770	0.2767
10.0000	0.2736	0.2722
11.0000	0.1677	0.1678
12.0000	0.0722	0.0723
13.0000	0.0238	0.0242
14.0000	0.0064	0.0066
16.0000	0.0003	0.0003

Chapter 3

A mesh free method for pricing options on a dividend paying asset

In this chapter we introduce a mesh free numerical method based on radial basis functions (RBFs) to solve problems for pricing American and European put options on a dividend paying asset. The system of differential equations that we obtain solved by a time integration methods. Again to resolve the difficulties associated in solving the free boundary problem associated with American options, we use a penalty approach. The resulting method is analyzed for stability. Comparative numerical results along with valuation of some Greeks are presented at the end.

3.1 Introduction

Options on dividend paying assets are more popular than those on non-dividend paying assets.

Several attempts are made in the past to solve these option pricing problems through a variety of techniques. We describe a few of them below.

Whaley [111] examined the pricing performance of the valuation equation for American call options on stocks with known dividends and compares it with two approximation methods. They showed that the approximation obtained by substituting the stock price net of the present value of the escrowed dividends into the Black-Scholes model induces spurious correlation between prediction error and (i) the standard deviation of stock return, (ii) the degree to which the option, is in-the-money or out-of-the-money, (iii) the probability of early exercise, (iv) the time to expiration of the option, and (v) the dividend yield of the stock.

Barone-Adesi and Whaley [2] gave simple analytic approximations for pricing exchange-traded American call and put options written on commodity futures contracts. Their approximations were computationally efficient than those obtained by binomial method or standard finite-difference methods.

Fischer [30] derived an analytic approximation for the valuation of American put options on stocks paying known dividends. The results obtained by his formula are comparable to other approximations seen in the literature.

Mallier and Alobaidi [72] used Laplace transform methods to study the valuation of American call and put options with constant dividend yield.

Meyer [75] illustrated that a straightforward numerical implementation of the time discrete method of lines for the Black-Scholes equation can readily cope with the disappearance and reappearance of the early exercise boundary. They discussed the performance of the method by computing option prices when dividends are paid discretely at a known rate or known amount as well as with a constant dividend yield.

Kallast and Kivinukk [52] derived a method for pricing and hedging American options written on a dividend-paying asset. This method is based on Kim equations presented in [58]. They demonstrated that a simple approximation of the Kim integral equations by quadrature formulas leads to an efficient and accurate numerical procedure. This approximation was accompanied by the Newton-Raphson iteration procedure in order to compute the optimal exercise boundary at each time. The proposed sequence of approximations converges monotonically.

Battauz and Pratelli [5] analyzed some problems arising in the evaluation of American options when the underlying security pays discrete dividends. They studied the problem of maximizing the expected gain process over stopping times taking values in the union of disjoint, real compact sets. The results that they obtained can be applied to evaluate options with restrictions on exercise periods.

Company *et al.* [21] obtained the numerical solution of a modified Black-Scholes equation modelling the valuation of stock options with discrete dividend payments. They used a delta-defining sequence of the involved generalized Dirac delta function and applied an approach based on the Mellin transforms.

Vellekoop and Nieuwenhuis [104] presented a method to deal with cash dividends pricing equity options, under the assumption that in between dividend dates the asset follows lognormal dynamics, and where the same dynamics are used to price all derivative products. They defined an algorithm which is computationally efficient and guarantees to generate prices that exclude arbitrage possibilities. They showed that for the method to work a mild uniform convergence condition must be satisfied which does happen in the case of standard options like European and American ones.

Some other relevant works that can be worth mentioning here are those of Khaliq *et al.* [57] who developed adaptive θ-methods for solving the Black-Scholes PDE for American options; Zhao *et al.* [115] who discussed some compact finite difference methods for pricing American options on a single asset with methods for dealing with optimal exercise boundary, and Tangman *et al.* [100] who described an improvement of Han and Wu's algorithm [37] for American options.

The rest of the chapter is organized as follows. The option pricing problems on dividend paying assets are described in Section 3.2. Section 3.3 deals with the application of radial basis functions to solve these problems. The stability analysis of the numerical methods is presented in Section 3.4. Finally some numerical results along with a discussion on them are given in Section 3.5.

3.2 Problem description

The Black-Scholes model for pricing American and European options on dividend paying assets is also an initial-boundary value problem. For European options this problem reads as

$$\frac{\partial V}{\partial t} + \frac{1}{2}\sigma^2 S^2 \frac{\partial^2 V}{\partial S^2} + (r - D)S\frac{\partial V}{\partial S} - rV = 0, \tag{3.2.1}$$

where r is the risk-free interest rate, S is the price of the stock, σ is the volatility of the stock price, D is the dividend yield (which is constant in the present case) on the stock, and $V(S,t)$ denotes the option's value at time t for the stock price S.

The initial condition is given by the terminal payoff function

$$V(S,T) = \begin{cases} \max(E - S, 0) & \text{for put} \\ \max(S - E, 0) & \text{for call} \end{cases} \tag{3.2.2}$$

whereas the boundary conditions are given by

$$V(S,T) = \begin{cases} V(0,t) = Ee^{-r(T-t)}, \quad V(S,t) \to 0 \text{ as } S \to \infty & \text{for put} \\ V(0,t) = 0, \quad V(S,t) \to Se^{-D(T-t)} \text{ as } S \to \infty & \text{for call} \end{cases} \tag{3.2.3}$$

where T is the maturity time and E is the strike price of the option.

The exact solution of the differential equation (3.2.1) with the initial condition (3.2.2) and the boundary conditions (3.2.3) is given by ([112]):

$$V(S,T) = \begin{cases} V(S,t) = Ee^{-r(T-t)}N(-\widetilde{d}_2) - e^{-D(T-t)}SN(-\widetilde{d}_1) & \text{for put} \\ V(S,t) = e^{-D(T-t)}SN(\widetilde{d}_1) - Ee^{-r(T-t)}N(\widetilde{d}_2) & \text{for call} \end{cases} \tag{3.2.4}$$

where $N(\cdot)$ is the cumulative distribution function of the standard normal distribution with

$$\widetilde{d}_1 = \frac{\log(S/E) + (r - D + \frac{1}{2}\sigma^2)(T-t)}{\sigma\sqrt{T-t}}, \tag{3.2.5}$$

and

$$\widetilde{d}_2 = d_1 - \sigma\sqrt{T-t}. \tag{3.2.6}$$

On the other hand, the American option pricing problem takes the form of a free-boundary problems. The early exercise possibility leads to the following model for the value $P(S,t)$ of an American put option to sell the underlying asset ([55]):

$$\frac{\partial P}{\partial t} + \frac{1}{2}\sigma^2 S^2 \frac{\partial^2 P}{\partial S^2} + (r-D)S\frac{\partial P}{\partial S} - rP = 0, \quad S > S_f(t),\ 0 \le t < T \quad (3.2.7)$$

$$P(S,T) = \max(E-S,0), \quad S \ge 0,$$

$$\frac{\partial P}{\partial S}(S_f,t) = -1,$$

$$P(S_f(t),t) = E - S_f(t),$$

$$\lim_{S\to\infty} P(S,t) = 0,$$

$$S_f(T) = E,$$

$$P(S,t) = E - S, \quad 0 \le S < S_f(t).$$

where $S_f(t)$ represents the free boundary, E represent the exercise price of the option, P denotes the value of the option and as before, σ is the volatility of the underlying asset, r is the risk-free interest rate, D is the dividend yield on the stock.

Since early exercise is permitted, the P of the option must satisfy

$$P(S,t) \ge \max(E-S,0), \quad S \ge 0,\ 0 \le t \le T. \quad (3.2.8)$$

In the next section, we explain how the radial basis functions are used to solve the above option pricing problems.

3.3 Application of radial basis functions in pricing options

In order for us to apply the radial basis function approach, we proceed in a manner similar to the one described in the previous chapter.

3.3.1 Pricing European options on a dividend paying asset

We approximate the unknown function V (the value of the European option) using the radial basis functions as

$$V(S,t) \approx \sum_{j=1}^{N} a_j(t)\phi(\|S - x_j\|), \tag{3.3.1}$$

where $a_j's$ are unknown coefficients and $\phi(\|S - x_j\|)$ are the RBFs. We will use the following radial basis functions for this problem

$$\phi(S) = e^{-\|S-x_j\|^2/c^2}, \tag{3.3.2}$$

where c is a positive parameter.

Collocating at the same N points $\{x_j\}_{j=1}^N$, equation (3.2.1) becomes

$$\frac{\partial V(x_i,t)}{\partial t} + \frac{1}{2}\sigma^2 S_i^2 \frac{\partial^2 V(x_i,t)}{\partial S^2} + (r - D)S_i \frac{\partial V(x_i,t)}{\partial S} - rV(x_i,t) = 0. \tag{3.3.3}$$

Differentiating (3.3.1), we get

$$\frac{\partial V(x_i,t)}{\partial t} = \sum_{j=1}^{N} \frac{da_j(t)}{dt}\phi(\|S - x_j\|), \tag{3.3.4}$$

$$\frac{\partial V(x_i,t)}{\partial S} = \sum_{j=1}^{N} a_j \frac{\partial \phi(\|S - x_j\|)}{\partial S}, \tag{3.3.5}$$

and

$$\frac{\partial^2 V(x_i,t)}{\partial S^2} = \sum_{j=1}^{N} a_j \frac{\partial^2 \phi(\|S - x_j\|)}{\partial S^2}. \tag{3.3.6}$$

In case of Gaussian basis functions, we have

$$\frac{\partial \phi(\|S - x_j\|)}{\partial S} = -\frac{2(S - x_j)}{c^2} e^{-\|S-x_j\|^2/c^2} \tag{3.3.7}$$

and

$$\frac{\partial^2 \phi(\|S - x_j\|)}{\partial S^2} = \frac{4(S - x_j)^2 - 2c^2}{c^4} e^{-\|S - x_j\|^2/c^2}. \qquad (3.3.8)$$

Substituting the expressions for various partial derivatives from equations (3.3.4)-(3.3.6) into (3.3.3), we obtain

$$\begin{aligned} &\sum_{j=1}^{N} \frac{d}{dt}(a_j(t))\phi(\|x_i - x_j\|) \\ &+\frac{1}{2}\sigma^2 x_i^2 \sum_{j=1}^{N} a_j(t) \left[\frac{4(x_i - x_j)^2 - 2c^2}{c^4}\phi(\|x_i - x_j\|)\right] \\ &+(r - D)x_i \sum_{j=1}^{N} a_j(t) \left[\frac{-2(x_i - x_j)}{c^2}\phi(\|x_i - x_j\|)\right] \\ &-r\sum_{j=1}^{N} a_j(t)\phi(\|x_i - x_j\|) = 0. \end{aligned} \qquad (3.3.9)$$

We can write equation (3.3.9) in form of a system of differential equations as

$$\Phi\frac{d\mathbf{a}}{dt} + R\mathbf{a} = 0, \qquad (3.3.10)$$

where

$$\Phi_{ij} = e^{-\|x_i - x_j\|^2/c^2} \qquad (3.3.11)$$

and

$$R_{ij} = \frac{1}{2}\sigma^2 x_i^2 \left(\frac{4(x_i - x_j)^2 - 2c^2}{c^4}\right)\Phi_{ij} + (r - D)x_i\left(\frac{-2(x_i - x_j)}{c^2}\right)\Phi_{ij} - r\Phi_{ij}. \qquad (3.3.12)$$

To solve the system described by (3.3.10), we use a θ-method

$$\Phi\frac{\mathbf{a}^{n+1} - \mathbf{a}^n}{\Delta t} + \theta R\mathbf{a}^{n+1} + (1 - \theta)R\mathbf{a}^n = 0, \qquad (3.3.13)$$

with the initial condition given by the first part of equation (3.2.2) and boundary conditions given by the first part of equation (3.2.3).

We can rewrite equation (3.3.13) as

$$[\Phi - (1-\theta)\Delta t R]\mathbf{a}^n = [\Phi + \theta \Delta t R]\mathbf{a}^{n+1}, \tag{3.3.14}$$

$$\mathbf{a}^n = [\Phi - (1-\theta)\Delta t R]^{-1}[\Phi + \theta \Delta t R]\mathbf{a}^{n+1}. \tag{3.3.15}$$

Equation (3.3.1) applied at all collocation point can be written in the matrix form as

$$\mathbf{V} = \Phi \mathbf{a}. \tag{3.3.16}$$

Using equation (3.3.16), equation (3.3.15) can be written as

$$V^n = \Phi[\Phi - (1-\theta)\Delta t R]^{-1}[\Phi + \theta \Delta t R]\Phi^{-1}V^{n+1}. \tag{3.3.17}$$

The above equation is solved along with (3.2.2) and the first part of equation (3.2.3) to obtain the numerical solution. Also the form of this equation should be read in context to the computing process because in the problems like those considered in this chapter, we usually have a final boundary value problem rather than an initial boundary value problem. To this end, note that the scheme given by (3.3.14) corresponding to $\theta = 0,\ 0.5,$ and 1 are the implicit Euler, Crank-Nicolson and explicit Euler methods, respectively.

3.3.2 Pricing American options on a dividend paying asset

To solve the American option problem (3.2.7), which is a free boundary problem, we approximate the model by adding a penalty term. This leads to a nonlinear partial differential equation on a fixed domain.

We consider the initial-boundary value problem

$$\frac{\partial P_\epsilon}{\partial t} + \frac{1}{2}\sigma^2 S^2 \frac{\partial^2 P_\epsilon}{\partial S^2} + (r-D)S\frac{\partial P_\epsilon}{\partial S} - rP_\epsilon + \frac{\epsilon C}{P_\epsilon + \epsilon - q(S)} = 0, \tag{3.3.18}$$

with the initial condition as the first part of equation (3.2.2), and the boundary conditions as

$$P_\epsilon(0,t) = E, \quad \lim_{S\to\infty} P_\epsilon(S,t) = 0, \tag{3.3.19}$$

where $C \geq rE$, $q(S) = E - S$, and $0 < \epsilon \ll 1$.

By inserting equations (3.3.1),(3.3.4)-(3.3.8) into equation (3.3.18), we obtain

$$\begin{aligned}
&\sum_{j=1}^{N} \frac{d}{dt}(a_j(t))\phi(\|x_i - x_j\|) + \frac{1}{2}\sigma^2 x_i^2 \sum_{j=1}^{N} a_j(t)\left[\frac{4(x_i-x_j)^2 - 2c^2}{c^4}\phi(\|x_i - x_j\|)\right] \\
&+(r-D)x_i \sum_{j=1}^{N} a_j(t)\left[\frac{-2(x_i-x_j)}{c^2}\phi(\|x_i - x_j\|)\right] - r\sum_{j=1}^{N} a_j(t)\phi(\|x_i - x_j\|) \\
&+\frac{\epsilon C}{\sum_{j=1}^{N} a_j(t)\phi(\|x_i - x_j\|) + \epsilon - q(S)} = 0.
\end{aligned} \tag{3.3.20}$$

We write equation (3.3.20) in form of a system of differential equations as

$$\Phi\frac{d\mathbf{a}}{dt} + R\mathbf{a} + Q(\mathbf{a}) = 0, \tag{3.3.21}$$

where

$$\Phi_{ij} = e^{-\|x_i - x_j\|^2/c^2}, \tag{3.3.22}$$

$$Q_i(\mathbf{a}) = \frac{\epsilon C}{\Phi_i \mathbf{a} + \epsilon - q(x_i)}, \quad i = 1, \cdots, N \tag{3.3.23}$$

with Φ_i denoting the i-th row of the matrix Φ and

$$R_{ij} = \frac{1}{2}\sigma^2 x_i^2\left(\frac{4(x_i-x_j)^2 - 2c^2}{c^4}\right)\Phi_{ij} + (r-D)x_i\left(\frac{-2(x_i-x_j)}{c^2}\right)\Phi_{ij} - r\Phi_{ij}. \tag{3.3.24}$$

The θ-method for equation (3.3.21) reads

$$\Phi\frac{\mathbf{a}^{n+1} - a^n}{\Delta t} + \theta R\mathbf{a}^{n+1} + (1-\theta)R\mathbf{a}^n + \theta Q(\mathbf{a}^{n+1}) + (1-\theta)Q(\mathbf{a}^n) = 0. \tag{3.3.25}$$

By replacing $\mathbf{a}^n$ in the penalty term by $\mathbf{a}^{n+1}$, the linearly implicit scheme for (3.3.25) is given by

$$\Phi\frac{\mathbf{a}^{n+1}-\mathbf{a}^{n}}{\Delta t}+\theta R\mathbf{a}^{n+1}+(1-\theta)R\mathbf{a}^{n}+Q(\mathbf{a}^{n+1})=0, \tag{3.3.26}$$

with the initial condition given by the first part of equation (3.2.2) and boundary conditions given by equation (3.3.19).

3.4 Stability analysis of the numerical method

To proceed with the stability analysis, let us define the error at the n^{th} time level by

$$e^n = V^n_{\text{exact}} - V^n_{\text{app}}, \tag{3.4.1}$$

where V^n_{exact} is the exact solution and V^n_{app} is the numerical solution obtained by either (3.3.13) or (3.3.26), respectively.

For the scheme given by (3.3.13) the error equation at $(n+1)^{th}$ level can be written as

$$e^n = Be^{n+1}, \tag{3.4.2}$$

where B is the amplification matrix is given by

$$B = \Phi^{-1}[\Phi+\theta\Delta tR][\Phi-(1-\theta)\Delta tR]^{-1}\Phi.$$

The numerical scheme is stable if $\rho(B)\le 1$, where $\rho(B)$ is the spectral radius of B. Substituting B in equation (3.4.2) and simplifying, we obtain

$$[\Phi-(1-\theta)\Delta tR]\Phi^{-1}e^n = [\Phi+\theta\Delta tR]\Phi^{-1}e^{n+1}. \tag{3.4.3}$$

This implies

$$[I-(1-\theta)\Delta tM]e^n = [I+\theta\Delta tM]e^{n+1}, \tag{3.4.4}$$

where $M = R\Phi^{-1}$ and $I\in\mathbb{R}^{N\times N}$ is the identity matrix.

It is clear from equation (3.4.4) that the numerical scheme is stable if all the eigenvalues of the matrix $[I-(1-\theta)\Delta tM]^{-1}[I+\theta\Delta tM]$ are less than unity, which means that

$$\left| \frac{1+\theta\Delta t\lambda_M}{1-(1-\theta)\Delta t\lambda_M} \right| \leq 1, \tag{3.4.5}$$

where λ_M represent the eigenvalues of the matrix M.

Now we consider different cases. Firstly, when $\theta = 1$, we have explicit Euler method. The above condition for stability becomes

$$|1+\Delta t\lambda_M| \leq 1. \tag{3.4.6}$$

Simplifying (3.4.6), we see that the explicit Euler method will be stable if

$$\Delta t \geq \frac{-2}{\lambda_M} \quad \text{and} \quad \lambda_M \leq 0. \tag{3.4.7}$$

Secondly, when $\theta = 0$, we have implicit Euler method which is clearly unconditionally stable as can be seen from (3.4.5). Finally, when $\theta = 0.5$, we have the Crank-Nicholson's method. Even in this case, the inequality (3.4.5) will hold as long as $\lambda_M \leq 0$ and this does happen. Therefore the Crank-Nicholson's method will be unconditionally stable.

3.5 Numerical results and discussion

Using the RBF approach, the resulting problems for European and American put options on dividend paying assets are solved via Crank-Nicolson's method (i.e., $\theta = 0.5$), for European put option problem (3.2.1). Results are presented in Table 3.5.1. The parameter values used in the simulation are $r = 0.05,\ \sigma = 0.2,\ D = 0.05,\ E = 10,\ t_0 = 0,\ T = 0.5,\ S_0 = 0,$ and $S_{\max} = 30$. The first column in this table represents values of the asset price S, the second column represents the exact solution and the other three columns indicated the numerical values of the European put option that we obtain using the radial basis function approach with 21, 41 and 101 nodes, respectively.

Figure 4.5.2 shows the value of a European put option at t_0 using 101 nodes and

Figure 3.5.2 shows the effect of the dividend paying in European put option with $D = 0, 0.05, 0.1$ and 0.2.

Table 3.5.1: Values of European put option using radial basis functions on a dividend paying asset

S	Exact	RBF21	RBF41	RBF101
2	7.8025	7.8044	7.8033	7.8026
4	5.8519	5.8527	5.8526	5.8519
6	3.9013	3.8987	3.9007	3.9013
8	1.9808	2.0232	1.9878	1.9820
10	0.5498	0.6357	0.5707	0.5532
12	0.0703	0.0731	0.0728	0.0706
13	0.0195	0.0310	0.0226	0.0200
14	0.0047	0.0068	0.0059	0.0049
15	0.0010	0.0006	0.0011	0.0010
16	0.0002	0.0004	0.0003	0.0002

RBF21: radial basis functions with 21 nodes.

RBF41: radial basis functions with 41 nodes.

RBF101: radial basis functions with 101 nodes.

As in the previous chapter, we chose $c = 2h$, where $h = (S_{max} - S_0)/(N-1)$ and done some numerical simulations. We search the value of shape parameter in RBFs by the step 0.01 and plot the relationship between shape parameter and max-error to select the optimal value of shape parameter. From Figure 3.5.3 we found that the optimal value of shape parameters using Gaussian RBFs is in the neighborhood of 0.44.

The numerical solution of American put option is obtained for $r = 0.08$, $\sigma = 0.2$, $D = 0.12, 0.08, 0.04$ and 0, $E = 100$, $t_0 = 0$, $T = 3$, $S_0 = 0$, and $S_{max} = 180$. We used the Crank-Nicolson method ($\theta = 0.5$) together with a constant time step of $\Delta t = 0.001$. The result listed in Table 3.5.2.

In Table 3.5.2, the first column represents the parameters used for simulation, the second column represents values of the asset price S, the next three columns represent results obtained by other researchers as mentioned below the table for the American put option on a dividend paying asset whereas the last column contains the numerical

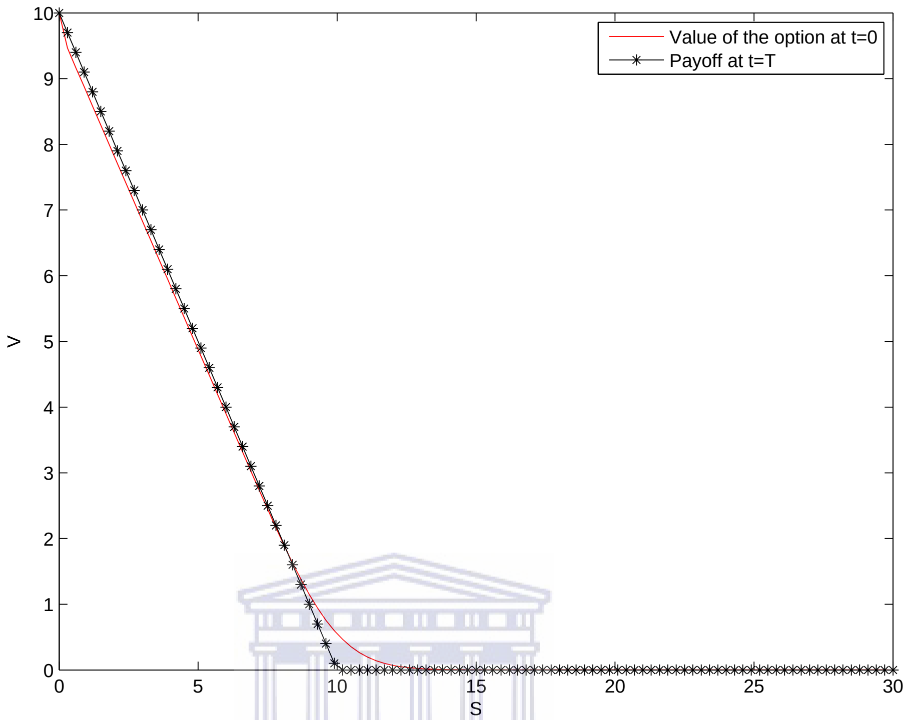

Figure 3.5.1: Values of a European put option on a dividend paying asset at t_0 using 101 points and $r = 0.05$, $\sigma = 0.2$, $E = 10$, $D = 0.05$, $t_0 = 0$, $T = 0.5$, $S_0 = 0$, and $S_{max} = 30$. The curve with '*' shows payoff whereas the solid curve represents the value of the option

results that we obtained using our RBF based mesh free approach.

Figure 3.5.4 illustrates the value of an American put option at different values of t using 101 points and Figure 3.5.5 shows value of the American put option for all cases.

Since the radial basis functions are infinitely differentiable, the computations of the derivatives of the options values are readily available from the derivatives of the basis functions. Then using equation (3.3.7) we can calculate the value of the delta of an option, which is the rate of change of the option value with respect to the asset price. Tables 3.5.3 and 3.5.5 present comparative results for the delta of European and American put options. It is clear from the results presented in these tables that the numerical values of the option's delta lie between -1 and 0 which is in agreement with what is mentioned in Hull [43].

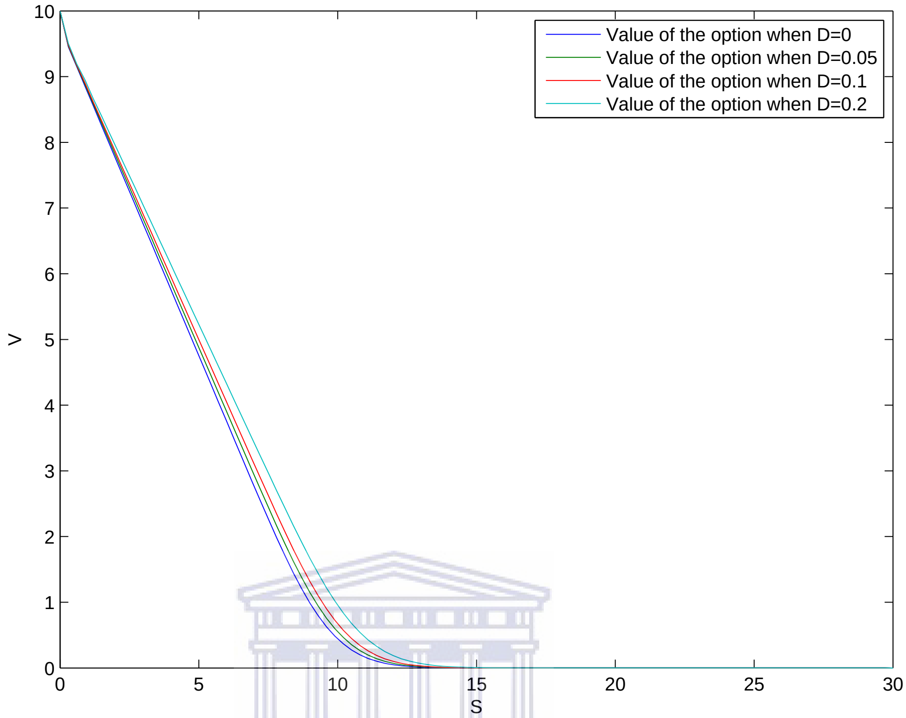

Figure 3.5.2: The effect of the dividend in European put option with $D = 0, 0.05, 0.1, 0.2$

We also calculate the gamma (Γ) using (3.3.7). Table 3.5.4 gives the values of gamma for European put options. The first column in this table represents the values of the asset price S, the second column represents the analytical values of option's gamma and the third column represents the numerical values of it using the proposed approach.

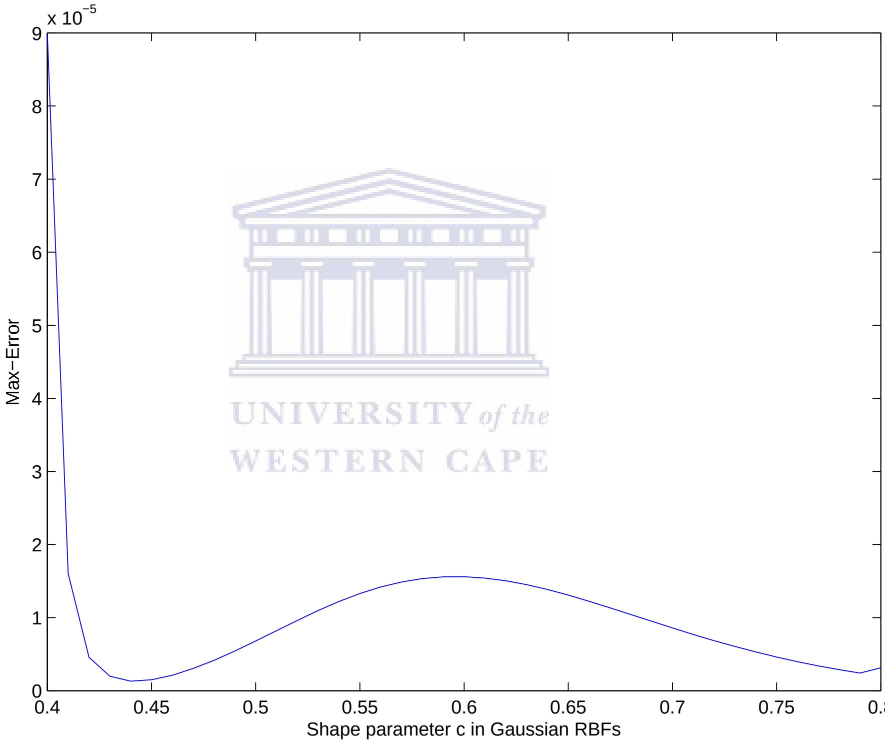

Figure 3.5.3: Effect of parameter c to computational error with $D = 0.05$ using radial basis functions

Table 3.5.2: Values of an American put option using radial basis functions on a dividend paying asset with $E = 100$

Parameters	S	FDM	COM	QFK	RBF
$D = 0.12,\ r = 0.08,$ $\sigma = 0.20,\ T = 3.$	80	25.66	25.59	25.66	25.83
	90	20.08	20.05	20.08	20.23
	100	15.50	15.51	15.50	15.61
	110	11.80	11.83	11.80	11.87
	120	8.88	8.91	8.89	8.89
$D = 0.08,\ r = 0.08,$ $\sigma = 0.20,\ T = 3.$	80	22.20	22.35	22.21	22.32
	90	16.21	16.18	16.21	16.31
	100	11.70	11.65	11.70	11.78
	110	8.37	8.34	8.37	8.43
	120	5.93	5.93	5.93	5.98
$D = 0.04,\ r = 0.08,$ $\sigma = 0.20,\ T = 3.$	80	20.35	20.60	20.35	20.42
	90	13.50	13.69	13.50	13.56
	100	8.94	8.95	8.94	8.99
	110	5.91	5.85	5.91	5.93
	120	3.90	3.85	3.89	3.89
$D = 0,\ r = 0.08,$ $\sigma = 0.20,\ T = 3.$	80	20.00	19.44	20.00	20.00
	90	11.69	11.96	11.69	11.75
	100	6.93	7.06	6.93	6.97
	110	4.15	4.13	4.15	4.17
	120	2.51	2.45	2.51	2.50

FDM: Finite Difference Method [2].

COM: Compound Option Methods [2].

QFK: Quadrature Formula of Kim equations [52].

RBF: Radial Basis Function approach proposed in this chapter.

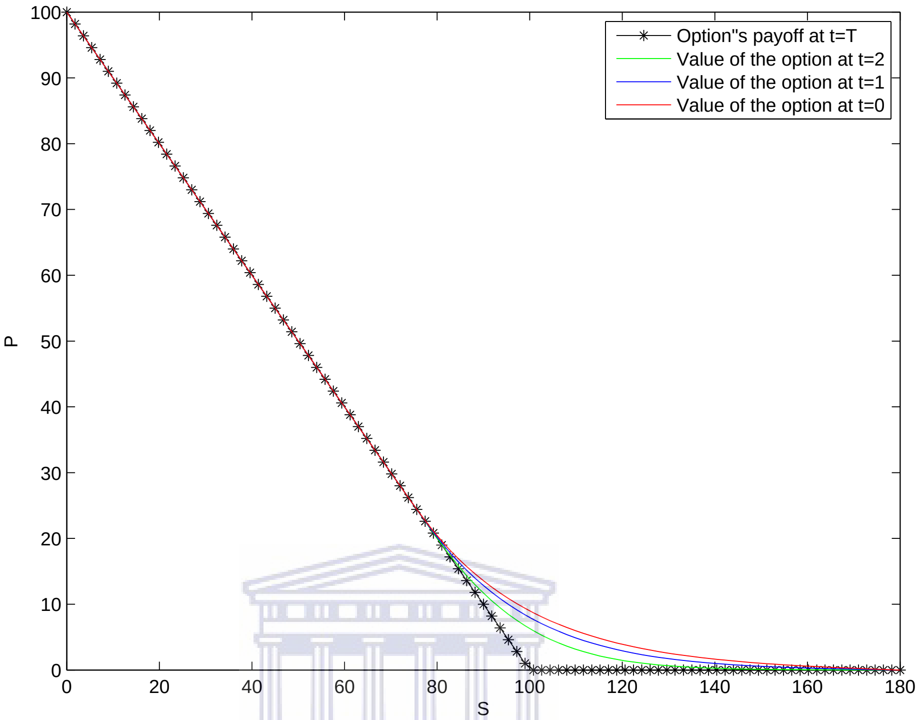

Figure 3.5.4: Values of an American put option on a dividend paying asset at different values of t and $r = 0.08,\ \sigma = 0.2,\ D = 0.04,\ E = 100,\ T = 3$

Table 3.5.3: Values of option's delta (Δ) for European put using radial basis functions on a dividend paying asset

S	Analytic values of option's Δ	Numerical values of option's Δ
2	-0.9753	-0.9831
4	-0.9753	-0.9781
6	-0.9751	-0.9741
7	-0.9684	-0.9680
8	-0.9111	-0.9095
9	-0.7314	-0.7310
10	-0.4602	-0.4605
11	-0.2226	-0.2239
12	-0.0848	-0.0850
13	-0.0264	-0.0269
14	-0.0070	-0.0072
15	-0.0016	-0.0016
16	-0.0003	-0.0004

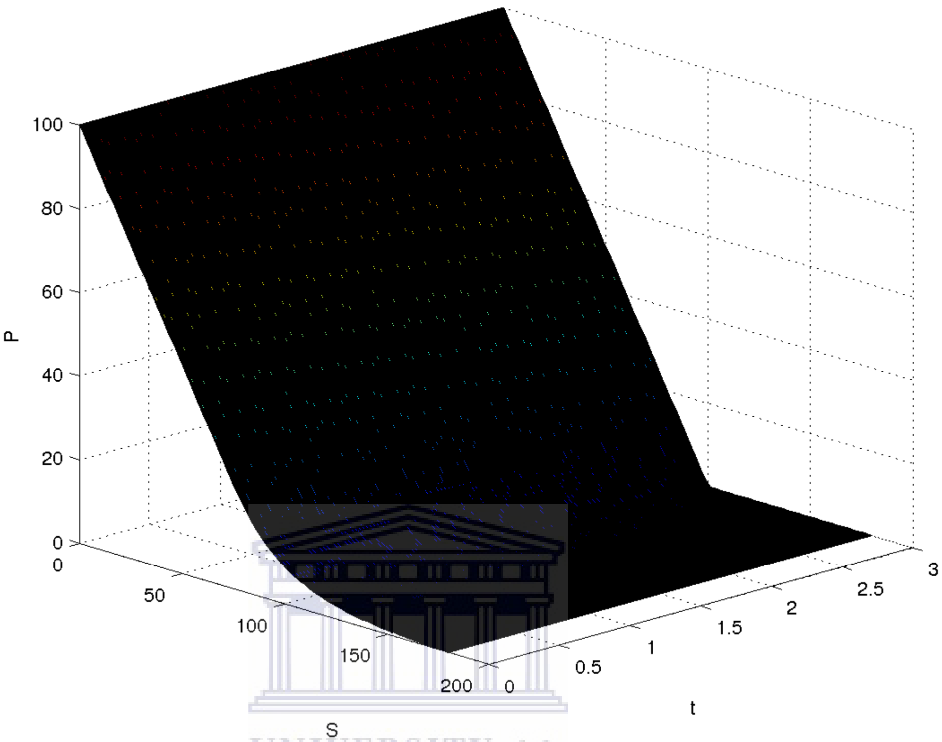

Figure 3.5.5: American put option using RBFs on a dividend paying asset

Table 3.5.4: Values of option's gamma (Γ) for European put using radial basis functions on a dividend paying asset

S	Analytic values of option's Γ	Numerical values of option's Γ
4	0.0000	0.0000
6	0.0009	0.0009
7	0.0195	0.0204
8	0.1105	0.1113
9	0.2435	0.2435
10	0.2744	0.2729
11	0.1896	0.1893
12	0.0909	0.0910
13	0.0331	0.0336
14	0.0098	0.0100
15	0.0025	0.0025
16	0.0005	0.0006

Table 3.5.5: Values of option's delta (Δ) for American put using radial basis functions on a dividend-paying asset with $E = 100$

Parameters	S	LUBA	EXP	QFE	RBF
$D = 0.12,\ r = 0.08,\ \sigma = 0.20,\ T = 3.$	80	-0.61	-0.61	-0.61	-0.61
	90	-0.50	-0.51	-0.51	-0.51
	100	-0.41	-0.41	-0.41	-0.42
	110	-0.33	-0.33	-0.33	-0.33
	120	-0.26	-0.26	-0.27	-0.27
$D = 0.08,\ r = 0.08,\ \sigma = 0.20,\ T = 3.$	80	-0.69	-0.69	-0.69	-0.69
	90	-0.52	-0.52	-0.52	-0.52
	100	-0.39	-0.39	-0.39	-0.39
	110	-0.28	-0.28	-0.28	-0.29
	120	-0.21	-0.21	-0.21	-0.21
$D = 0.04,\ r = 0.08,\ \sigma = 0.20,\ T = 3.$	80	-0.83	-0.84	-0.84	-0.84
	90	-0.55	-0.55	-0.55	-0.55
	100	-0.37	-0.37	-0.37	-0.37
	110	-0.25	-0.25	-0.25	-0.25
	120	-0.16	-0.16	-0.16	-0.17
$D = 0,\ r = 0.08,\ \sigma = 0.20,\ T = 3.$	80	-1.00	-1.00	-1.00	-1.00
	90	-0.62	-0.62	-0.62	-0.62
	100	-0.36	-0.36	-0.36	-0.36
	110	-0.21	-0.21	-0.21	-0.21
	120	-0.13	-0.13	-0.13	-0.13

LUBA: Lower and Upper bound Approximations [10].

EXP: The multipiece Exponention [51].

QFE: Quadrature Formula of Eim equations [52].

RBF: Radial Basis Function approach proposed in this chapter.

Chapter 4

A mesh free method for pricing exotic options

In this chapter, we extend the mesh free method that developed in previous chapters to solve problems for pricing two type of exotic options, namely, European barrier and Asian options. Even in these cases we obtain a system of ordinary differential equations which are then solved by a time integration techniques. As compared to the work done in Goto *et al.* [36], in this chapter we provide a simplified presentation of the approach. We also analyzed the method for stability which was not done in the above mentioned work. The proposed approach in this chapter is further extended to solve problems of pricing European style double barrier options and digital options. Finally, we present some numerical experiments using a number of radial basis functions.

4.1 Introduction

Exotic options are non-standard options. The features of these options are more complex features than the standard (plain vanilla) European and American options. These exotic options are option contracts that can be exercised according to the average value of the asset price during a specified period of time and their maximum and minimum prices. There are many exotic options available in the literature. However, in this chapter, we will focus on the European barrier and Asian options. Below we describe each one of them along with some literature work.

Barrier options are options where the payoff depends on whether the underlying asset's price reaches a certain level during a certain period of time. These barrier options can be classified as either knock-out options or knock-in options. A knock-out option ceases to exist when the underlying asset price reaches a certain barrier whereas a knock-in option comes into existence only when the underlying asset price reaches a barrier [43]. Most of these options are priced by means of partial differential equations. Below we describe some of the techniques that are used in the past to solve the problems that price the barrier options.

Zvan *et al.* [118] described an implicit finite difference method to solve the problem of pricing barrier options. They illustrated its application to a variety of such contracts. They handled barrier options with and without American-style features in a similar way. They found that the use of the implicit method leads to convergence in fewer time steps as compared to explicit schemes.

Sanfelici [95] analyzed the Galerkin infinite element method for pricing European barrier options with discontinuous payoff. They considered three main aspects: the degeneracy of the pricing PDE models; the presence of discontinuities at the barriers or in the payoff clause and their effects on the numerical approximation process; and the need for resorting to suitable numerical methods for unbounded domains when appropriate asymptotic conditions are not specified.

In [86], Pelsser provided valuation formulas for a wide range of double-barrier knock-out and knock-in options. They derived Laplace transforms which were inverted analytically using contour integration methods.

Using an optimal portfolio framework, Chao *et al.* [14] developed an algorithm to price the barrier options in the presence of proportional transaction costs. They computed the option prices numerically by using a Markov chain approximation to the continuous-time singular stochastic optimal control problem.

Wade *et al.* [105] presented some higher order schemes for pricing barrier options.

They explored the smoothing strategy for the Crank-Nicolson's method in an attempt to achieve optimal order of convergence for barrier option problems. They discussed numerical experiments for one asset and two asset problems.

In [82], Ökten *et al.* used a Monte Carlo Simulation technique to price down-and-in barrier options. Their approach was based on two variance reduction techniques: the use of conditional expectation and importance sampling. They used a simulated annealing algorithm to estimate the optimal parameters of exponential twisting in importance sampling.

On the other hand, the Asian options are popular path-dependent financial derivatives. These options are securities with payoff which depend on the average value of an underlying stock price over some time interval. These options have either fixed strike (also known as an average rate) or a floating strike (or floating rate). The pricing of arithmetic Asian options has been tackled by a variety of analytical approximations and numerical algorithms. Below we describe some of them.

In the methods based on Monte Carlo simulations, researchers usually calculate the price by directly simulating the stock price process. Joy *et al.* [50] introduced a different version of the Monte Carlo method that has attractive properties for the numerical valuation of derivatives. They suggested Quasi-Monte Carlo methods that use sequences that are deterministic instead of random. This improved convergence and gave rise to deterministic error bounds. The method is well explained and illustrated through several examples including complex derivatives such as basket options, Asian options, and energy swaps.

Methods based on partial differential equation (PDE) approaches are mostly based on finite differences methodology. Sak *et al.*[94] discussed the use of parallel computing for pricing Asian options and evaluated the efficiency of various algorithms. They implemented a PDE approach that involves a single state variable to price the Asian option, and implemented the same methodology to price a standard European option to check the accuracy. They solved a parabolic PDE by using both explicit and Crank-Nicolson's implicit finite-difference methods.

Some researchers used lattices and Binomial trees which are closely related to finite-difference methods. Costabile *et al.* [22] proposed a model for pricing both European and American Asian options based on the arithmetic average of the underlying asset prices. Their approach relies on a binomial tree describing the underlying asset evolution. They associated a set of representative averages chosen among all the effective averages realized at that node at each node of the tree. They used backward recursion and linear interpolation to compute the option price.

Hsu and Lyuu [41], used lattices to price fixed-strike European-style Asian options that are discretely monitored. They presented the first provably quadratic-time convergent lattice algorithm for pricing fixed-strike European-style discretely monitored Asian options.

Vanmaele *et al.* [103] studied the pricing of European-style discrete arithmetic Asian options with fixed and floating strike by deriving analytical lower and upper bounds. They used a general technique for deriving upper (and lower) bounds for stop-loss premiums of sums of dependent random variables. It is to be noted that analytical representations in terms of infinite series and integral formula (including Laplace transforms) usually require numerical algorithms in order to recover the price.

Tsao and Huang [102] solved European and American discrete average price Asian options by using Taylor expansion to obtain the approximation formula for continuous average strike Asian options. They showed numerically that their formula are robust in terms of volatility.

Rogers and Shi [93] approached the problem of computing the price of an Asian option in two different ways. Firstly, exploiting a scaling property, they reduced the problem to the problem of solving a parabolic PDE in two variables. Secondly, they provided a sufficiently accurate lower bound.

The rest of the chapter is organized as follows. Some pricing problems for exotic options are described in Section 4.2. Section 4.3 deals with the application of radial basis functions to solve these problems. The stability analysis of the numerical methods is presented in Section 4.4. Finally some numerical results along with a discussion on them are given in Section 4.5.

4.2 Problem description

In this section we describe the pricing problems for two type of exotic options, namely, barrier and Asian options.

Barrier option

The Black-Scholes partial differential equation for the valuation of an option V is

$$\frac{\partial V}{\partial t} + \frac{1}{2}\sigma^2 S^2 \frac{\partial^2 V}{\partial S^2} + rS\frac{\partial V}{\partial S} - rV = 0, \tag{4.2.1}$$

where r is the risk-free interest rate, σ is the volatility of the stock price, and $V(S,t)$ is the option value at time t for the stock's price S.

With boundary conditions

$$V(0,t) = 0, \quad V(X,t) = 0, \tag{4.2.2}$$

and barrier constraint:

- For a single barrier option

$$V(S,t) = \begin{cases} 0 & S \leq K \\ \\ V(S,t) & S > K. \end{cases} \tag{4.2.3}$$

- For a double barrier option

$$V(S,t) = \begin{cases} 0 & S \leq K_1 \; or \; S \geq K_2 \\ V(S,t) & \text{otherwise,} \end{cases} \tag{4.2.4}$$

and initial condition (payoff):

- For a single barrier option

$$V(S,0) = \begin{cases} 0, & S \leq K, \\ S - E & S > K. \end{cases} \tag{4.2.5}$$

- For a double barrier option

$$V(S,0) = \begin{cases} 0, & S \leq K_1, \\ S - E & K_1 \geq S < K_2, \\ 0, & S \geq K_2, \end{cases} \tag{4.2.6}$$

where K is the barrier level in the case of a single barrier option whereas K_1 and K_2 are the lower and upper barriers in the case of a double barrier option, respectively; E is the strike price, and X is chosen sufficiently large in this case.

Digital option

A digital call option, also known as cash-or-nothing call or binary option, is an option with payoff zero before the strike price and one (or any fixed amount) after the strike price [56]. This is modeled by the Black-Scholes PDE (4.2.1) with the payoff function given as

$$V(S,T) = \begin{cases} 1, & \text{for } S > E \\ 0, & \text{for } S < E. \end{cases} \tag{4.2.7}$$

Using the average of the payoff, equation (4.2.7) can be written as

$$V(S,T) = \begin{cases} 1, & \text{for } S > E \\ 0.5, & \text{for } S = E \\ 0, & \text{for } S < E. \end{cases} \tag{4.2.8}$$

The boundary conditions are given by

$$C(0,t) = 0, \quad 0 \leq t \geq T, \tag{4.2.9}$$

$$C(S,t) \approx e^{-rT}, \quad S \to \infty. \tag{4.2.10}$$

The analytic solution for the digital option is

$$V(S,t) = e^{-rT} N(d), \tag{4.2.11}$$

where $N(d)$ is the cumulative distribution function of the standard normal distribution with

$$d = \frac{\log(S/E) + (r - \frac{1}{2}\sigma^2)T}{\sigma\sqrt{T}}. \tag{4.2.12}$$

Asian option

Typically an Asian option is a contract giving the holder the right to buy an asset for its average price over some prescribed time period. The average rate of an asset S is given as

$$\frac{1}{t}\int_0^t S(\tau)d\tau.$$

Introducing the function

$$I = \int_0^t S(\tau)d\tau. \tag{4.2.13}$$

The partial differential equation pricing on European Asian option is

$$\frac{\partial V}{\partial t} + S\frac{\partial V}{\partial I} + \frac{1}{2}\sigma^2 S^2 \frac{\partial^2 V}{\partial S^2} + rS\frac{\partial V}{\partial S} - rV = 0. \tag{4.2.14}$$

At the expiration date $t = T$, we have the

$$\text{payoff} \;=\; \begin{cases} \max\left(S - \frac{1}{T}\int_0^t S(\tau)d\tau, 0\right) & \text{for call option} \\ \max\left(\frac{1}{T}\int_0^t S(\tau)d\tau - S, 0\right) & \text{for put option.} \end{cases} \tag{4.2.15}$$

In this chapter, we will consider only a call option. We can write the payoff for the call option as

$$S\left[\max\left(1 - \frac{1}{ST}\int_0^t S(\tau)d\tau, 0\right)\right].$$

Introducing the variable

$$R = \frac{1}{S}\int_0^t S(\tau)d\tau, \tag{4.2.16}$$

the payoff at the expiry can be written as

$$S\left[\max\left(1 - \frac{R}{T}, 0\right)\right].$$

In view of the form of the payoff function mentioned above, the option value takes the form

$$V(S, R, t) = SH(R, t), \quad \text{with} \;\; R = I/S. \tag{4.2.17}$$

Combining the above, we obtain a one dimensional PDE pricing the European Asian options (see [112] for further details):

$$\frac{\partial H}{\partial t} + \frac{1}{2}\sigma^2 R^2 \frac{\partial^2 H}{\partial R^2} + (1 - rR)\frac{\partial H}{\partial R} = 0, \tag{4.2.18}$$

with

$$H(R, T) = \max\left(1 - \frac{R}{T}, 0\right). \tag{4.2.19}$$

The above problems are solved by applying the mesh free method discussed in next section.

4.3 Application of radial basis functions in pricing exotic options

The use of radial basis functions is demonstrated here for two type of exotic options.

4.3.1 Pricing barrier options using RBFs

We approximate the unknown function V (the value of the European barrier option) using the radial basis functions as

$$V(S, t) \approx \sum_{j=1}^{N} a_j(t)\phi(\|S - x_j\|), \tag{4.3.1}$$

where a_j are unknown coefficients and $\phi(\|S - x_j\|)$ are the RBFs. We will use the following Gaussian radial basis functions for this problem

$$\phi(S) = e^{-\|S - x_j\|^2/c^2}, \tag{4.3.2}$$

where c is a positive parameter.

Collocating at the N points x_j $(j = 1, 2, \cdots, N)$, equation (4.2.1) becomes

$$\frac{\partial V(x_i,t)}{\partial t} + \frac{1}{2}\sigma^2 S_i^2 \frac{\partial^2 V(x_i,t)}{\partial S^2} + rS_i \frac{\partial V(x_i,t)}{\partial S} - rV(x_i,t) = 0. \tag{4.3.3}$$

Differentiating (4.3.1) we get

$$\frac{\partial V(x_i,t)}{\partial t} = \sum_{j=1}^{N} \frac{da_j(t)}{dt}\phi(\|S - x_j\|), \tag{4.3.4}$$

$$\frac{\partial V(x_i,t)}{\partial S} = \sum_{j=1}^{N} a_j \frac{\partial \phi(\|S - x_j\|)}{\partial S}, \tag{4.3.5}$$

$$\frac{\partial^2 V(x_i,t)}{\partial S^2} = \sum_{j=1}^{N} a_j \frac{\partial^2 \phi(\|S - x_j\|)}{\partial S^2}. \tag{4.3.6}$$

Now from (4.3.2) we have

$$\frac{\partial \phi(\|S - x_j\|)}{\partial S} = -\frac{2(S - x_j)}{c^2} e^{-\|S - x_j\|^2/c^2}, \tag{4.3.7}$$

and

$$\frac{\partial^2 \phi(\|S - x_j\|)}{\partial S^2} = \frac{4(S - x_j)^2 - 2c^2}{c^4} e^{-\|S - x_j\|^2/c^2}. \tag{4.3.8}$$

Substituting equations (4.3.4)-(4.3.8) into (4.3.3), we obtain

$$\sum_{j=1}^{N} \frac{d}{dt}(a_j(t))\phi(\|x_i - x_j\|) + \frac{1}{2}\sigma^2 x_i^2 \sum_{j=1}^{N} a_j(t) \left[\frac{4(x_i - x_j)^2 - 2c^2}{c^4}\phi(\|x_i - x_j\|)\right]$$
$$+ rx_i \sum_{j=1}^{N} a_j(t) \left[\frac{-2(x_i - x_j)}{c^2}\phi(\|x_i - x_j\|)\right] - r\sum_{j=1}^{N} a_j(t)\phi(\|x_i - x_j\|) = 0. \tag{4.3.9}$$

We write equation (4.3.9) in form of a system of differential equations as

$$\Phi \frac{d\mathbf{a}}{dt} + G\mathbf{a} = 0, \tag{4.3.10}$$

where

$$\Phi_{ij} = e^{-\|x_i - x_j\|^2/c^2}, \tag{4.3.11}$$

and

$$G_{ij} = \frac{1}{2}\sigma^2 x_i^2 \left(\frac{4(x_i - x_j)^2 - 2c^2}{c^4}\right)\Phi_{ij} + r x_i \left(\frac{-2(x_i - x_j)}{c^2}\right)\Phi_{ij} - r\Phi_{ij}. \tag{4.3.12}$$

To solve the system described by equation (4.3.10), we use a θ-method

$$\Phi\frac{\mathbf{a}^{n+1} - \mathbf{a}^n}{\Delta t} + \theta G\mathbf{a}^{n+1} + (1-\theta)G\mathbf{a}^n = 0, \tag{4.3.13}$$

with the initial condition given by equation(4.2.6).

We can rewrite equation (4.3.13) as

$$[\Phi - (1-\theta)\Delta t G]\mathbf{a}^n = [\Phi + \theta\Delta t G]\mathbf{a}^{n+1}, \tag{4.3.14}$$

$$\mathbf{a}^n = [\Phi - (1-\theta)\Delta t G]^{-1}[\Phi + \theta\Delta t G]\mathbf{a}^{n+1}. \tag{4.3.15}$$

Equation (4.3.1) applied for all collocation point can be written in the matrix form as

$$\mathbf{V} = \Phi\mathbf{a}. \tag{4.3.16}$$

Using equation (4.3.20), equation (4.3.19) can be written as

$$V^n = \Phi[\Phi - (1-\theta)\Delta t G]^{-1}[\Phi + \theta\Delta t G]\Phi^{-1}V^{n+1}. \tag{4.3.17}$$

The above equation is solved along with (4.2.6) to obtain the numerical solution. Also the form of this equation should be read in context to the computing process because in the problems like those considered in this chapter, we usually have a final boundary value problem rather than an initial boundary value problem. Also note that the scheme (4.3.18) corresponding to $\theta = 0,\ 0.5,$ and 1 are the implicit Euler, Crank-Nicolson and explicit Euler methods, respectively.

4.3.2 Pricing Asian options using RBFs

To solve an Asian option problem (4.2.18) with initial condition given by equation (4.2.19) we use inverse multiquadric radial basis function given by

$$\phi(S) = \frac{1}{\sqrt{\|S - R_j\|^2 + c^2}}. \tag{4.3.18}$$

Differentiating we get

$$\frac{\partial \phi(\|S - R_j\|)}{\partial S} = \frac{-(S - R_j)}{(\|S - R_j\|^2 + c^2)^{3/2}}, \tag{4.3.19}$$

and

$$\frac{\partial^2 \phi(\|S - R_j\|)}{\partial S^2} = \frac{2(S - R_j)^2 - c^2}{(\|S - R_j\|^2 + c^2)^{5/2}}. \tag{4.3.20}$$

Substituting equations (4.3.4) - (4.3.6) and (4.3.18) - (4.3.20) into (4.2.18), we obtain

$$\sum_{j=1}^{N} \frac{d}{dt}(a_j(t)) \left[\frac{1}{\sqrt{\|R_i - R_j\|^2 + c^2}}\right] + \frac{1}{2}\sigma^2 x_i^2 \sum_{j=1}^{N} a_j(t) \left[\frac{2(R_i - R_j)^2 - c^2}{(\|R_i - R_j\|^2 + c^2)^{5/2}}\right]$$
$$+(1 - r)R_i \sum_{j=1}^{N} a_j(t) \left[\frac{-(R_i - R_j)}{(\|R_i - R_j\|^2 + c^2)^{3/2}}\right] = 0. \tag{4.3.21}$$

We can write equation (4.3.21) in form of a system of differential equations as

$$\Phi \frac{d\mathbf{a}}{dt} + G\mathbf{a} = 0, \tag{4.3.22}$$

where

$$\Phi_{ij} = \frac{1}{\sqrt{\|R_i - R_j\|^2 + c^2}}, \tag{4.3.23}$$

and

$$G_{ij} = \frac{1}{2}\sigma^2 R_i^2 \left(\frac{1}{\sqrt{\|R_i - R_j\|^2 + c^2}}\right) + (1 - r)R_i \left(\frac{-(R_i - R_j)}{(\|R_i - R_j\|^2 + c^2)^{(3/2)}}\right). \tag{4.3.24}$$

To solve the system described by equation (4.3.22), we use a θ-method

$$\Phi\frac{\mathbf{a}^{n+1}-\mathbf{a}^{n}}{\Delta t}+\theta G\mathbf{a}^{n+1}+(1-\theta)G\mathbf{a}^{n}=0, \tag{4.3.25}$$

with the initial condition given by equation(4.2.19).

Also note that the scheme corresponding to $\theta = 0,\ 0.5,$ and 1 are the implicit Euler, Crank-Nicolson and explicit Euler methods, respectively.

4.4 Stability analysis of the numerical method

To proceed with the stability analysis, let us define the error at the n^{th} time level by

$$e^n = V^n_{\text{exact}} - V^n_{\text{app}}, \tag{4.4.1}$$

where V^n_{exact} is the exact solution and V^n_{app} is the numerical solution obtained by either (4.3.17) or (4.3.25).

For the scheme given by (4.3.17) the error equation at $(n+1)^{th}$ level can be written as

$$e^n = Pe^{n+1}, \tag{4.4.2}$$

where P is the amplification matrix is given by

$$B = \Phi^{-1}[\Phi + \theta\Delta t G][\Phi - (1-\theta)\Delta t G]^{-1}\Phi.$$

The numerical scheme is stable if $\rho(B) \leq 1$, where $\rho(B)$ is the spectral radius of B. Substituting B in equation (4.4.2), we obtain

$$[\Phi - (1-\theta)\Delta t G]\Phi^{-1}e^n = [\Phi + \theta\Delta t G]\Phi^{-1}e^{n+1}. \tag{4.4.3}$$

This implies

$$[I - (1-\theta)\Delta t M]e^n = [I + \theta\Delta t M]e^{n+1}, \tag{4.4.4}$$

where $M = G\Phi^{-1}$ and $I \in \mathbb{R}^{N\times N}$ is the identity matrix.

It is clear from equation (4.4.4) that the numerical scheme is stable if all the eigenvalues of the matrix $[I-(1-\theta)\Delta tM]^{-1}[I+\theta\Delta tM]$ are less than unity, which means that

$$\left| \frac{1+\theta\Delta t\lambda_M}{1-(1-\theta)\Delta t\lambda_M} \right| \leq 1. \tag{4.4.5}$$

where λ_M represent the eigenvalues of the matrix M.

Now we consider different cases. Firstly, when $\theta = 1$, we have explicit Euler method. The above condition for stability becomes

$$|1+\Delta t\lambda_M| \leq 1, \tag{4.4.6}$$

which implies that the explicit Euler method will be stable if

$$\Delta t \geq \frac{-2}{\lambda_M} \quad \text{and} \quad \lambda_M \leq 0. \tag{4.4.7}$$

Secondly, when $\theta = 0$, we have implicit Euler method which is clearly unconditionally stable as can be seen from (4.4.5). Finally, when $\theta = 0.5$, we have the Crank-Nicolson's method. Even in this case, the inequality (4.4.5) will hold as long as $\lambda_M \leq 0$ and this does happen. Therefore, the Crank-Nicolson's method will be unconditionally stable. The stability analysis for (4.3.25) can be done along the similar lines.

4.5 Numerical results and discussion

Using the RBF approach, the resulting problems for European barrier and European Asian call options are solved via Crank-Nicolson's method (i.e., $\theta = 0.5$). Results are presented in Table 4.5.1 and Figure 4.5.1.

The parameters used for the simulations for European barrier option problem are: $r = 0.05$, $\sigma = 0.2$, $E = 10$, $t_0 = 0$, $T = 0.5$, $\Delta t = 0.005$, $K = 9$, $x_0 = 0$ and $X = 30$. We have set the parameter c in the radial basis function as $2h$

where $h = (X - x_0)/(N - 1)$. The first column in Table 4.5.1 represents values of the asset price S, the second column represents the exact solution as in [36] and the other three columns indicated the numerical values of the European barrier option that we obtain using the radial basis functions with Gaussian, Inverse Multiquadratic, Multiquadratic respectively.

For double barrier option we used Multiquadratic RBFs with parameters:$r = 0.05,\ \sigma = 0.25,\ E = 100,\ t_0 = 0,\ T = 0.5,\ K_1 = 95,\ K_2 = 110,\ x_0 = 0$ and $X = 115$. We used Crank-Nicolson's method (i.e., $\theta = 0.5$)and the numerical results are presented in Table 4.5.2. The first column of this table represents the time step Δt, the second and third column represents the option values at barriers K_1 and K_2, the next two columns represents the errors at K_1 and K_2. We used a reference solution 0.09697960007895 at $K_1 = 95$ and 0.08148159339106 at $K_2 = 110$. We found that our results for double barrier option are close to those presented in Table 1 in Wade *et al.* [105].

Figure 4.5.2 and Table 4.5.3 contain results for digital call option at strike price $E = 0.5$ using Multiquadric radial basis functions. The other parameter used are: $S_0 = 0,\ S_{\max} = 1,\ T = 0.25,\ r = 0.05,$ and $\sigma = 0.2$ with $N = 101$ and $\Delta t = 0.0025$. The first column of this table represents the asset price S, the second column represents the exact solution using (4.2.11), the third column represents the value of the option using RBFs, and the last column represents the errors.

For the European Asian call options, we choose $r = 0.1,\ \sigma = 0.2,\ D = 0,\ t_0 = 0,\ T = 0.5,\ R_0 = 0,$ and $R_{\max} = 1$. We again use the Crank-Nicolson's method with $\Delta t = 0.005$.

Using the multiquadratic and inverse multiquadratic radial basis functions, we obtain reasonably accurate results in the sense that they are very close to those obtained by Goto *et al.* in [36].

Numerical results are shown in Table 4.5.4 and Figures 4.5.3, 4.5.4 and 4.5.5. The values of c used for the simulation are respectively, 0.02, 0.03 and 0.04 in the cases when Gaussian, Multiquadratic and Inverse Multiquadratic RBFs are used. It is worth mentioning here that the authors in [36] pointed out that the Multiquadratic RBFs when used with $c = 0.04$ do not provide correct numerical value of the option. Taking this into account, we have used the value of c as 0.03 and obtained desired results (see the results in Figure 4.5.4). A slight change in the results as compared to those in [36] are due to the difference in the value of σ that they have used. The first column in Table 4.5.4 represents the values of the asset price R and the other three columns indicated the numerical values of the European barrier option that we obtain using the radial basis functions with Gaussian, Multiquadratic, Inverse Multiquadratic, respectively.

Table 4.5.1: Values of a European down-and-out call option using Radial Basis Functions

S	Exact	RBF(G)	RBF(IMQ)	RBF(MQ)
1	0.0000	0.0000	0.0000	0.0000
3	0.0000	0.0000	0.0000	0.0000
5	0.0000	0.0000	0.0000	0.0000
7	0.0000	0.0000	0.0000	0.0000
9	0.0000	0.0000	0.0000	0.0000
11	1.3998	1.4065	1.4065	1.4065
13	3.2591	3.2591	3.2591	3.2591
15	5.2475	5.2474	5.2474	5.2474
17	7.2469	7.2458	7.2465	7.2469
19	9.2469	9.2243	9.2383	9.2466

G: Gaussian.

MQ: Multiquadratic.

IMQ: Inverse Multiquadratic.

Table 4.5.2: Values of a double barrier European down-and-out call option using Radial Basis Functions

Δt	Option value at K_1	Option value at K_2	Error at K_1	Error at K_2
0.025	0.0235	0.2105	7.35E-2	1.29E-2
0.0125	0.0449	0.0503	5.21E-2	3.12E-2
0.00625	0.0411	0.0349	5.58E-2	4.66E-2
0.003125	0.0388	0.0311	5.81E-2	5.04E-2
0.0015625	0.0377	0.0293	5.93E-2	5.22E-2

Table 4.5.3: Values of digital call Option using radial basis functions with $\Delta t = 0.0025$

S	Exact	RBF101	Error
0.1000	0.0000	0.0000	0.0000
0.2000	0.0000	0.0000	0.0000
0.3000	0.0000	0.0000	0.0000
0.4000	0.0153	0.0152	0.0001
0.5000	0.5233	0.5233	0.0000
0.6000	0.9591	0.9594	0.0003
0.7000	0.9873	0.9874	0.0001
0.8000	0.9876	0.9874	0.0001
0.9000	0.9876	0.9858	0.0018
1.0000	0.9876	0.9876	0.0000

Table 4.5.4: Values of European Asian call option using Radial Basis Functions

R	RBF(G)	RBF(MQ)	RBF(IMQ)
0.0	0.0527	0.0518	0.0519
0.1	0.0019	0.0017	0.0018
0.2	0.0002	0.0000	0.0001
0.3	0.0001	0.0000	0.0000
0.4	0.0000	0.0001	0.0000
0.5	0.0000	0.0003	0.0002
0.6	0.0000	0.0005	0.0003
0.7	0.0000	0.0005	0.0002
0.8	0.0000	0.0004	0.0001
0.9	0.0000	0.0002	0.0001
1.0	0.0000	0.0000	0.0000

G: Gaussian.

MQ: Multiquadratic.

IMQ: Inverse Multiquadratic.

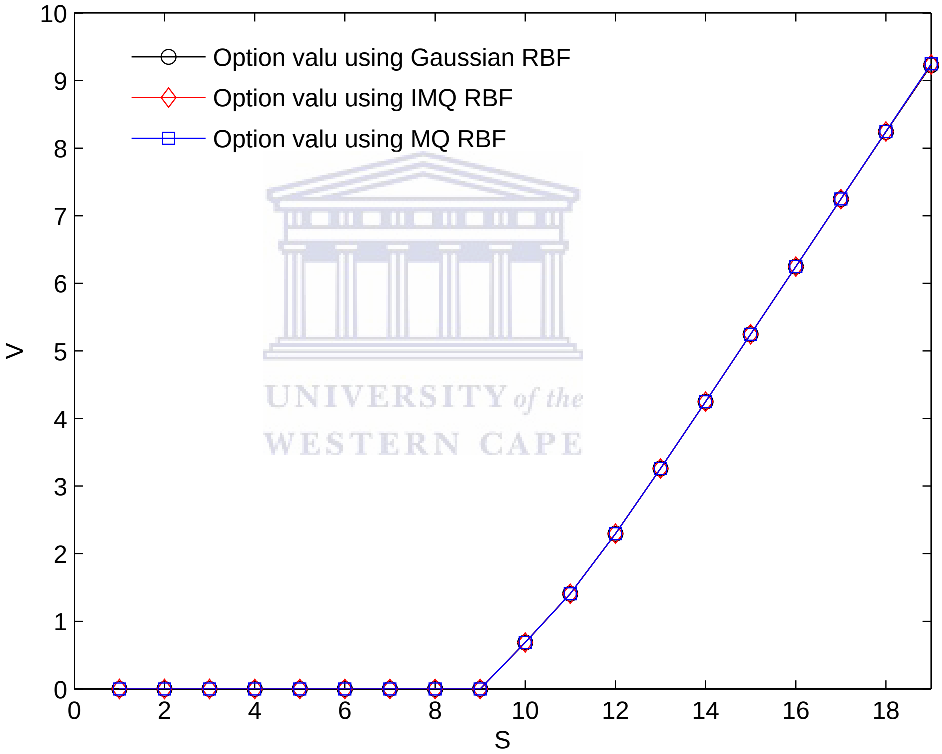

Figure 4.5.1: Values of the European barrier (down-and-out) option at t_0 using 121 points and $r = 0.05,\ \sigma = 0.2,\ E = 10,\ t_0 = 0,\ T = 0.5,\ S_0 = 0$ and $S_{\max} = 30$

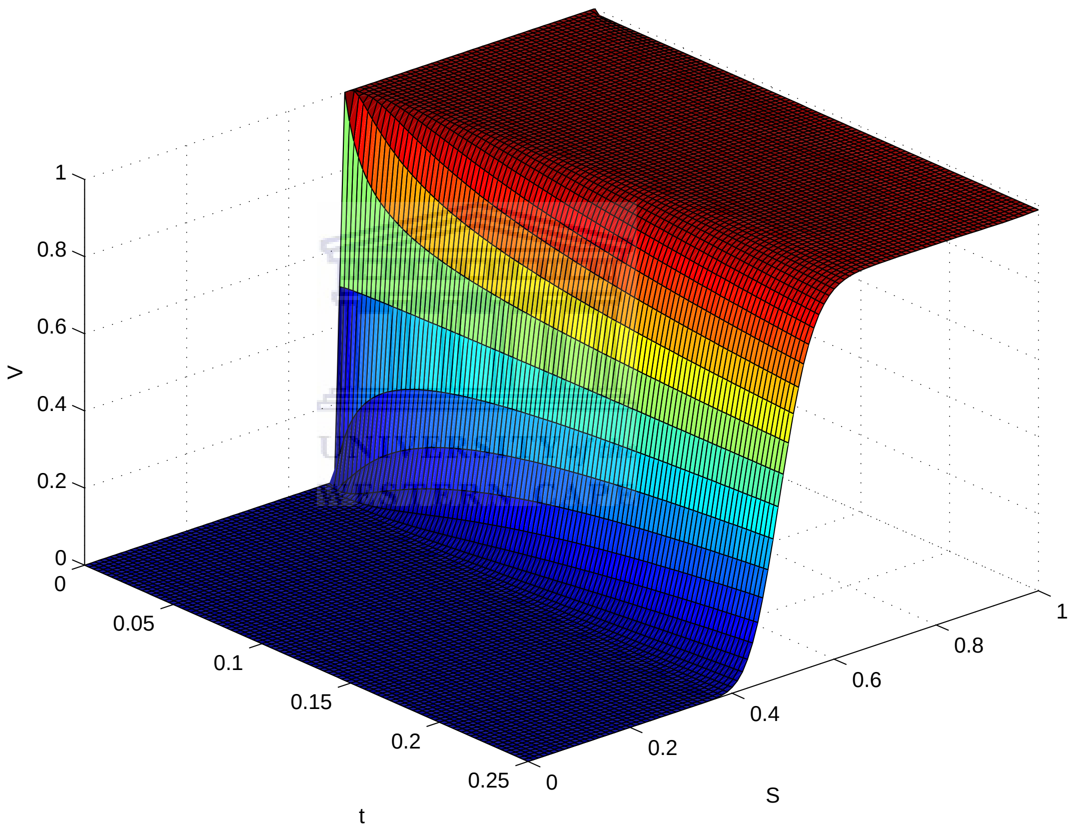

Figure 4.5.2: Values of the digital call option using 101 points and $r = 0.05$, $\sigma = 0.2$, $E = 0.5$, $t_0 = 0$, $T = 0.25$, $S_0 = 0$ and $S_{\max} = 1$

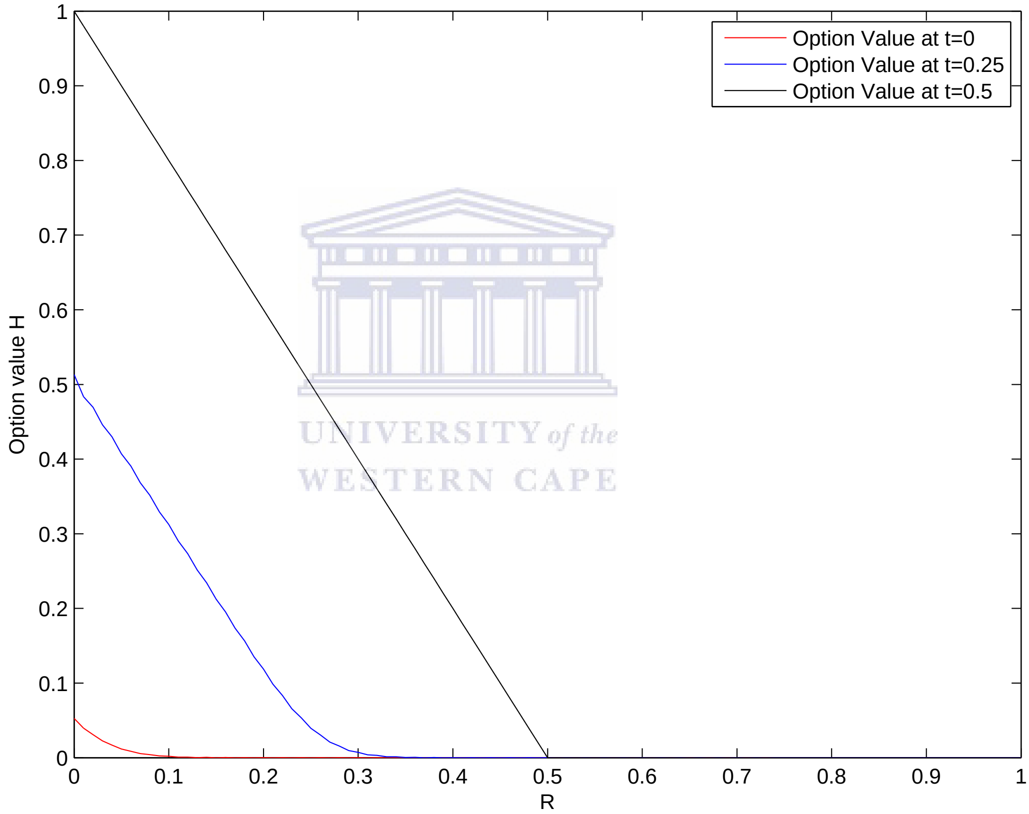

Figure 4.5.3: Values of the European Asian call option using RBF (Gaussian) with 101 points and $r = 0.1,\ \sigma = 0.2,\ t_0 = 0,\ T = 0.5,\ R_0 = 0$ and $R_{\max} = 1$

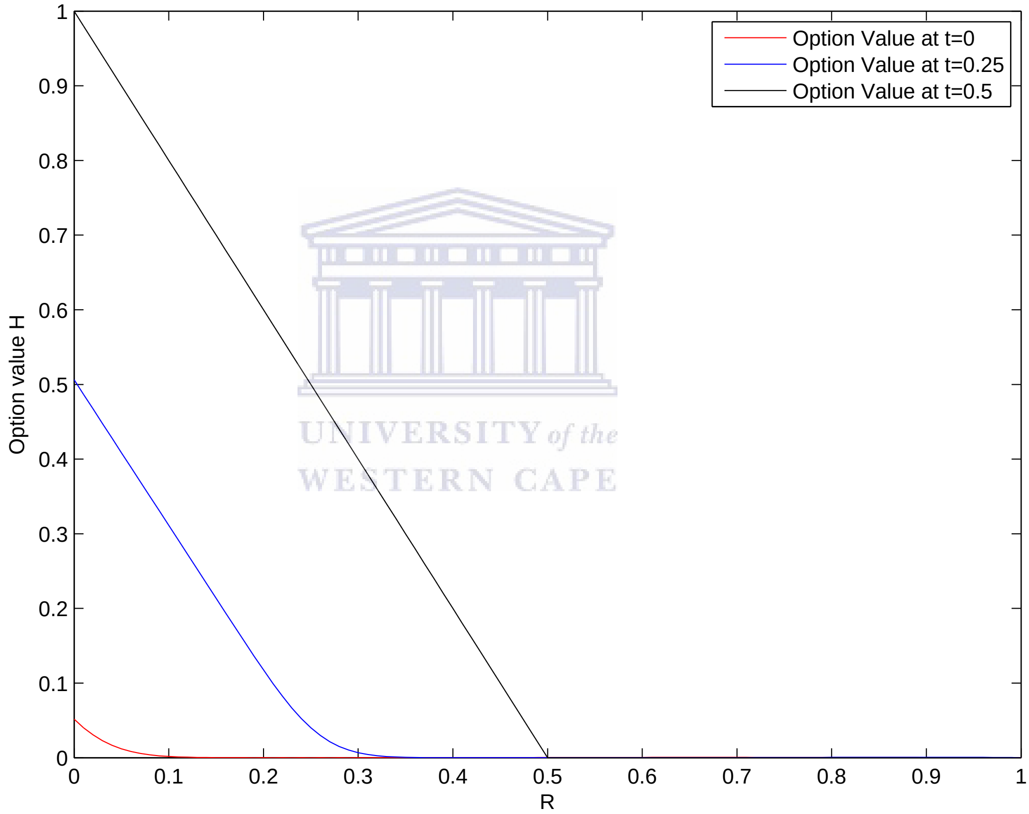

Figure 4.5.4: Values of the European Asian call option using RBF (Multiquadric) with 101 points and $r = 0.1,\ \sigma = 0.2,\ t_0 = 0,\ T = 0.5,\ R_0 = 0$ and $R_{\max} = 1$

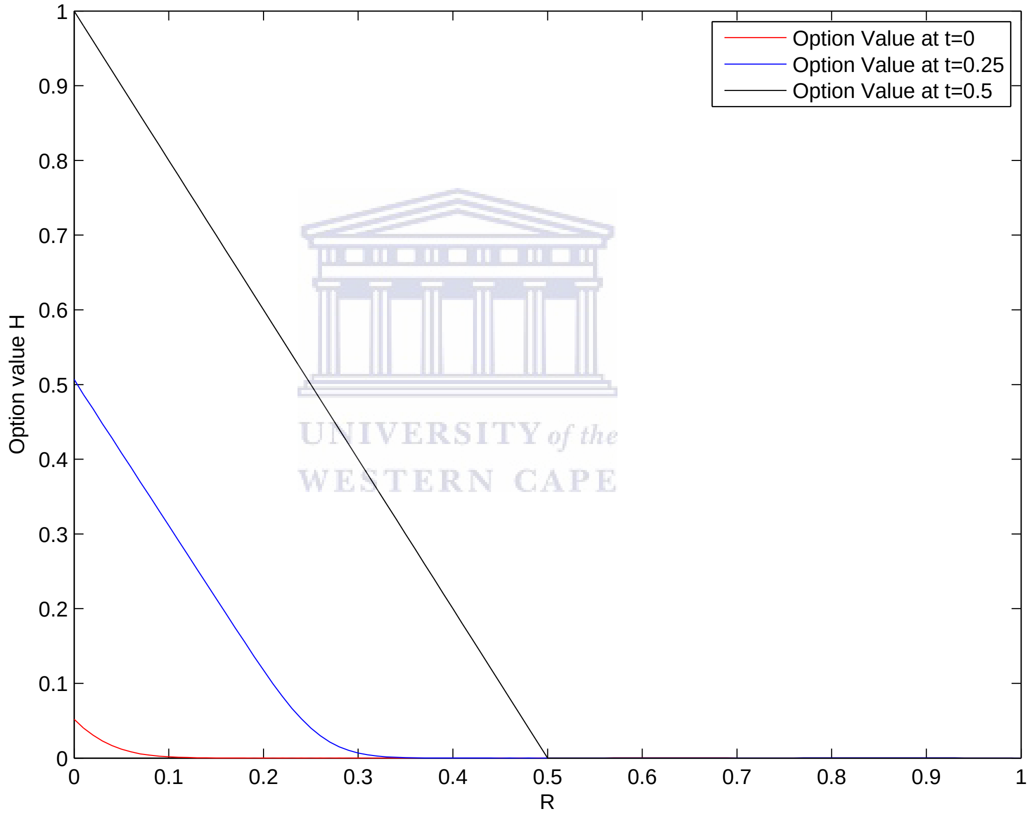

Figure 4.5.5: Values of the European Asian call option using RBF (Inverse multi-quadric) with 101 points and $r = 0.1,\ \sigma = 0.2,\ t_0 = 0,\ T = 0.5,\ R_0 = 0$ and $R_{\max} = 1$

Chapter 5

A radial point interpolation method to price options

In this chapter we introduce a radial point interpolation method (RPIM) to price European and American put options. The case when no polynomial basis functions are used, the RPIM approach reduces to the RBFs approach. The proposed method is analyzed for stability. Some comparative numerical results are also presented. The approach presented here is more beneficial for multi-asset problems which is out of the scope of this thesis due to space limitation. However, it is the scope for our future research.

5.1 Introduction

There are numerous variants of the mesh free approaches. One of the most popular ones is the radial point interpolation method (RPIM) which is the subject of study in this chapter and therefore we provide below a brief account of work using RPIMs.

Wang and Liu [106] proposed a point interpolation meshless method based on combining radial and polynomial basis functions. The interpolation function thus obtained passes through all scattered points and has an influence on the domain and therefore shape functions have delta function property. This makes the implementation of essential boundary conditions much easier than the other meshless methods based on the moving least-squares approximation. In addition, the partial derivatives of shape functions are easily obtainable.

In [107], Wang *et al.* proposed an algorithm to solve Biots consolidation problem using a RPIM. In time domain they proposed fully implicit integration scheme to avoid spurious ripple effects. They studied some examples with structured and unstructured nodes.

Dai *et al.* [24] presented a mesh free method for the static and dynamic analysis of functionally graded material (FGM) plates based on the radial point interpolation method (RPIM). They studied the convergence properties of their approach and compared their results with those obtained by the finite element method.

In this chapter we present a radial point interpolation method for pricing American and European put options. Using RPIM, we obtain a system of ordinary differential equations which is then solved by a time integration methods. Since the American options are allowed to be exercised any time before their expiry; they in turn lead to a free boundary problem. To resolve the difficulties associated in solving this free boundary problem, we use a penalty method.

The RPIM has the following advantages [69]: The shape function has the Kronecker delta property, which facilitates easy treatment of the essential boundary conditions; the moment matrix used in constructing shape functions is always invertible for irregular nodes; and the polynomials can be exactly reproduced up to desired order by polynomial augmentation. Some of these properties make the RPIM as a very powerful tool when solving complex problems like those considered in this chapter as well as their possible extensions to price multi-asset options.

The rest of the chapter is organized as follows. The partial differential equation models for pricing the two type of options described in Chapter 2 are again described in Section 5.2 so as to keep this chapter self-contained. In Section 5.3 we discuss the development of the radial point interpolation method. Section 5.4 deals with the application of this method to solve these problems. The stability analysis of the full numerical methods is presented in Section 5.5. Some numerical results along with a discussion on them are given in Section 5.6.

5.2 Problem description

The Black-Scholes model for pricing American and European options is an initial-boundary value problem. For European options this problem reads as

$$\frac{\partial V}{\partial t} + \frac{1}{2}\sigma^2 S^2 \frac{\partial^2 V}{\partial S^2} + rS\frac{\partial V}{\partial S} - rV = 0, \tag{5.2.1}$$

where r is the risk-free interest rate, S is the price of the stock, σ is the volatility of the stock price, D is the dividend yield (which is constant in the present case) on the stock, and $V(S,t)$ denotes the option's value at time t for the stock price S.

The initial condition is given by the terminal payoff function

$$V(S,T) = \begin{cases} \max(E - S, 0) & \text{for put} \\ \max(S - E, 0) & \text{for call} \end{cases} \tag{5.2.2}$$

and the boundary conditions are given by

$$V(S,T) = \begin{cases} V(0,t) = Ee^{-r(T-t)}, & V(S,t) \to 0 \ \text{ as } \ S \to \infty \quad \text{for put} \\ V(0,t) = 0, & V(S,t) \to S \ \text{ as } \ S \to \infty \quad \text{for call} \end{cases} \tag{5.2.3}$$

where T is the maturity time and E is the strike price of the option.

The exact solution of equation (5.2.1) with the initial condition (5.2.2) and the boundary conditions (5.2.3) is given by ([112])

$$V(S,T) = \begin{cases} Ee^{-r(T-t)}N(-d_2) - SN(-d_1) & \text{for put} \\ SN(d_1) - Ee^{-r(T-t)}N(d_2) & \text{for call} \end{cases} \tag{5.2.4}$$

where $N(\cdot)$ is the cumulative distribution function of the standard normal distribution with

$$d_1 = \frac{\log(S/E) + (r + \frac{1}{2}\sigma^2)(T-t)}{\sigma\sqrt{T-t}} \tag{5.2.5}$$

and

$$d_2 = \frac{\log(S/E) + (r - \frac{1}{2}\sigma^2)(T-t)}{\sigma\sqrt{T-t}}. \tag{5.2.6}$$

On the other hand, the American option pricing problem takes the form of a free-boundary problems. The early exercise possibility leads to the following model for the value $P(S,t)$ of an American put option to sell the underlying asset [55]:

$$\begin{aligned}
&\frac{\partial P}{\partial t} + \frac{1}{2}\sigma^2 S^2 \frac{\partial^2 P}{\partial S^2} + rS\frac{\partial P}{\partial S} - rP = 0, \quad S > S_f(t),\ 0 \le t < T \\
&P(S,T) = \max(E-S,0), \quad S \ge 0, \\
&\frac{\partial P}{\partial S}(S_f,t) = -1, \\
&P(S_f(t),t) = E - S_f(t), \\
&\lim_{S\to\infty} P(S,t) = 0, \\
&S_f(T) = E, \\
&P(S,t) = E - S, \quad 0 \le S < S_f(t),
\end{aligned} \tag{5.2.7}$$

where $S_f(t)$ represents the free boundary, E represent the exercise price of the option, P denotes the value of the option and as before, σ is the volatility of the underlying asset, r is the risk-free interest rate, D is the dividend yield on the stock.

Since early exercise is permitted, the P of the option must satisfy

$$P(S,t) \ge \max(E-S,0), \quad S \ge 0,\ 0 \le t \le T. \tag{5.2.8}$$

In the next section, we give a brief discussion on how to construct the shape functions and their various derivatives using RPIM.

5.3 The Radial point interpolation method

Following [69], we approximate the solution using the RPIM as

$$u(x) = \sum_{i=1}^{n} R_i(x)a_i + \sum_{j=1}^{m} P_j(x)b_j = \mathbf{R}^T(\mathbf{x})\mathbf{a} + \mathbf{P}^T(\mathbf{x})\mathbf{b}, \tag{5.3.1}$$

where $R_i(x)$ is the i-th radial basis function (RBF), n is the number of RBFs, m is the number of polynomial basis functions (PBFs), and $P_j(x)$ is monomial in the space coordinates $x^T = [x, y]$. It is clear that the conventional RBF is augmented with m polynomial basis functions or in another words we can say that when $m = 0$, this RPIM will coincide with the conventional RBF approach. Coefficients **a** and **b** are constant vectors yet to be determined. The RBFs that we use in this chapter are described in Table 1.2.1 in Chapter 1.

Coefficients a_i and b_j in equation (5.3.1), can be determined by enforcing equation (5.3.1) to be satisfied at n nodes surrounding the point of interest x. This leads to n linear equations, one at each node. The matrix form of these equations can be expressed as

$$\mathbf{U}_s = \mathbf{R}\mathbf{a} + \mathbf{P}_m\mathbf{b}, \tag{5.3.2}$$

where the solution vector is

$$\mathbf{U}_s = [u_1 \;\; u_2 \;\; \cdots \;\; u_n]^T, \tag{5.3.3}$$

the moment matrix of RBFs is

$$\mathbf{R} = \begin{bmatrix} R_1(r_1) & R_2(r_1) & \cdots & R_n(r_1) \\ R_1(r_2) & R_2(r_2) & \cdots & R_n(r_2) \\ \vdots & \vdots & & \vdots \\ R_1(r_n) & R_2(r_n) & \cdots & R_n(r_n) \end{bmatrix}_{(n\times n)}, \tag{5.3.4}$$

with

$$r_k = \sqrt{(x_k - x_i)^2 + (y_k - y_i)^2}, \tag{5.3.5}$$

and the polynomial moment matrix is

$$\mathbf{P}_m = \begin{bmatrix} 1 & x_1 & y_1 & \cdots & P_m(x_1) \\ 1 & x_2 & y_2 & \cdots & P_m(x_2) \\ \vdots & \vdots & \vdots & & \vdots \\ 1 & x_n & y_n & \cdots & P_m(x_n) \end{bmatrix}_{(n\times m)}. \tag{5.3.6}$$

The coefficient vector multiplying to RBFs in (5.3.1) is

$$\mathbf{a} = [a_1 \ \ a_2 \ \ \cdots \ \ a_n]^T, \tag{5.3.7}$$

and the coefficient vector multiplying to PBFs in (5.3.1) is

$$\mathbf{b} = [b_1 \ \ b_2 \ \ \cdots \ \ b_m]^T. \tag{5.3.8}$$

There are $n + m$ variables in equation (5.3.2). The additional m equations comes from the following m constraints

$$\sum_{i=1}^{n} P_j(x_i)a_i = \mathbf{P}_m^T\mathbf{a} = 0, \quad j = 1, 2, \cdots, m. \tag{5.3.9}$$

Combining equations (5.3.2) and (5.3.9) we obtain the following system of equations

$$\widehat{\mathbf{U}}_s = \begin{bmatrix} \mathbf{U}_s \\ \mathbf{0} \end{bmatrix} = \begin{bmatrix} \mathbf{R} & \mathbf{P}_m \\ \mathbf{P}_m^T & \mathbf{0} \end{bmatrix} \begin{bmatrix} \mathbf{a} \\ \mathbf{b} \end{bmatrix} = \mathbf{G}\widetilde{\mathbf{a}} \tag{5.3.10}$$

where

$$\widetilde{\mathbf{a}} = [a_1 \ \ a_2 \ \ \cdots \ \ a_n \ \ b_1 \ \ b_2 \ \ \cdots \ \ b_m]^T, \tag{5.3.11}$$

and

$$\widehat{\mathbf{U}}_s = [u_1 \;\; u_2 \;\; \cdots \;\; u_n \;\; 0 \;\; 0 \;\; \cdots \;\; 0]^T. \tag{5.3.12}$$

Because the matrix $\mathbf{R}$ is symmetric, it is therefore clear from the structure of the matrix $\mathbf{G}$ that it will also be symmetric.

Solving system (5.3.10), we obtain

$$\widetilde{\mathbf{a}} = \begin{bmatrix} \mathbf{a} \\ \mathbf{b} \end{bmatrix} = \mathbf{G}^{-1}\widehat{\mathbf{U}}_s. \tag{5.3.13}$$

Now equation (5.3.1) can be written as

$$\begin{aligned} u(x) &= \mathbf{R}^T(x)\mathbf{a} + \mathbf{P}^T(x)\mathbf{b} = [\mathbf{R}^T(x) \;\; \mathbf{P}^T(x)] \begin{bmatrix} \mathbf{a} \\ \mathbf{b} \end{bmatrix} \\ &= [\mathbf{R}^T(x) \;\; \mathbf{P}^T(x)]G^{-1}\widehat{\mathbf{U}}_s \qquad \text{using (5.3.13)} \\ &= \widehat{\Phi}^T(x)\widehat{\mathbf{U}}_s, \end{aligned} \tag{5.3.14}$$

where the RPIM shape functions can be expressed as

$$\widehat{\Phi}^T(x) = [\mathbf{R}^T(x) \;\; \mathbf{P}^T(x)]G^{-1} \tag{5.3.15}$$

$$= [\phi_1(x) \;\; \phi_2(x) \;\; \cdots \;\; \phi_n(x) \;\; \phi_{n+1}(x) \;\; \cdots \;\; \phi_{n+m}(x)]. \tag{5.3.16}$$

Finally, the RPIM shape functions corresponding to the nodal displacements vector $\Phi(x)$ are obtained as

$$\Phi(x) = [\phi_1(x) \;\; \phi_2(x) \;\; \cdots \;\; \phi_n(x)], \tag{5.3.17}$$

where

$$\Phi_k(x) = \sum_{i=1}^{n} R_i(x)\bar{G}_{i,k} + \sum_{j=1}^{m} P_j(x)\bar{G}_{n+j,k}, \quad k = 1, 2, \cdots, n, \tag{5.3.18}$$

in which $\bar{G}_{i,k}$ is the $(i,k)^{th}$ element of matrix G^{-1}.

Equation (5.3.14) can be re-written as

$$u(x) = \Phi(x)\mathbf{U}_s = \sum_{i=1}^{n} \phi_i u_i. \tag{5.3.19}$$

The derivatives of $u(x)$ are obtained as

$$u_x(x) = \Phi_x^T(x)\mathbf{U}_s. \tag{5.3.20}$$

In the above, u_x indicates a partial differentiation with x.

Equation (5.3.20) gives

$$\frac{\partial \Phi_k}{\partial x} = \sum_{i=1}^{n} \frac{\partial R_i}{\partial x}\bar{G}_{i,k} + \sum_{j=1}^{m} \frac{\partial P_j}{\partial x}\bar{G}_{n+j,k} \tag{5.3.21}$$

and

$$\frac{\partial^2 \Phi_k}{\partial x^2} = \sum_{i=1}^{n} \frac{\partial^2 R_i}{\partial x^2}\bar{G}_{i,k} + \sum_{j=1}^{m} \frac{\partial^2 P_j}{\partial x^2}\bar{G}_{n+j,k}. \tag{5.3.22}$$

In case of Multiquadric radial basis function

$$R(\|S - x_j\|) = \sqrt{(\|S - x_j\|)^2 + c^2}, \tag{5.3.23}$$

the partial derivatives are obtained as

$$\frac{\partial R(\|S - x_j\|)}{\partial S} = \frac{(\|S - x_j\|)}{\sqrt{(\|S - x_j\|)^2 + c^2}} \tag{5.3.24}$$

and

$$\frac{\partial^2 R(\|S - x_j\|)}{\partial S^2} = \frac{c^2}{((\|S - x_j\|)^2 + c^2)^{3/2}}. \tag{5.3.25}$$

In the next section we will discuss the use of above RPIM in pricing European and American put options.

5.4 Application of the radial point interpolation method for pricing options

5.4.1 Pricing European options using RPIM

We approximate the unknown function, the value of the European option, V, using the radial basis functions as

$$V(S,t) \approx \sum_{j=1}^{N} a_j(t)\Phi(\|S-x_j\|), \tag{5.4.1}$$

where $\Phi(\|S-x_j\|)$ are the RPIM shape functions given by equation (5.3.17).

Collocating at the points x_j $j = 1, 2, \cdots, N$, equation (5.2.1) becomes

$$\frac{\partial V(x_i,t)}{\partial t} + \frac{1}{2}\sigma^2 S_i^2 \frac{\partial^2 V(x_i,t)}{\partial S^2} + rS_i \frac{\partial V(x_i,t)}{\partial S} - rV(x_i,t) = 0. \tag{5.4.2}$$

Differentiating (5.4.1), we get

$$\frac{\partial V(x_i,t)}{\partial t} = \sum_{j=1}^{N} \frac{da_j(t)}{dt}\Phi(\|S-x_j\|), \tag{5.4.3}$$

$$\frac{\partial V(x_i,t)}{\partial S} = \sum_{j=1}^{N} a_j \frac{\partial \Phi(\|S-x_j\|)}{\partial S} \tag{5.4.4}$$

and

$$\frac{\partial^2 V(x_i,t)}{\partial S^2} = \sum_{j=1}^{N} a_j \frac{\partial^2 \Phi(\|S-x_j\|)}{\partial S^2}. \tag{5.4.5}$$

In the construction of our radial point interpolation method, we use Multiquadric radial basis functions (mentioned in Table 1.2.1) and the polynomial basis functions (as indicated in (5.3.6)). By using equations (5.3.21)-(5.3.25) and substituting equations (5.4.3)-(5.4.5) into (5.4.2), we obtain

$$\mathbf{\Phi}\frac{d\mathbf{a}}{dt} + \widetilde{H}\mathbf{a} = 0, \tag{5.4.6}$$

where

$$\widetilde{H} = \frac{1}{2}\sigma^2 x_i^2 \frac{\partial^2 \Phi}{\partial x^2} + r x_i \frac{\partial \Phi}{\partial x} - r\Phi. \tag{5.4.7}$$

To solve the system described by equation (5.4.6), we use a θ-method

$$\mathbf{\Phi}\frac{\mathbf{a}^{n+1} - \mathbf{a}^n}{\Delta t} + \theta\widetilde{H}\mathbf{a}^{n+1} + (1-\theta)\widetilde{H}\mathbf{a}^n = 0, \tag{5.4.8}$$

with the initial condition given by the first part of equation (5.2.2) and boundary conditions given by the first part of equation (5.2.3).

We can rewrite equation (5.4.8) as

$$[\mathbf{\Phi} - (1-\theta)\Delta t\widetilde{H}]\mathbf{a}^n = [\mathbf{\Phi} + \theta\Delta t\widetilde{H}]\mathbf{a}^{n+1}, \tag{5.4.9}$$

$$\mathbf{a}^n = [\mathbf{\Phi} - (1-\theta)\Delta t\widetilde{H}]^{-1}[\mathbf{\Phi} + \theta\Delta t\widetilde{H}]\mathbf{a}^{n+1}. \tag{5.4.10}$$

Equation (5.4.1) applied for all collocation points can be written in the matrix form as

$$\mathbf{V} = \mathbf{\Phi}\mathbf{a}. \tag{5.4.11}$$

Using equation (5.4.11), equation (5.4.10) can be written as

$$V^n = \mathbf{\Phi}[\mathbf{\Phi} - (1-\theta)\Delta t\widetilde{H}]^{-1}[\mathbf{\Phi} + \theta\Delta t\widetilde{H}]\mathbf{\Phi}^{-1}V^{n+1}. \tag{5.4.12}$$

The above equation is solved along with (5.2.2) and the first part of equation (5.2.3) to obtain the numerical solution. Also the form of this equation should be read in context to the computing process because in the problems like those considered in this chapter, we usually have a final boundary value problem rather than an initial boundary value problem. Note that the scheme given by (5.4.9) corresponding to $\theta = 0,\ 0.5,$ and 1 are the implicit Euler, Crank-Nicolson and explicit Euler methods, respectively.

5.4.2 Pricing American options using RPIM

In the case of the American option problem (5.2.7), we note that it is a free boundary problem. Therefore before we proceed we modify the model by adding a penalty term. This leads to the following nonlinear partial differential equation on a fixed domain which is an initial-boundary value problem:

$$\frac{\partial P_\epsilon}{\partial t} + \frac{1}{2}\sigma^2 S^2 \frac{\partial^2 P_\epsilon}{\partial S^2} + rS\frac{\partial P_\epsilon}{\partial S} - rP_\epsilon + \frac{\epsilon C}{P_\epsilon + \epsilon - q(S)} = 0, \tag{5.4.13}$$

with the initial condition as the first part of equation (5.2.2), and the boundary conditions as

$$P_\epsilon(0,t) = E, \qquad \lim_{S\to\infty} P_\epsilon(S,t) = 0, \tag{5.4.14}$$

where $C \geq rE$, $q(S) = E - S$, and $0 < \epsilon \ll 1$.

Again as before, in the construction of our radial point interpolation method, we use Multiquadric radial basis functions (mentioned in Table 1.2.1) and the polynomial basis functions (as indicated in (5.3.6)).

By using equations (5.3.21)-(5.3.25) and substituting equations (5.4.3)-(5.4.5) into (5.4.2), we get

$$\mathbf{\Phi}\frac{d\mathbf{a}}{dt} + \widetilde{H}\mathbf{a} + Q(\mathbf{a}) = 0, \tag{5.4.15}$$

where

$$Q_i(\mathbf{a}) = \frac{\epsilon C}{\mathbf{\Phi}_i\mathbf{a} + \epsilon - q(x_i)}, \quad i = 1, \cdots, N$$

with Φ_i denoting the i-th row of the matrix Φ and

$$\widetilde{H} = \frac{1}{2}\sigma^2 x_i^2 \frac{\partial^2 \mathbf{\Phi}}{\partial x^2} + rx_i\frac{\partial \mathbf{\Phi}}{\partial x} - r\mathbf{\Phi}. \tag{5.4.16}$$

Now we use a θ-method to solve (5.4.15) which gives

$$\mathbf{\Phi}\frac{\mathbf{a}^{n+1}-\mathbf{a}^{n}}{\Delta t}+\theta\widetilde{H}\mathbf{a}^{n+1}+(1-\theta)\widetilde{H}\mathbf{a}^{n}+\theta Q(\mathbf{a}^{n+1})+(1-\theta)Q(\mathbf{a}^{n})=0. \quad (5.4.17)$$

The nonlinear penalty term gives rise to a nonlinear system of equations whose solution is usually found by a modified Newton's method. However, by replacing a^n in the penalty term by a^{n+1}(as in [55]), we obtain a linearly implicit scheme corresponding to equation (5.4.17) which is given by

$$\mathbf{\Phi}\frac{\mathbf{a}^{n+1}-\mathbf{a}^{n}}{\Delta t}+\theta\widetilde{H}\mathbf{a}^{n+1}+(1-\theta)\widetilde{H}\mathbf{a}^{n}+Q(\mathbf{a}^{n+1})=0, \quad (5.4.18)$$

with the initial condition given by the first part of equation (5.2.2) and boundary conditions given by equation (5.4.14).

5.5 Stability analysis of the numerical method

To proceed with the stability analysis, let us define the error at the n^{th} time level by

$$e^n = V^n_{\text{exact}} - V^n_{\text{app}}, \quad (5.5.1)$$

where V^n_{exact} is the exact solution and V^n_{app} is the numerical solution obtained by either (5.4.8) or (5.4.18).

For the scheme given by (5.4.12) the error equation at $(n+1)^{th}$ level can be written as

$$e^n = Be^{n+1}, \quad (5.5.2)$$

where B, the amplification matrix, given by

$$B = \mathbf{\Phi}^{-1}[\mathbf{\Phi}+\theta\Delta t\widetilde{H}][\mathbf{\Phi}-(1-\theta)\Delta t\widetilde{H}]^{-1}\mathbf{\Phi}.$$

The numerical scheme is stable if $\rho(B)\le 1$, where $\rho(B)$ is the spectral radius of B.

Substituting B in equation (5.5.2) and simplifying, we obtain

$$[\mathbf{\Phi} - (1-\theta)\Delta t\widetilde{H}]\mathbf{\Phi}^{-1}e^{n} = [\mathbf{\Phi} + \theta\Delta t\widetilde{H}]\mathbf{\Phi}^{-1}e^{n+1}, \qquad (5.5.3)$$

equation (5.5.3) can be written as

$$[I - (1-\theta)\Delta tM]e^{n} = [I + \theta\Delta tM]e^{n+1}, \qquad (5.5.4)$$

where $M = \widetilde{H}\Phi^{-1}$ and $I \in \mathbb{R}^{N\times N}$ is the identity matrix.

It is clear from equation (5.5.4) that the numerical scheme is stable if all the eigenvalues of the matrix $[I-(1-\theta)\Delta tM]^{-1}[I+\theta\Delta tM]$ are less than unity, which means that

$$\left| \frac{1+\theta\Delta t\lambda_M}{1-(1-\theta)\Delta t\lambda_M} \right| \leq 1. \qquad (5.5.5)$$

where λ_M represent the eigenvalues of the matrix M.

Equation (5.5.5) is similar to the one obtained in Chapter 2 and therefore we conclude that the explicit Euler method will be stable if $\Delta t \geq -2/\lambda_M\,, \quad \lambda_M \leq 0$; and the implicit Euler and Crank-Nicholson's methods are unconditionally stable.

5.6 Numerical results and discussion

Using the RPIM approach, the resulting problems for European and American put options are solved via Crank-Nicolson's method (i.e., $\theta = 0.5$) with $\Delta t = 0.01$. Results are presented in Table 5.6.1 and Figure 5.6.3, respectively.

The parameters used for the simulations for European put option problem using the multiquadratic radial point interpolation method are: $r = 0.05$, $\sigma = 0.2$, $D = 0$, $E = 10$, $t_0 = 0$, $T = 0.5$, $S_0 = 0$ and $S_{max} = 30$. We have set the parameter c in the radial basis function as $2h$ where $h = (S_{max} - S_0)/(N-1)$. The first column in this table represents values of the asset price S, the second column represents the exact solution and the other three columns indicated the numerical values of the European put option that we obtain using the radial basis function approach with 21, 41 and 101 nodes, respectively.

For the American put options, we choose $r = 0.1,\ \sigma = 0.2,\ D = 0,\ E = 1,\ t_0 = 0,\ T = 1, \epsilon = 0.01,\ S_0 = 0,$ and $S_{max} = 2$. We again use the Crank-Nicolson method with $\Delta t = 0.01$. Using the multiquadratic radial point interpolation method, we obtain reasonably accurate results in the sense that they are very close to those obtained by Fasshauer in [27]. This can be seen from Table 5.6.2.

Table 5.6.1: Values of European put option using radial point interpolation method

S	Exact	RPIM21	RPIM41	RPIM101
2	7.7531	7.7530	7.7533	7.7531
4	5.7531	5.7533	5.7531	5.7531
6	3.7532	3.7530	3.7593	3.7532
7	2.7568	2.7657	2.7593	2.7572
8	1.7987	1.8508	1.8080	1.8003
9	0.9880	1.0085	0.9909	0.9886
10	0.4420	0.5281	0.4628	0.4454
11	0.1606	0.2086	0.1754	0.1629
12	0.0483	0.0499	0.0504	0.0486
13	0.0124	0.0205	0.0147	0.0127
14	0.0028	0.0040	0.0035	0.0029
15	0.0006	0.0005	0.0006	0.0006
16	0.0001	0.0002	0.0001	0.0001

RPIM21: radial point interpolation method with 21 nodes.

RPIM41: radial point interpolation method with 41 nodes.

RPIM101: radial point interpolation method with 101 nodes.

Finally, figures 5.6.1 and 5.6.2 depict some special cases for European and American put options as indicated in the figure captions.

In our numerical experiments, we search the value of shape parameter c in RBFs by proceeding with the step 0.01 and plot the relationship between shape parameter and max-error to select the optimal value of shape parameter. From Figure 5.6.4 we found that the optimal value of shape parameters using Multiquadric is in the neighborhood of 0.53.

Since the radial basis functions are infinitely differentiable, the computations of the

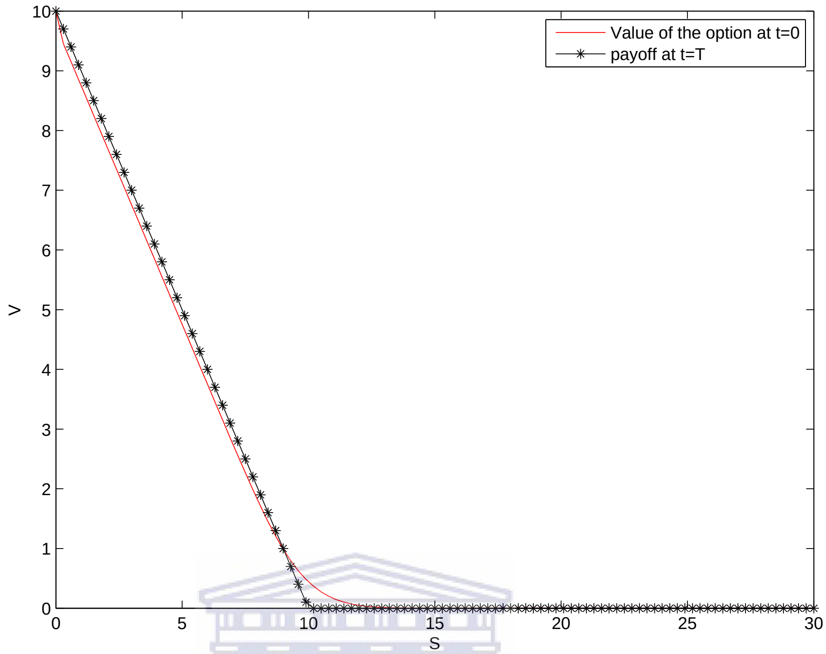

Figure 5.6.1: Values of the European put on a dividend paying asset at t_0 using 101 points and $r = 0.05,\ \sigma = 0.2,\ E = 10,\ t_0 = 0,\ T = 0.5,\ S_0 = 0$ and $S_{\max} = 30$. The curve with '*' shows payoff whereas the solid curve represents the value of the option

Table 5.6.2: Values of American put option using radial point interpolation method

S	RPIM21	RPIM41	RPIM101
0.6	4.00E-01	4.00E-01	4.00E-01
0.7	3.00E-01	3.00E-01	3.00E-01
0.8	2.02E-01	2.02E-01	2.02E-01
0.9	1.17E-01	1.17E-01	1.17E-01
1.0	5.97E-02	6.02E-02	6.03E-02
1.1	2.88E-02	2.92E-02	2.93E-02
1.2	1.37E-02	1.40E-02	1.41E-02
1.3	6.79E-03	6.99E-03	7.05E-03
1.4	3.70E-03	3.84E-03	3.896E-03

RPIM21: radial point interpolation method with 21 nodes.

RPIM41: radial point interpolation method with 41 nodes.

RPIM101: radial point interpolation method with 101 nodes.

derivatives of the option's values are readily available from the derivatives of the basis functions. Using equation (5.4.3) we can easily calculate the value of the delta of an option, which is the rate of change of the option value with respect to the asset price.

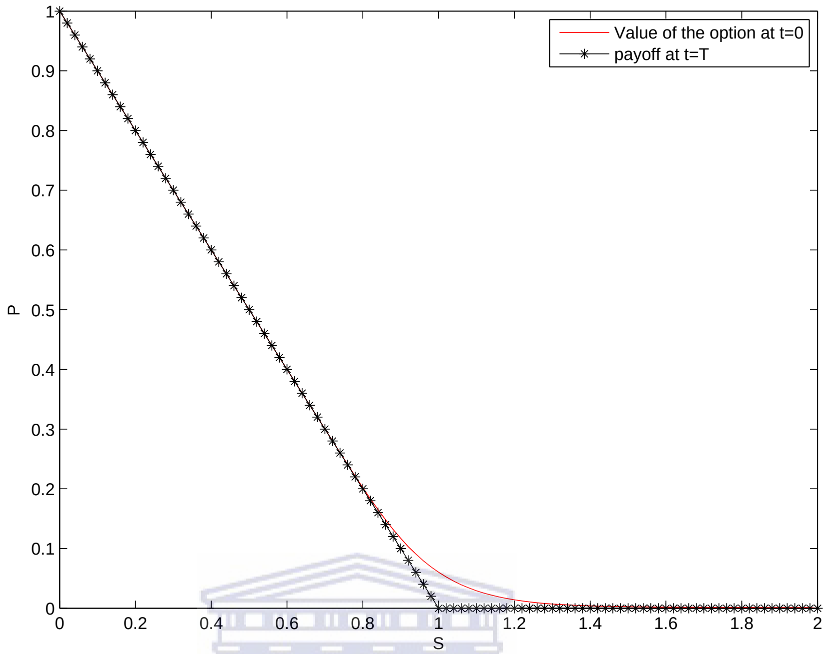

Figure 5.6.2: Values of an American put on a dividend paying asset at t_0 using 101 points and $r = 0.1, \sigma = 0.2, E = 1, T = 1, \epsilon = 0.01$. The curve with '*' shows payoff whereas the solid curve represents the value of the option

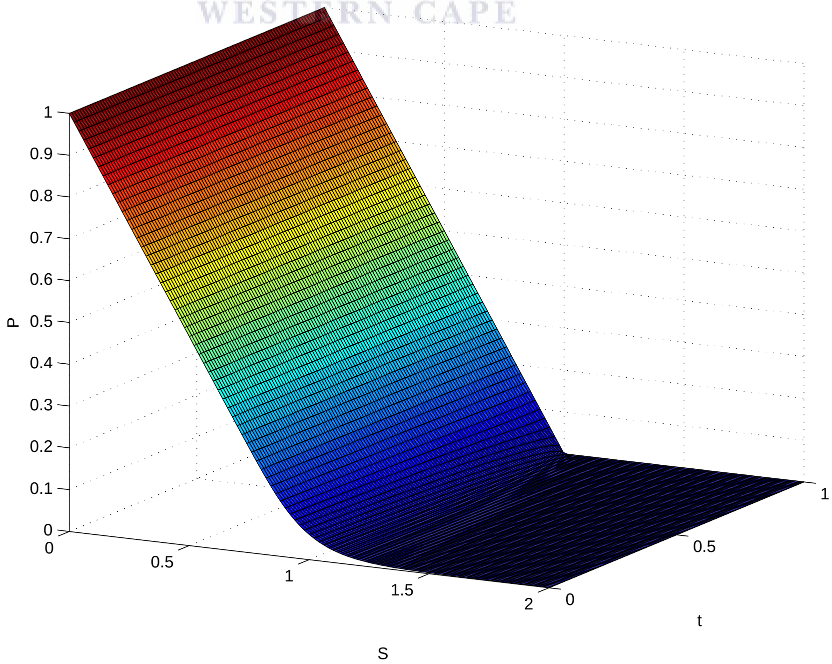

Figure 5.6.3: Values of American put option using radial point interpolation method

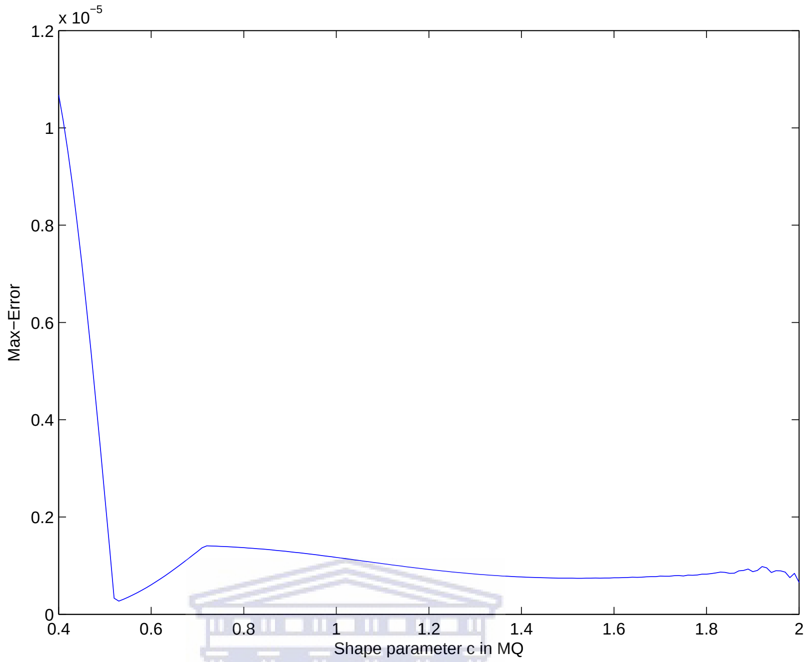

Figure 5.6.4: Effect of parameter c to computational error using radial point interpolation method

Table 5.6.3 and Table 5.6.4 give the values of delta for European and American put options using radial point interpolation method. It is clear from the results presented in these tables that the numerical values of the option's delta lie between -1 and 0 which is in agreement with what is mentioned in Hull [43]. Furthermore, in Table 5.6.5 we compare the option's delta for American put with some other works seen in the literature and found that our results are comparable with those obtained by others. Figure 5.6.5 shows the values of European delta put option using radial point interpolation method.

We also calculate the gamma (Γ) using (5.4.5). Table 5.6.6 gives the values of gamma for European put options. The first column in this table represents the values of the asset price S, the second column represents the analytical values of option's gamma and the third column represents the numerical values of it using the proposed approach.

Table 5.6.3: Values of option's delta (Δ) for European put using radial point interpolation method

S	Analytic values of option's Δ	Numerical values of option's Δ
4	-1.0000	-1.0000
6	-0.9996	-0.9996
7	-0.9885	-0.9878
8	-0.9083	-0.9065
9	-0.6906	-0.6903
10	-0.4023	-0.4031
11	-0.1784	-0.1798
12	-0.0622	-0.0624
13	-0.0177	-0.0181
14	-0.0043	-0.0045
15	-0.0009	-0.0009
16	-0.0002	-0.0002

Table 5.6.4: Values of option's delta (Δ) for American put using radial point interpolation method

S	Numerical values of option's Δ
0.6	-0.9999
0.7	-0.9964
0.8	-0.9480
0.9	-0.7202
1.0	-0.4219
1.1	-0.2155
1.2	-0.1017
1.3	-0.0459
1.4	-0.0206

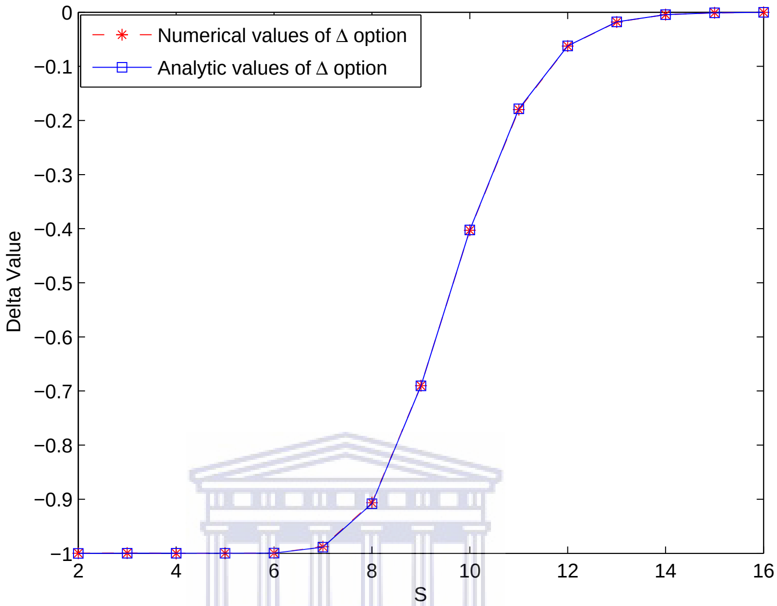

Figure 5.6.5: Values of option's delta (Δ) for European put option using radial point interpolation method (Multiquadric)

Table 5.6.5: Comparison of option's delta (Δ) for American Put options

S	LUBA	EXP	QFK	RPIM
80	-1.0000	-1.0000	-1.0000	-0.9997
90	-0.6173	-0.6207	-0.6212	-0.6216
100	-0.3588	-0.3582	-0.3581	-0.3593
110	-0.2108	-0.2109	-0.2108	-0.2112
120	-0.1256	-0.1257	-0.1256	-0.1249

LUBA: Lower and Upper bound Approximations [10].

EXP: The multipiece Exponention [51].

QFK: Quadrature Formula of Kim equations [52].

RBF: Radial Basis Function approach proposed in this chapter.

Table 5.6.6: Values of option's gamma (Γ) for European put using radial point interpolation method

S	Analytic values of option's Γ	Numerical values of option's Γ
4	0.0000	0.0000
6	0.0016	0.0017
7	0.0303	0.0315
8	0.1455	0.1461
9	0.2770	0.2768
10	0.2736	0.2722
11	0.1677	0.1678
12	0.0722	0.0723
13	0.0238	0.0242
14	0.0064	0.0066
15	0.0015	0.0015
16	0.0003	0.0003

Chapter 6

A mesh free method for solving the Heston's volatility model

In this chapter we construct a mesh free method by using radial basis functions (RBFs) to price some put options of European and American type for the Heston's model [38]. Using this RBFs approximation, we again obtain a system of ordinary differential equations in each case which is then solved by a time integration methods. We use an update procedure to solve this free boundary problem associated with the American style options in the Heston's model. The resulting method is analyzed for stability and comparative numerical results are presented.

6.1 Introduction

The Heston's model is named after Steven Heston (a professor in the Robert H. Smith School of Business at the University of Maryland). It is a mathematical model that describes the evolution of the volatility of an underlying asset [38]. Many attempts were made to solve this model in the past. Below we provide some literature on the approaches that are used to solve the problems described by the Heston's model.

By transforming the original linear two dimensional stochastic volatility option pricing PDE into a PDE with a nonlinear source term, Zvan *et al.* [117] proposed a penalty method for American options with stochastic volatility. They described several methods for enforcing the early exercise constraint by using a penalty source term in the discrete equations. The resulting nonlinear algebraic equations are solved using a Newton's method.

Clarke and Parrott [20] described an implicit finite difference approach for pricing of American options on assets with a stochastic volatility. They used a multigrid procedure for the fast iterative solution of the discrete linear complementarity problems. They further improved the accuracy and performance of their approach by a strike-price related analytic transformation of asset prices and adaptive time-stepping.

Dehgha [26] developed three new fully implicit methods which are based on the (5,5) Crank-Nicolson method, the (5,5) N-H (Noye–Hayman) implicit method and the (9,9) N-H implicit method for solving the heat equation in two dimensional space with non-local boundary conditions.

Oosterlee [83] discussed a nonlinear multigrid method for a linear complementarity problem to solve an American style option pricing problem. The convergence was improved by a recombination of iterates. He discretized a 2D convection-diffusion type operator with the help of second order upwind discretizations. The properties of smoothers are analyzed with Fourier two-grid analysis. He compared his numerical solutions with some reference results from the literature.

Ikonen and Toivanen [45] considered the numerical pricing of American options under Heston's stochastic volatility model. The price was given by a linear complementarity problem with a two-dimensional parabolic partial differential operator. They proposed operator splitting methods for performing time stepping after a finite difference space discretization. Their numerical experiments show that the operator splitting methods have comparable discretization errors. They also demonstrated the efficiency of the operator splitting methods when a multigrid method is used for solving the systems of linear equations.

Recently, Hout and Foulon [40] investigated four splitting schemes of the Alternating Direction Implicit (ADI) type: the Douglas scheme, the Craig-Sneyd scheme, the Modified Craig-Sneyd scheme, and the Hundsdorfer-Verwer scheme, each of which contains a free parameter. They discuss the adaptation of the above four ADI schemes to the Heston's PDE. They presented various numerical examples with realistic data sets from the literature, where they considered European call options as well as down-and-out barrier options.

In [116], Zhu and Chen applied singular perturbation techniques to price European puts with a stochastic volatility model, and derived a simple and elegant analytical formula as an approximation for the value of European put options.

The rest of the chapter is organized as follows. The option pricing problem is described in Section 6.2. Section 6.3 deals with the application of radial basis functions to solve this problem. The stability analysis of the numerical methods is presented in Section 6.4. Finally some numerical results along with a discussion are given in Section 6.5.

6.2 The Heston's model

The Heston's model [38] is described by the stochastic differential equations

$$dx_t = \mu x_t dt + \sqrt{y_t} x_t d\omega_1, \tag{6.2.1}$$

and

$$dy_t = \alpha(\beta - y_t)dt + \sigma\sqrt{y_t} d\omega_2. \tag{6.2.2}$$

Equation (6.2.1) models the stock price process x_t . The parameter μ is the deterministic growth rate of the stock price and $\sqrt{y_t}$ is the standard deviation (the volatility) of the stock returns dx/x. The model for the variance process y_t is given by (6.2.2). The volatility of the variance process y_t is denoted by σ and the variance will drift back to a mean value $\beta > 0$ at a rate $\alpha > 0$. These two processes contain randomness as w_1 and w_2 are Brownian motions with a correlation factor $\rho \in [-1, 1]$ (see, [45] for further details).

Heston's model is derived by deriving a two-dimensional parabolic partial differential equation can be derived for the price of the American option using the above stochastic volatility model ([117]):

$$\frac{\partial u}{\partial t}+\frac{1}{2}yx^2\frac{\partial^2 u}{\partial x^2}+\rho\sigma yx\frac{\partial^2 u}{\partial x\partial y}+\frac{1}{2}\sigma^2 y\frac{\partial^2 u}{\partial y^2}+rx\frac{\partial u}{\partial x}+(\alpha(\beta-y)-\vartheta\sigma\sqrt{y})\frac{\partial u}{\partial y}-ru=0, \quad (6.2.3)$$

where r is a risk free interest rate, and ϑ is a market price of the risk.

In the following, we assume ϑ to be zero as has been done in many previous studies, for example, in [83].

The option pricing problem is defined in an unbounded domain

$$(x,y,t)|x\geq 0, y\geq 0, t\in[0,T].$$

In order to use radial basis function approximations for space variables, we truncate a finite computational domain

$$(x,y,t)\in[0,X]\times[0,Y]\times[0,T]=\Omega\times[0,T], \quad (6.2.4)$$

with $\Omega:=[0,X]\times[0,Y]$ where X and Y are sufficiently large.

For a put option the payoff function is

$$g(x)=\max(E-x,0), \quad (6.2.5)$$

where E is the exercise price.

The value at the expiry gives the initial value for u, that is,

$$u(x,y,0)=g(x)\in[0,X]\times[0,Y]. \quad (6.2.6)$$

On the truncation boundaries, we use the Neumann boundary conditions

$$\frac{\partial u}{\partial x}(X, y, t) = \frac{\partial g}{\partial x}(X), \quad (y, t) \in [0, Y] \times [0, T] \tag{6.2.7}$$

and

$$\frac{\partial u}{\partial y}(x, Y, t) = 0, \qquad (x, t) \in [0, X] \times [0, T]. \tag{6.2.8}$$

Because of the early exercise of the American option, we have to include the following early exercise constraint for the option price

$$u(x, y, t) \geq g(x), \quad (x, y, t) \in \Omega \times [0, T]. \tag{6.2.9}$$

We will solve (6.2.3) using the RBF approach described in the next section.

6.3 Application of RBFs for solving Heston's model

The radial basis function approach proposed for single asset problems in the previous chapters is now being extended to solve a Heston's model here. To begin with, we approximate the unknown function u as

$$u(x, y, t) \approx \sum_{j=1}^{N} a_j(t)\phi\left(\|x - x_j\|, \|y - y_j\|\right), \tag{6.3.1}$$

where $a_j's$ are unknown coefficients and $\phi(\|x - x_j\|, \|y - y_j\|)$ are the RBFs.

We will use the following radial basis functions for this problem

$$\phi(\|x - x_j\|, \|y - y_j\|) = e^{-\left(\|x-x_j\|^2+\|y-y_j\|^2\right)/c^2}, \tag{6.3.2}$$

where c is a positive parameter.

Collocating at the same N points $\{x_j\}_{j=1}^N$ and $\{y_j\}_{j=1}^N$, equation (6.2.3) becomes

$$\begin{aligned}\frac{\partial u}{\partial t} &+ \frac{1}{2} y_i x_i^2 \frac{\partial^2 u}{\partial x^2} + \rho\sigma y_i x_i \frac{\partial^2 u}{\partial x \partial y} + \frac{1}{2}\sigma^2 y_i \frac{\partial^2 u}{\partial y^2} + r x_i \frac{\partial u}{\partial x} \\ &+ \alpha(\beta - y_i)\frac{\partial u}{\partial y} - rV = 0. \end{aligned} \tag{6.3.3}$$

In case of Gaussian basis functions differentiating (6.3.1), we get

$$\frac{\partial u(x,y,t)}{\partial t} = \sum_{j=1}^{N} \frac{d a_j(t)}{dt} \phi(\|x - x_j\|, \|y - y_j\|), \tag{6.3.4}$$

$$\frac{\partial u(x,y,t)}{\partial x} = \sum_{j=1}^{N} a_j \frac{-2(x - x_j)}{c^2} e^{-\left(\|x-x_j\|^2 + \|y-y_j\|^2\right)/c^2}, \tag{6.3.5}$$

$$\frac{\partial u(x,y,t)}{\partial y} = \sum_{j=1}^{N} a_j \frac{-2(y - y_j)}{c^2} e^{-\left(\|x-x_j\|^2 + \|y-y_j\|^2\right)/c^2}, \tag{6.3.6}$$

$$\frac{\partial^2 u(x,y,t)}{\partial x \partial y} = \sum_{j=1}^{N} a_j \frac{4(x - x_j)(y - y_j)}{c^4} e^{-\left(\|x-x_j\|^2 + \|y-y_j\|^2\right)/c^2}, \tag{6.3.7}$$

$$\frac{\partial^2 u(x,y,t)}{\partial x^2} = \sum_{j=1}^{N} a_j \frac{(4(x - x_j)^2 - 2c^2)}{c^4} e^{-\left(\|x-x_j\|^2 + \|y-y_j\|^2\right)/c^2}, \tag{6.3.8}$$

$$\frac{\partial^2 u(x,y,t)}{\partial y^2} = \sum_{j=1}^{N} a_j \frac{(4(y - y_j)^2 - 2c^2)}{c^4} e^{-\left(\|x-x_j\|^2 + \|y-y_j\|^2\right)/c^2}. \tag{6.3.9}$$

Substituting the above expressions for various partial derivatives into (6.3.3), we obtain

$$\Phi \frac{d\mathbf{a}}{dt} + R\mathbf{a} = 0, \tag{6.3.10}$$

where

$$\Phi_{ij} = e^{-\left(\|x_i-x_j\|^2 + \|y_i-y_j\|^2\right)/c^2}, \tag{6.3.11}$$

and

$$\begin{aligned} R_{ij} &= \frac{1}{2} y_i x_i^2 \left(\frac{4(x_i - x_j)^2 - 2c^2}{c^4} \right) \Phi_{ij} + \rho \sigma y_i x_i \left(\frac{4(x_i - x_j)(y_i - y_j)}{c^4} \right) \Phi_{ij} \\ &+ \frac{1}{2} \sigma^2 y_i \left(\frac{4(y_i - y_j)^2 - 2c^2}{c^4} \right) \Phi_{ij} + r x_i \left(\frac{-2(x_i - x_j)}{c^2} \right) \Phi_{ij} \\ &+ (\alpha(\beta - y_i) \left(\frac{-2(y_i - y_j)}{c^2} \right) \Phi_{ij} - r \Phi_{ij}. \end{aligned} \tag{6.3.12}$$

To solve the system described by (6.3.10), we use a θ-method:

$$\Phi \frac{\mathbf{a}^{n+1} - \mathbf{a}^n}{\Delta t} + \theta R \mathbf{a}^{n+1} + (1 - \theta) R \mathbf{a}^n = 0, \tag{6.3.13}$$

with the initial condition given by equation (6.2.6) and boundary conditions given by equations (6.2.7)-(6.2.8).

We can rewrite equation (6.3.13) as

$$[\Phi - (1 - \theta)\Delta t R]\mathbf{a}^n = [\Phi + \theta \Delta t R]\mathbf{a}^{n+1}, \tag{6.3.14}$$

$$\mathbf{a}^n = [\Phi - (1 - \theta)\Delta t R]^{-1}[\Phi + \theta \Delta t R]\mathbf{a}^{n+1}. \tag{6.3.15}$$

Equation (6.3.1) applied at all collocation point can be written in the matrix form as

$$\mathbf{u} = \Phi \mathbf{a}. \tag{6.3.16}$$

Using equation (6.3.16), equation (6.3.15) can be written as

$$u^n = \Phi[\Phi - (1 - \theta)\Delta t R]^{-1}[\Phi + \theta \Delta t R]\Phi^{-1} u^{n+1}. \tag{6.3.17}$$

The above equation is solved along with (6.2.6) and equations (6.2.7)-(6.2.8) to obtain the numerical solution. Also the form of this equation should be read in context to the computing process because in the problems like those considered in this chapter, we usually have a final boundary value problem rather than an initial boundary value problem. To this end, note that the scheme given by (6.3.14) corresponding to $\theta = 0,\ 0.5,$ and 1 are the implicit Euler, Crank-Nicolson and explicit Euler methods, respectively.

6.4 Stability analysis of the numerical method

To proceed with the stability analysis, let us define the error at the n^{th} time level by

$$e^n = u^n_{\text{exact}} - u^n_{\text{app}}, \tag{6.4.1}$$

where u^n_{exact} and u^n_{app} are the exact and numerical solutions for the Heston's model.

For the scheme given by (6.3.17) the error equation at $(n+1)^{th}$ level can be written as

$$e^n = Be^{n+1}, \tag{6.4.2}$$

where B is the amplification matrix is given by

$$B = \Phi^{-1}[\Phi + \theta\Delta tR][\Phi - (1-\theta)\Delta tR]^{-1}\Phi.$$

The numerical scheme is stable if $\rho(B) \leq 1$, where $\rho(B)$ is the spectral radius of B. Substituting B in equation (6.4.2) and simplifying, we obtain

$$[\Phi - (1-\theta)\Delta tR]\Phi^{-1}e^n = [\Phi + \theta\Delta tR]\Phi^{-1}e^{n+1}. \tag{6.4.3}$$

This implies

$$[I - (1-\theta)\Delta tM]e^n = [I + \theta\Delta tM]e^{n+1}, \tag{6.4.4}$$

where $M = R\Phi^{-1}$ and $I \in \mathbb{R}^{N\times N}$ is the identity matrix.

It is clear from equation (6.4.4) that the numerical scheme is stable if all the eigenvalues of the matrix $[I - (1-\theta)\Delta tM]^{-1}[I + \theta\Delta tM]$ are less than unity, which means that

$$\left| \frac{1+\theta\Delta t\lambda_M}{1-(1-\theta)\Delta t\lambda_M} \right| \leq 1, \tag{6.4.5}$$

where λ_M represent the eigenvalues of the matrix M.

Note that it is the matrix R that significantly differs in this case. However, the form of (6.4.4)is similar to the one obtained previously and therefore we conclude that the explicit Euler method will be stable if $\Delta t \geq -2/\lambda_M, \ \lambda_M \leq 0$, and the implicit Euler and Crank-Nicholson's methods will be unconditionally stable.

6.5 Numerical results and discussion

Using the RBF approach, the resulting problems for European put options in Heston's model are solved via implicit Euler methods (i.e., $\theta = 0$). The parameter values used in the simulation are given in Table 6.5.1. Results are presented in Table 6.5.2. We use the computational domain as

$$[0, X] \times [0, Y] \times [0, T] = [0, 20] \times [0, 1] \times [0, 0.25].$$

We computed the prices of the American put options using radial basis functions based on the Crank-Nicolson's method. These prices are presented in Table 6.5.5 for the asset values $x = 8.0, \ 9.0, \ 10.0, \ 11.0, \ 12.0$, and for the variance values $y = 0.0625$ and $y = 0.25$ with $N = 32, \ L = 32$ and $M = 20$.

We also note that even in this case the radial basis functions are infinitely differentiable, therefore, the computations of the derivatives of the options values are readily available from the derivatives of the basis functions. Thus using equations (6.3.5) and (6.3.6) we can calculate the value of the delta and vega of an option, which is the rate of change of the option value with respect to the asset price and volatility, respectively. Table 6.5.3 present results for the delta and vega of European put options in Heston's model using radial basis functions.

We also calculate the gamma (Γ) using equation (6.3.8). It is the second partial

Table 6.5.1: The parameter values used for European and American put options for the Heston's model

Parameter	Value
σ	0.9
ρ	0.1
α	5
β	0.16
ϑ	0
r	0.1
Time to expiry (T)	0.25
Exercise price (E)	10

Table 6.5.2: Values of European put option using radial basis functions in Heston's model ($y = 0.25$)

Asset value	Exact [45]	Option value using RBFs	Errors
8	1.9773	1.9855	0.0082
9	1.2780	1.2687	0.0093
10	0.7697	0.7704	0.0007
11	0.4360	0.4369	0.0008
12	0.2373	0.2462	0.0089

derivative of the portfolio with respect to the asset price. If the absolute value of gamma is large, delta is highly sensitive to the price of the underlying asset. Table 6.5.4 gives the values of gamma for European put options.

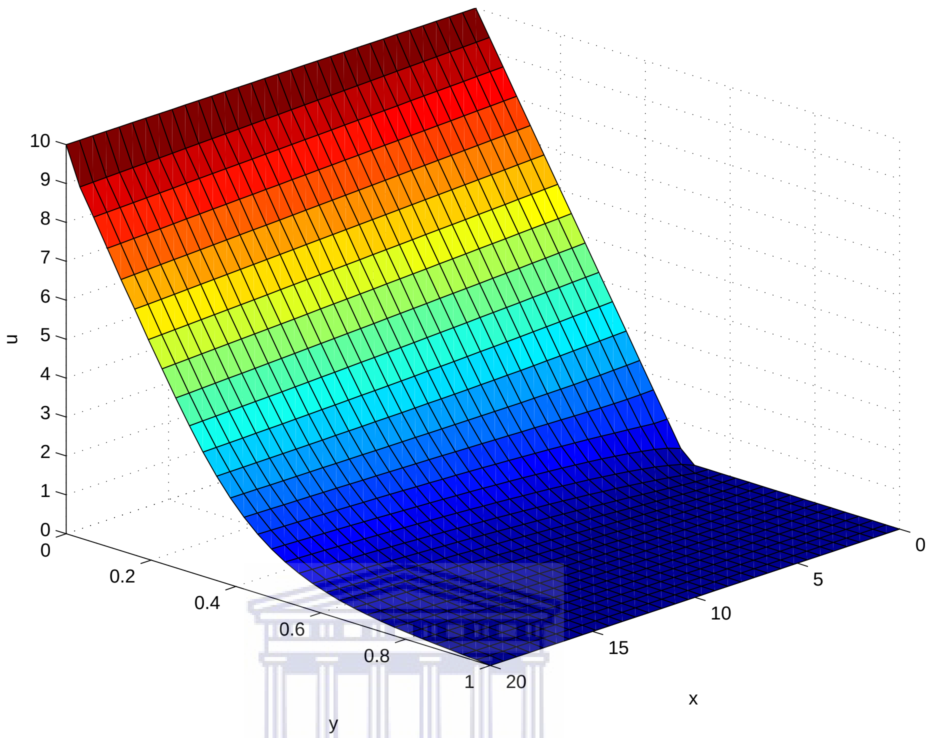

Figure 6.5.1: Values of European put option in Heston's model using radial basis functions

Table 6.5.3: Values of option's delta (Δ) and vega for European put option using radial basis functions in Heston's model

Asset value	Δ	Vega
4	-0.9619	-0.0481
5	-0.9656	-0.0483
6	-0.8979	-0.0449
7	-0.7643	-0.0382
8	-0.6100	-0.0305
9	-0.4658	-0.0233
10	-0.3475	-0.0174
11	-0.2532	-0.0127
12	-0.1848	-0.0092
13	-0.1344	-0.0067
14	-0.0993	-0.0050

Table 6.5.4: Values of option's gamma (Γ) for European put option using radial basis functions in Heston's model

Asset value	Γ
5	0.0299
6	0.0886
7	0.1308
8	0.1390
9	0.1246
10	0.1001
11	0.0756
12	0.0552
13	0.0392
14	0.0276

Table 6.5.5: Values of American put option in Heston's model

Methods	y	Asset value				
		8	9	10	11	12
RBFs	0.0625	2.0081	1.1277	0.5444	0.2097	0.0762
	0.25	2.0590	1.3066	0.7907	0.4475	0.2520
OS [45]	0.0625	2.0000	1.1061	0.5178	0.2122	0.0815
	0.25	2.0778	1.3323	0.7944	0.4470	0.2420
[83]	0.0625	2.0000	1.1070	0.5170	0.2120	0.0815
	0.25	2.0790	1.3340	0.7960	0.4490	0.2430
[117]	0.0625	2.0000	1.1076	0.5202	0.2138	0.0821
	0.25	2.0784	1.3337	0.7961	0.4483	0.2428

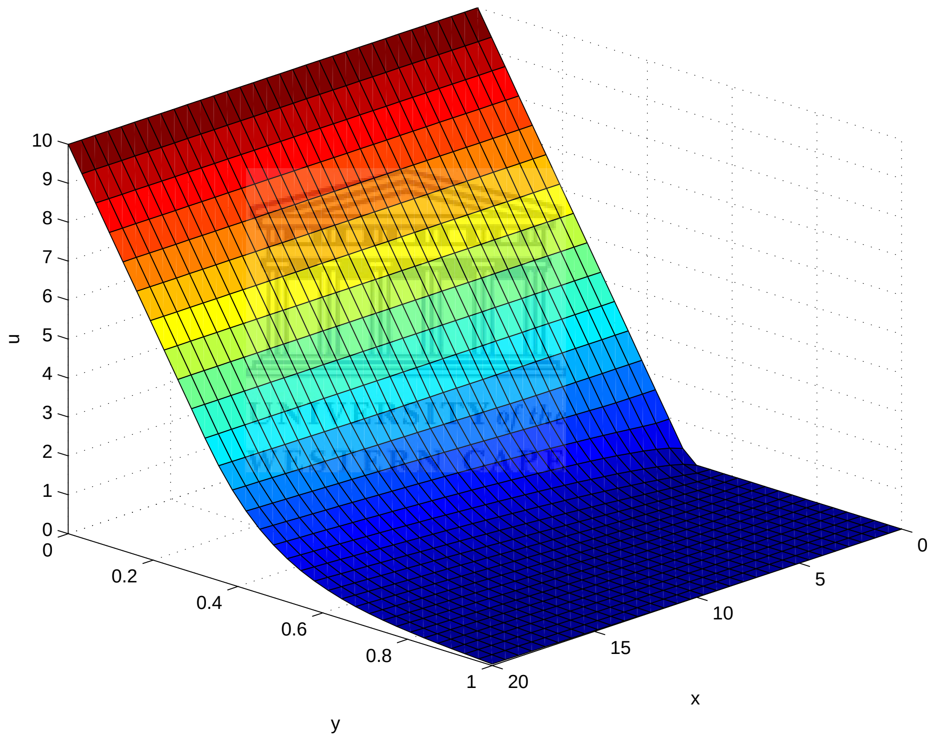

Figure 6.5.2: Values of American put option in Heston's model using using radial basis functions

Chapter 7

Concluding remarks and scope for future research

In this thesis, we used a special class of numerical methods, namely, Mesh Free Methods, to study the differential models for pricing options. We applied this method to solve some standard and nonstandard options and then extended to solve the Heston's model. The methods in each of these cases are analyzed for stability and thorough numerical results are presented and compared with those seen in the literature.

In Chapter 2, We developed an efficient mesh free methods based on the radial basis functions (RBFs) to solve European and American option pricing problems in computational finance. The application of RBFs leads to system of differential equations which are then solved by a time integration scheme. The main difficulty in pricing the American options lies in the fact that these options are allowed to be exercised at any time before their expiry. Such an early exercise right purchased by the holder of the option results into a free boundary problem. We added a small penalty term to covering PDEs to removed the free boundary. The proposed method is analyzed for stability. Numerical results describing the payoff functions and option values are also presented. We also performed some simulations for Greeks, in particular, option's delta and gamma.

In Chapter 3, we extend the approach used in Chapter 2 to solve problems of pricing European and American put options with dividend yield.

In Chapter 4, we extend the approach to solve two type of exotic options, namely, European barrier and European Asian options. This approach is further extended to solve problems of pricing European style double barrier options and digital options. Finally, we presented some numerical experiments using a number of radial basis functions.

In Chapter 5, we described the valuation of European and American put options using a mesh free method which is based on a radial point interpolation approximations. The valuation of European options explained thoroughly and the numerical results are compared with the analytical ones. In the case of American options, we have a free boundary condition which usually places a great difficulty for many numerical methods. We added a penalty term to fix this boundary and obtained reasonably accurate results. We performed some simulations for Greeks, in particular, option's delta and gamma. Furthermore, the proposed method is analyzed for stability and we found that it is unconditionally stable.

Finally, in Chapter 6, we extend the radial basis functions (RBFs) for solving Heston's model. Both European and American style options are solved.

Overall we found the proposed numerical methods very pleasing. However, we discover that much more can be done using this approaches. Therefore, below we list some research issues that we would like to address in future.

- Using RBF approximation we obtain a systems of ordinary differential equations, which are then solved by time integration techniques. When we attempted to solve multi-dimensional problems, we found that these systems are highly ill-conditioned. We have partly solved such problems using matrix decomposition approach (LU factorization). However, currently we are exploring the use of some matrix regularization technique, for example, truncated singular value decomposition (TSVD).

- Another aspect that we are looking at currently is to devise high order time integration schemes.
- RPIM approach presented in Chapter 5 seem a very powerful approach for multi-asset options. We are exploring it currently.
- Recently we have also started experimenting our approach to solve some partial integro-differential models in finance. This includes a jump-diffusion model in which the asset price motion is given by a process of the form

$$\frac{dS}{S} = \nu dt + \sigma dz + (\eta - 1)dq, \tag{7.0.1}$$

where ν is the drift rate, σ is the volatility of the Brownian part of the process, and dq is a Poisson process. Here $dq = 0$ with probability $(1 - \lambda)$, and $dq = 1$ with probability $\lambda\ dt$, where λ is the Poisson arrival intensity, and $\eta - 1$ is an impulse function giving a jump from S to $S\eta$. The average relative jump size, $E(\eta - 1)$ is denoted by k. The Poisson process dq is assumed to be independent of the Wiener process dz.

Merton [77] showed that with the above assumptions that the value of a contingent claim $V(S, \tau)$ depending on the asset price S and time τ satisfies the following partial integro-differential equation:

$$V_t = \frac{\sigma^2 S^2}{2} V_{SS} + (r - \lambda k)SV_S - (r + \lambda)V + \lambda \int_0^\infty V(S\eta)g(\eta)d\eta, \tag{7.0.2}$$

where $t = T - \tau$ is the time till expiration at T, r is the risk free interest rate, and $g(\eta)$ is the probability density function of the jump size η.

With the change of variables (cf. Cruz-Báez and Rodriguez [23])

$$S = e^x, \quad \eta = e^y, \quad t = 2\frac{\tilde{\tau} - T}{\sigma^2}, \quad V(S, t) = e^{\alpha x + \beta \tilde{\tau}} u(x, \tilde{\tau}),$$

where

$$\alpha = \frac{1}{2} - \frac{(r - \lambda k)}{\sigma^2}, \quad \beta = -\frac{1}{4}\left(\frac{2r}{\sigma^2} - \frac{2\lambda k}{\sigma^2} + 1\right)^2 - 2\frac{\lambda k}{\sigma^2}.$$

The equation (7.0.2) takes the form

$$u_{\tilde{\tau}} = u_{xx} - \lambda u + \lambda \int_{-\infty}^{\infty} h(y - x)u(y, \tilde{\tau})dy, \quad \tilde{\tau} \in \left(0, \frac{1}{2}\sigma^2 T\right], \tag{7.0.3}$$

where $h(y) = g(e^y)e^{\delta y}$, for some suitable real constant δ.

With the help of some adaptive quadrature formula to solve the above integral, we are busy extending the proposed mesh free method to solve problem described by equation (7.0.3).

Bibliography

[1] E. Banks and P. Siegel, *The Options Applications Handbook: Hedging and Speculating Techniques for Professional Investors*, McGraw-Hill Professional, 2006.

[2] G. Barone-Adesi and E. Whaley, Efficient analytic approximation of American option values. *The Journal of Finance* **XLII (2)** (1987).

[3] G. Barone-Adesi, The saga of the American put, *Journal of Banking and Finance* **29 (11)** (2005), 2909-2918.

[4] D.S. Bates, Jumps and stochastic volatility: exchange rate Processes implicit in Deutshe mark options, *Review of Financial Studies* **9** (1996), 69-107.

[5] A. Battauz and M. Pratelli, Optimal stopping and American options with discrete dividends and exogenous risk, *Insurance: Mathematics and Economics* **35** (2004), 255-265.

[6] T. Belytschko, Y. Krongauz, D. Organ, M. Fleming and P. Krysl, Meshless methods: An overview and recent developments, *Computer Methods in Applied Mechanics and Engineering* **139** (1996), 3-47.

[7] F. Black and M. Scholes, The pricing of options and corporate liabilities, *Journal of Political Economy* **81** (1973), 637-659.

[8] P. Brandimarte, *Numerical Methods in Finance and Economics*, Second ed., Wiley, New Jersey, 2006.

[9] M.J. Brennan and E.S. Schwartz, The valuation of American put options, *Journal of Finance* **32 (2)** (1977), 449-462.

[10] M. Broadie and J. Detemple, American option valuation: New bounds, approximations, and a comparison of existing methods, *Review of Financial Studies* **9** (1996), 1211-1250.

[11] B. Carole, O.L Courtois and F. Quittard-Pinon, Pricing derivatives with barriers in a stochastic interest rate environment, *Journal of Economic Dynamics and Control* **32(9)** (2008), 2903-2938.

[12] P. Carr, R. Jarrow and R. Myneni, Alternative characterizations of American put options, *Mathematical Finance* **2** (1992), 87-106.

[13] Z. Cen and A. Le, A robust finite difference scheme for pricing American put options with Singularity-Separating method, *Numerical Algorithms* **53** (2010), 497-510.

[14] S. Chao, Y. Jing-Yang and L. Sheng-Hong, On barrier option pricing in binomial market with transaction costs, *Applied Mathematics and Computation* **189** (2007), 1505-1516.

[15] M.M. Chawla, M.A. AL-Zanaidi and D.J. Evans, Generralized trapezoidal formulas for the Black-Scholes equation of option pricing, *International Journal of Computer Mathematics* **80 (12)** (2003), 1521-1526.

[16] M.M. Chawla, M.A. AL-Zanaidi and D.J. Evans,Generralized trapezoidal formulas for valuing American options, *International Journal of Computer Mathematics* **81 (3)** (2004), 375-381.

[17] C. Chiarella, N. El-Hassan and A. Kucera, Evaluation of American option prices in a path integral framework using Fourier-Hermite series expansions, *Journal of Economic Dynamics and Control* **23** (1999), 1387-1424.

[18] C. Chiarella, B. Kang, G.H. Meyer and A. Ziogas, The evaluation of American option prices under stochastic volatility and jump-diffusion dynamics using the method of lines, *Research Report: Quantitative Finance Research Centre, University of Technology*, Sydney, 2008.

[19] N. Chriss, *Black-Scholes and Beyond: Option Pricing Models*, McGraw-Hill Professional, 1996.

[20] N. Clarke and K. Parrott, Multigrid for American option pricing with stochastic volatility, *Applied Mathematical Finance* **6** (1999), 177-195.

[21] R. Company, A.L. Gonzalez and L. Jodar, Numerical solution of modified Black-Scholes equation pricing stock options with discrete dividend, *Mathematical and Computer Modelling* **44** (2006), 1058-1068.

[22] M. Costabile, I. Massab and E. Russo, An adjusted binomial model for pricing Asian options, *Review of Quantitative Finance and Accounting* **27** (2006), 285-296.

[23] D.I Cruz-Báez and J.M. González-Rodríguez, A semigroup approach to American options, *Journal of Mathematical Analysis and Applications* 302 (2005), 157-165.

[24] K.Y. Dai, G.R. Liu, K.M. Lim, X. Han and S.Y. Du, A meshfree radial point interpolation method for analysis of functionally graded material (FGM) plates, *Computational Mechanics* **34** (2004), 213-223.

[25] D.J. Duffy, *Finite Difference Methods in Financial Engineering:A Partial Differential Equation Approach*, Wiley, West Sussex, 2006.

[26] M. Dehghan, Fully implicit finite differences methods for two-dimensional diffusion with a non-local boundary condition, *Journal of Computational and Applied Mathematics* **106** (1999), 255-269.

[27] G.E. Fasshauer, A.Q.M. Khaliq and D.A. Voss, Using meshfree approximation for multi-asset American option, *Journal of the Chinese Institute of Engineers* **27 (4)** (2004), 563-571.

[28] G.E. Fasshauer, *Meshfree Approximation Methods with Matlab*, World Scientific Publishers, Singapore, 2007.

[29] A.I. Fedoseyev, M.J. Friedman and E.J. Kansa, Improved Multiquadric method for elliptic partial differential equations via PDE collocation on the boundary, *Computers and Mathematics with Applications* **43** (2002), 439-455.

[30] E.O. Fischer, Analytic approximation for the valuation of American put options on stocks with known dividends, *International Review of Economics & Finance* **2 (2)** (1993), 115-127.

[31] B. Fornberg and C. Piret, On choosing a radial basis function and a shape parameter when solving a convective PDE on a sphere, *Journal of Computational Physics* **227** (2008), 2758-2780.

[32] A. Friedman, *Variational Principles and Free-boundary Problems*, Wiley, New York, 1982.

[33] G. Fusai and M. C. Recchioni, Analysis of quadrature methods for pricing discrete barrier options, *Journal of Economic Dynamics and Control* **31(3)** (2007), 826-860.

[34] L. Gao-lian and L. Xiao-wei, Mesh free method based on local cartesian frame, *Applied Mathematics and Mechanics* **27** (2006), 1-6.

[35] F.C. Giinther and W.K. Liu, Implementation of boundary conditions for meshless methods, *Computer Methods in Applied Mechanics and Engineering* **163** (1998), 205-230.

[36] Y. Goto, Z. Fei, S. Kan and E. Kita, Options valuation by using radial basis function approximation, *Engineering Analysis with Boundary Elements* **31** (2007), 836-843.

[37] H. Han and X.Wu, A fast numerical method for the Black-Scholes equation of American options, *SIAM Journal of Numerical Analysis* **41 (6)** (2003), 2081-2095.

[38] S.L. Heston, A closed-form solution for options with stochastic volatility with applications to bonds and currency options, *The Review of Financial Studies* **6(2)** (1993), 327-343.

[39] Y.C. Hon, A Quasi-Radial Basis Functions Method for American Options Pricing, *Computers and Mathematics with Applications* **43** (2002), 513-524.

[40] K.J. Hout and S. Foulon, ADI Finite difference schemes for option pricing in the Heston model with correlation, *Numerical Analysis and Modeling* **7(2)** (2010), 303-320.

[41] W.W.Y. Hsu and Y-D Lyuu, Efficient pricing of discrete Asian options, *Applid Mathematics and Computtation* (2011), **doi: 10.1016/j.amc.2011.01.015**.

[42] H.Y. Hu, J.S. Chen and W. Hu, Weighted radial basis collocation method for boundary value problems, *International Journal for Numerical Methods in Engineering* **69** (2007), 2736-2757.

[43] J.C. Hull, *Options, Futures, and Other Derivatives*, Pearson/Prentice Hall, Upper Saddle River, NJ, 2009.

[44] S. Ikonen and J. Toivanen, Componentwise splitting methods for pricing American options under stochastic volatility, *International Journal of Theoretical and Applied Finance* **10 (2)** (2007), 331-361.

[45] S. Ikonen and J. Toivanen, Operator splitting methods for pricing American options under stochastic volatility, *Numerische Mathematik* **113** (2009), 299-324.

[46] S. Islam, S. Haq and A. Ali, A meshfree method for the numerical solution of the RLW equation, *Journal of Computational and Applied Mathematics* **223** (2009), 997-1012.

[47] S. Islam, S. Haq and M. Uddin, A meshfree interpolation method for the numerical solution of the coupled nonlinear partial differential equations, *Engineering Analysis with Boundary Elements* **33** (2009), 399-409.

[48] P. Jaillet, D. Lamberton and B. Lapeyre, Variational inequalities and the pricing of American options, *Acta Applicandae Mathematicae* **21** (1990), 263-289.

[49] G.R. Johnson and S.R. Beissel, Normalized smoothing functions for SPH impact computations, *International Journal for Numerical Methods in Engineering* **39** (1996), 2725-2741.

[50] C. Joy, P.P. Boyle and K.S. Tan, Quasi-Monte Carlo Methods in Numerical Finance, *Management Science* **42(6)** (1996), 926-938.

[51] N. Ju, Pricing an American option by approximating its early exercise boundary as a multipiece exponential function, *Review of Financial Studies* **11** (1998), 627-646.

[52] S. Kallast and A. Kivinukk, Pricing and Hedging American Options Using Approximations by Kim Integral Equations, *European Finance Review* **7** (2003), 361-383.

[53] E.J. Kansa, Multiquadrics- A Scatered data approximation scheme with applications to computional Fluid-Dynamics-I, *Computers & Mathematics with Applications* **19** (1990), 127-145.

[54] E.J. Kansa, Multiquadrics - A scattered data approximation scheme with applications to computational fluid-dynamics. II. Solutions to parabolic, hyperbolic and elliptic partial differential equations, *Computers & Mathematics with Applications* **19 (8-9)** (1990), 147-161.

[55] A.Q.M. Khaliq, D.A. Voss and S.H.K. Kazmi, A linearly implicit predictor-corrector scheme for pricing American options using a penalty method approach, *Journal of Banking & Finance* **30** (2006) 489-502.

[56] A.Q.M. Khaliq, D.A. Voss and M. Yousuf, Pricing exotic options with L-stable Padé schemes, *Journal of Banking and Finance* **31(11)** (2007), 3438-3461.

[57] A.Q.M. Khaliq, D.A. Voss, and K. Kazmi, Adaptive θ-methods for pricing American options, *Journal of Computational and Applied Mathematics* **222** (2008), 210-227.

[58] I.K. Kim, The analytical valuation of American options, *Review of Financial Studies* **3** (1990), 547-572.

[59] M. Kindelan, F. Bernal, P. Gonzalez-Rodriguez and M. Moscoso, Application of the RBF meshless method to the solution of the radiative transport equation, *Journal of Computational Physics* **229** (2010), 1897-1908.

[60] P.E. Kloeden and E. Platen, *Numerical Solution of Stochastic Differential Equations*, Springer-Verlag, Berlin, 1999.

[61] H.G. Landau, Heat conduction in a melting solid, *Quarterly Applied Mathematics* **8** (1950), 81-95.

[62] E. Larsson, K. Ahlander and A. Hal, Multi-dimensional option pricing using radial basis functions and the generalized Fourier transform, *Journal of Computational and Applied Mathematics 222* (2008), 175-192.

[63] W. Liao and J. Zhu, An accurate and efficient numerical method for solving Black-Scholes equation in option pricing, *International Journal of Mathematics in Operational Research* **1 (1/2)** (2009), 191-210.

[64] J. Li, Y. Chen and D. Pepper, Radial basis function method for 1-D and 2-D groundwater contaminant transport modeling, *Computational Mechanics* **32** (2003), 10-15.

[65] W. Liao and A.Q.M. Khaliq, High-order compact scheme for solving nonlinear Black-Scholes equation with transaction cost, *International Journal of Computer Mathematics* **86 (6)**, (2009), 1009-1023.

[66] W.K. Liu, S. Jun, S. Li, J. Adee and T. Belytschko, Reproducing kernel particle methods for structural dynamics, *International Journal for Numerical Methods in Engineering* **38** (1995), 1655-1679.

[67] G.R. Liu, *Mesh Free Methods: Moving Beyond The Finite Element Method*, CRC Press, 2002.

[68] G.R. Liu and M.B. Liu, *smooth particle hydrodynamics*, World Scientific Publishing Company, London, 2003.

[69] G.R. Liu and Y.T. Gu, *An Introduction to Meshfree Methods and Their Programming*, Springer, 2005.

[70] L.B. Lucy, A numerical approach to the testing of the fission hypothesis, *The Astronomical Journal* **82** (1977), 1013-1024.

[71] L.G. Macmillan, *Options as a Strategic Investment*, (3rd ed.), New York Institute of Finance, 1993.

[72] R. Mallier and G. Alobaidi, Laplace transforms and American options, *Applied Mathematical Finance* **7** (2000), 241-256.

[73] R.C. Merton, Theory of rational option pricing, *Bell Journal of Economics and Management Science* **4** (1973), 141-183.

[74] G.H. Meyer, The numerical valuation of options with underlying jumps, *Acta Mathematica* **47** (1998), 69-82.

[75] G.H. Meyer, Numerical investigation of early exercise in American puts with discrete dividends, *Journal of Computational Finance* **5 (2)** (2002), 37-53.

[76] J.J. Monaghan, An introduction to SPH, *Computer Physics Communications* **48** (1988), 89-96.

[77] R.C. Merton, Option pricing when underlying stock returns are discontinuous, *Journal of Financial Economics* **3** (1976), 125-144.

[78] K. Muthuraman, A moving boundary approach to American option pricing, *Journal of Economic Dynamics and Control*, **32(11)** (2008), 3520-3537.

[79] R. Myneni, The pricing of the American option, *The Annals of Applied Probability* **2 (1)** (1992), 1-23.

[80] B.F. Nielsen, O. Skavhaug and A. Tveito, Penalty and front-fixing methods for the numerical solution of American option problems, *The Journal of Computational Finance* **5 (4)** (2002), 69-97.

[81] B.F. Nielsen, O. Skavhaug and A. Tveito, Penalty methods for the numerical solution of American multi-asset option problems, *Journal of Computational and Applied Mathematics* **222** (2008), 3-16.

[82] G. Ökten, E. Salta and A. Göncü, On pricing discrete barrier options using conditional expectation and importance sampling Monte Carlo, *Mathematical and Computer Modelling* **47** (2008), 484-494.

[83] C.W. Oosterlee, On multigrid for linear complementarity problems with application to American-style options, *Electronic Transactions on Numerical Analysis* **15** (2003), 165-185.

[84] K.N. Pantazopoulos, *Numerical Methods and Software for the Pricing of American Financial Derivatives*, Ph.D. Thesis, Computer Science Department, Purdue University Computer Science Department, Purdue University, 1998.

[85] K.C. Patidar and A.O.M. Sidahmed, An efficient meshfree method for option pricing problems, T.E. Simos, G. Psihoyios and Ch. Tsitouras (eds.), *ICNAAM, Numerical Analysis and Applied Matheamtics, International Conference 2010*, American Institute of Physics, 1824-1827, 2010.

[86] A. Pelsser, Pricing double barrier options using Laplace transforms, *Finance and Stochastics* **4** (2000), 95-104.

[87] J. Persson and L. Sydow, Pricing American options using a space-time adaptive finite difference method, *Mathematics and Computers in Simulation* **80** (2010), 1922-1935.

[88] U. Pettersson, E. Larsson, G. Marcusson and J. Persson, Improved radial basis function methods for multi-dimensional option pricing, *Journal of Computational and Applied Mathematics* **222** (2008), 82-93.

[89] C. Piret, *Analytical and Numerical Advances in Radial Basis Functions*, Ph.D. thesis, 2007.

[90] E. Platen and J. West, Fair pricing of weather derivatives, *Research Paper Series No. 106, Quantitative Finance Research Centre, University of Technology, Sydney*, Australia, 2004.

[91] N. Rambeerich, D.Y. Tangman, A. Gopaul and M. Bhuruth, Exponential time integration for fast finite element solutions of some financial engineering problems, *Journal of Computational and Applied Mathematics* **224(2)** (2009), 668-678.

[92] P.W. Randles and L.D. Libersky, Smoothed particle hydrodynamics: Some recent improvements and applications, *Computer Methods in Appllied Mechanics and Engineering* **139** (1996), 375-408.

[93] L.C.G. Rogers and Z. Shi, The Value of an Asian Option, *Journal of Applied Probability* **32(4)** (1995), 1077-1088.

[94] H. Sak, S.Ozekici and I. Boduroglu, Parallel computing in Asian option pricing, *Parallel Computing* **33** (2007), 92-108.

[95] S. Sanfelici, Galerkin infinite element approximation for pricing barrier options and options with discontinuous payoff, *Decisions in Economics and Finance* **27** (2004), 125-151.

[96] R. U. Seydel, *Tools for Computational Finance*, Springer, 2006.

[97] M. Sharan, E.J. Kansa and S. Gupta, Application of the Multiquadric method for numerical solution of elliptic partial differential equations, *Applied Mathematics and Computation*, **84** (1997), 275-302.

[98] J.W. Swegle, D.L. Hicks and S.W. Attaway, Smoothed particle hydrodynamics stability analysis, *Journal of Computational Physics* **116** (1995), 123-134.

[99] C. Sun, J.-Y. Yang and S.-H. Li, On barrier option pricing in binomial market with transaction costs, *Applied Mathematics and Computation* **189(2)** (2007), 1505-1516.

[100] D.Y. Tangman, A. Gopaul and M. Bhuruth, A fast high-order finite difference algorithm for pricing American options, *Journal of Computational and Applied Mathematics* **222 (1)** (2008), 17-29.

[101] M. Tatari and M. Dehghan, A method for solving partial differential equations via radial basis functions: Application to the heat equation, *Engineering Analysis with Boundary Elements* **34** (2010), 206-212.

[102] C. Tsao and C. Huang, Efficient solutions for discrete Asian options, *Soft Computing - A Fusion of Foundations, Methodologies and Applications - Special issue on intelligent systems for financial engineering and computational finance* **11** (2007), 1131-1140.

[103] M. Vanmaele, G. Deelstra, J. Liinev, J. Dhaene and M.J. Goovaerts, Bounds for the price of discrete arithmetic Asian options, *Journal of Computational and Applied Mathematics* **185** (2006), 51-90.

[104] M.H. Vellekoop and J.W. Nieuwenhuis, Efficient pricing of derivatives on assets with discrete dividends, *Applied Mathematical Finance*, **13 (3)** (2006), 265-284.

[105] B.A. Wadea, A.Q.M. Khaliq, M. Yousuf, J. Vigo-Aguiard and R. Deiningere, On smoothing of the Crank-Nicolson scheme and higher order schemes for pricing barrier options, *Journal of Computational and Applied Mathematics* **204** (2007), 144-158.

[106] J.G. Wang and G.R. Liu, A point interpolation meshless method based on radial basis functions, *International Journal for Numerical Methods in Engineering* **38** (2002), 1623-1648.

[107] J.G. Wang, G.R. Liu and P. Lin, Numerical analysis of Biots consolidation process by radial point interpolation method, *International Journal of Solids and Structures* **39** (2002), 1557-1573.

[108] H.Y. Wen, X.H. Dong, and X.Y. Ruan, Mesh free method based on point collocation for metal forming simulation, *Acta Metallurgica Sinica* **19** (2006), 79-84.

[109] H. Wendland, Error estimates for interpolation by compactly supported radial basis functions of minimal degree, *Journal of Approximation Theory* **93** (1998), 258-396.

[110] H. Wendland, *Scattered Data Approximation*, Cambridge University Press, Cambridge 2005.

[111] R.E. Whaley, Valuation of American call options on dividend-paying stocks, *Journal of Financial Economics* **10** (1982), 29-58.

[112] P. Wilmott, S. Howison and J. Dewynne, *The Mathematical Financial Derivatives: A Student Introduction*, Cambridge University Press, Oxford, UK, 1995.

[113] L. Wu and Y. Kwok, A front-fixing finite difference method for the valuation of American options, *Journal of Financial Engineering* **6** (1997), 83-97.

[114] Z. Wua and Y.C. Hon, Convergence error estimate in solving free boundary diffusion problem by radial basis functions method, *Engineering Analysis with Boundary Elements* **27** (2003), 73-79.

[115] J. Zhao, M. Davison and R.M. Corless, Compact finite difference method for American option pricing, *Journal of Computational and Applied Mathematics* **206** (2007), 306 - 321.

[116] S.P. Zhu and W.T. Chen, A new analytical approximation for European puts with stochastic volatility, *Applied Mathematics Letters* **23** (2010), 687-692.

[117] R. Zvan, P.A. Forsyth and K.R. Vetzal, Penalty methods for American options with stochastic volatility, *Journal of Computational and Applied Mathematics* **91** (1998), 199-218.

[118] R. Zvan, K.R. Vetzal and P.A. Forsyth, PDE methods for pricing barrier options, *Journal of Economic Dynamics & Control* **24** (2000), 1563-1590.